

General Disclaimer

One or more of the Following Statements may affect this Document

- This document has been reproduced from the best copy furnished by the organizational source. It is being released in the interest of making available as much information as possible.
- This document may contain data, which exceeds the sheet parameters. It was furnished in this condition by the organizational source and is the best copy available.
- This document may contain tone-on-tone or color graphs, charts and/or pictures, which have been reproduced in black and white.
- This document is paginated as submitted by the original source.
- Portions of this document are not fully legible due to the historical nature of some of the material. However, it is the best reproduction available from the original submission.

THE MARINE RESOURCES EXPERIMENT PROGRAM (MAREX)

(NASA-TM-87368) THE MARINE RESOURCES
EXPERIMENT PROGRAM (MAREX) (NASA) 119 p
HC A06/MF A01 CSCL 08C

N85-10560

Unclas

G3/48 01090

Report of the Ocean Color
Science Working Group



NASA

Goddard Space Flight Center
Greenbelt, Maryland 20771



Front Cover

NIMBUS 7 CZCS view of the Northwest Atlantic. The brown to red areas off the coast and in the vicinity of Georges Bank are high in phytoplankton plant life, while the blue areas of the North Wall of the Gulf Stream, and the circular "warm core ring" spun off the Gulf Stream are relative deserts of plant life.

Back Cover

This is the same view as the front cover, showing infra-red sea surface temperatures. The cold shelf water is shown in blue, while the warmer Gulf Stream and ring are red to yellow.

THE MARINE RESOURCES EXPERIMENT PROGRAM
(MAREX)

Report of
The Ocean Color Science Working Group

GODDARD SPACE FLIGHT CENTER
Greenbelt, Maryland 20771
1982

ORIGINAL PAGE IS
OF POOR QUALITY



Visibility Laboratory Processed CZCS Image of the Southern California Bight
(Orbit 1915, 11 March 1979)

CONTENTS

<u>Section</u>	<u>Page</u>
FOREWORD.	ix
EXECUTIVE SUMMARY	xi
1. INTRODUCTION.	1-1
2. PRESENT LIMITATIONS	2-1
2.1 Ship <u>in situ</u> Sensing	2-1
2.2 Satellite Remote Sensing	2-4
2.3 Aircraft Remote Sensing.	2-10
2.4 Fluorometer <u>in situ</u> Sensing.	2-14
3. MAREX Project Plan Objectives	3-1
3.1 C/N and Climate.	3-1
3.2 Food Webs and Fisheries.	3-5
3.3 Waste Disposal	3-7
4. EXPERIMENTAL DESIGN	4-1
4.1 Previous Studies	4-1
4.2 MAREX Shelf Studies.	4-2
4.3 Reliability of Individual Measurements	4-5
4.4 Frequency of Sampling.	4-15
4.5 Additional Oceanic Studies	4-17
5. REQUIREMENTS.	5-1
5.1 Spacecraft	5-1
5.2 Measurement Channels	5-5
5.3 Spatial Resolution	5-5
5.4 Observational Coverage	5-6
5.5 Navigational Accuracy.	5-7
5.6 Data Delivery.	5-7
5.7 Mission Length	5-9
APPENDIX A. SENSORS.	A-1
APPENDIX B. ALGORITHMS	B-1
APPENDIX C. DATA REDUCTION	C-1
APPENDIX D. DEFENSE AND COMMUNICATION APPLICATIONS	D-1
APPENDIX E. MAREX WORKING GROUP.	E-1

CONTENTS (cont.)

<u>Section</u>	<u>Page</u>
APPENDIX F. LITERATURE CITED	F-1
APPENDIX G. GLOSSARY OF ACRONYMS	G-1

ILLUSTRATIONS

<u>Figure</u>	<u>Page</u>
2-1 Simplified Space and Time Domains for Some Oceanic Processes and Sampling	2-2
2-2 The Distribution of CZCS-derived and <u>In Vitro</u> Measurements of Chlorophyll Along a Ship's Track from Georges Bank to Delaware Bay	2-7
2-3 The Distribution of CZCS-derived and <u>In Vitro</u> Measurements of Chlorophyll Along a Ship's Track from the Gulf of Mexico to the West Florida Shelf.	2-9
2-4 Airborne Remote Sensor Mappings of the Lower Chesapeake Bay and Plume Mode on June 23, 1980.	2-13
2-5 Initial Mooring Design for High Frequency Time Series of Chlorophyll from <u>In Situ</u> Fluorometers off Long Island	2-15
2-6 Time Series of Chlorophyll at 10.5 m Between Temperature, Salinity, and Current Sensors and 8 m and 16 m During the 1977 Fall Bloom off Long Island	2-17
4-1 Functional Response of Photosynthesis to Light Intensity. . .	4-7
4-2 Arrhenius Plots of Light-saturated Photosynthetic Rate of <u>Phaeodactylum tricornutum</u> Previously Grown at 5°C, 10°C, and 25°C, from Li (1981).	4-10
4-3 Scatter Diagrams of Temperature Versus Nitrate Along the West Coast of America	4-11
4-4 Depth Profiles of Photosynthesis Simulated by Random Walk Model of Phytoplankton Circulation with Time-dependent Photosynthetic Rate at High Irradiance.	4-12
4-5 Photosynthetic Efficiency per g Chlorophyll as a Function of PSU Size for Marine Phytoplankton.	4-14
5-1 Possible Location of CZCS on NOAA-I Satellites.	5-4

TABLES

<u>Table</u>	<u>Page</u>
1-1 Uncertainty of Carbon Fixation Within the Sea.	1-3
1-2 A Balanced Budget of Annual Net Fluxes of the Global CO ₂ Cycle.	1-4
1-3 Ocean-related NASA Spacecraft Activities: Previous Decade . .	1-7
2-1 Scaled Biological Patterns in the Ocean and Their Driving Mechanisms	2-3
2-2 Space-borne Ocean Sensing Techniques	2-5
2-3 Aircraft Remote Sensors Used in Marine Productivity Experiments.	2-11
4-1 Variability in Nitrogen Inputs and Subsequent Primary Production on American Shelves	4-3
4-2 MAREX Biomass/Productivity Experiments in 1987-89.	4-6
5-1 Ocean Related Spacecraft Activities: Next Decade.	5-2
5-2 NOAA-I/CZCS Orbit Parameters	5-3

FOREWORD

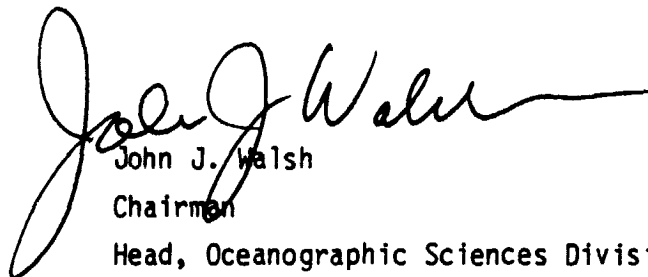
As a result of the launch of the Nimbus-7 Coastal Zone Color Scanner (CZCS) in October 1978 and the subsequent progress with data analysis, it is now possible to determine ocean chlorophyll concentrations from space to better than ± 30 percent for values of $0-5 \mu\text{g l}^{-1}$ in Case I waters (little sediment or humic matter). Calculations of annual ocean primary production vary from 20 to 55×10^9 tons C yr^{-1} and may be underestimated by three to ten fold, leading to unreliable estimates of world fish production and of the role of ocean biota in global CO_2 cycles. With some modest improvements in similar satellite instrumentation, together with a limited amount of in situ data, it appears feasible to determine global marine algal biomass and primary productivity with sufficient accuracy that future changes, induced by overfishing or anthropogenic nutrient inputs, for example, can be detected.

With this prospect in mind, the Satellite Ocean Color Science Working Group was established in October 1981 to consider the scientific utility of repeated satellite measurements of ocean color, especially for measuring global ocean chlorophyll and for studying the fate of global primary productivity in the sea. The group was specifically asked:

- a. What are major scientific problems that can be studied using satellite-derived measurements of near-surface ocean color?
- b. To what extent can satellite ocean color measurements make a significant improvement over conventional observations?
- c. To what extent can complementary satellite measurements, such as sea surface temperature and wind speed, or airborne and in situ measurements, significantly augment the value of ocean color measurement?
- d. What are the options on accuracy, resolution, areal coverage, and revisit time of the satellite ocean color observations that best satisfy the data requirements of these scientific problems?

This document presents the results of the Working Group's deliberations. In particular, it states the scientific requirements for ocean color data from a CZCS follow-on sensor (hereafter designated the Ocean Color Imager or OCI) in order to address global primary productivity, fishery, and carbon storage problems. It also outlines some specific experiments (called the Marine Resources Experiment or MAREX) which are designed to determine critical nutrient fluxes, photosynthetic rates, and the fate of the resultant primary productivity and biomass for a variety of continental shelf and open ocean ecosystems which are representative of those found in the world oceans.

Concurrently with the activities of this group, Goddard Space Flight Center has been studying the feasibility of including an Ocean Color Imager on the NOAA series of polar-orbiting, operational meteorological satellites. Results to date indicate that it is indeed feasible. NASA is developing a plan which could result in the flight of an Ocean Color Imager aboard one of the NOAA satellites around 1988.

A handwritten signature in black ink, appearing to read "John J. Walsh", with a long horizontal flourish extending to the right.

John J. Walsh

Chairman

Head, Oceanographic Sciences Division

Brookhaven National Laboratory

EXECUTIVE SUMMARY

I. SCIENCE BASIS

Primary production in the sea accounts for at least 30 percent of the total global annual plant fixation of CO_2 . Marine primary production is the basis for almost all life in the sea, and is an integral to major biogeochemical cycles, such as the CO_2 cycle. However, uncertainties exist in the magnitude of annual marine CO_2 fixation and its variability. The highly productive continental shelves of the world, where 95 percent of the estimated fishery yield and most of the carbon sink of atmospheric CO_2 occur, may actually be two or three times more productive than presently estimated. Open ocean productivity estimates have recently been challenged and could be underestimated by an order of magnitude.

These uncertainties are due to a wide range of variability of biomass in the shelf waters and to problems in growth rate measurement techniques in the open ocean. Significant improvement in the estimates of shelf productivity, and in understanding the controlling mechanisms for productivity variations are expected when satellite measurements of ocean color are combined with appropriate in situ observations. Such a capability is clearly needed if we are to understand biological variability in response to discrete and climatic changes, anthropogenic nutrient inputs on fisheries, and fossil-fuel CO_2 load in the atmosphere.

The Nimbus-7 Coastal Zone Color Scanner (CZCS) has shown that the pigment concentrations of the upper ocean can be measured from space with enough accuracy for determining phytoplankton biomass and, in certain areas, net primary productivity. Improved in situ chlorophyll sensors can now provide complementary calibration and interpolation data. Thus, by using satellites, buoys, aircraft and ships, it is now possible to significantly lower the variances in estimates of phytoplankton abundance and population growth rates in the ocean, and to identify biological and physical factors responsible for these variances. With the appropriate data sets, and from ongoing development of phytoplankton models, future

fluxes of carbon and nitrogen in the open ocean regions can then be addressed in the context of changes in coastal eutrophication, storage pools of CO₂, and fishery yields, at daily and decadal time scales.

To improve our estimates of phytoplankton abundance and growth rates, we recommend that NASA fly a CZCS follow-on (Ocean Color Imager, OCI) with improvements in channels, bit accuracy, calibration, data storage and handling, and real time accessability. This could be achieved by flying an OCI on the NOAA series of satellites and by implementing the focused field experiments discussed as part of the Marine Resources Experiment (MAREX). MAREX is conceived as an integrated, interdisciplinary and multi-agency research opportunity, likely including elements of future NASA, NOAA, NSF, DOE and ONR programs and inviting international collaboration. In conjunction with the development of a new OCI, it is necessary that selected data sets of the current CZCS be processed to the best possible Level II product and analyzed in biological scientific literature to demonstrate the techniques to be used in MAREX, evaluate the limits of biological use of the data, and provide the basis for algorithms for the OCI.

Color Scanner data are extremely useful for other applications in addition to those previously mentioned. Identification of fronts, eddies, turbidity, and regions of bioluminescence are a few of the defense applications of OCI data. Albacore and salmon feeding habitats and anchovy spawning habitats, are examples of the fisheries-related changes that can be detected with satellite ocean color/temperature data for improved fisheries management. Thus, while this document largely discusses ocean primary productivity research, a wide variety of other research and operational users will also benefit from the flight of a future Ocean Color Imager.

A number of measurements will be needed. The aims of MAREX are: (1) measure global chlorophyll; (2) relate chlorophyll to global biomass;

(3) relate chlorophyll, light, and efficiency determinations to global oceanic CO₂ fixation; (4) relate changes in mesoscale or regional biomass to primary production, or changed biomass (this has implications for effects of nutrients and for the settling loss of CO₂); (5) include fishery information to get correlations between the extent and timing of phytoplankton blooms and subsequent effects on larger species.

II. EXPERIMENTAL REQUIREMENTS

A set of minimum spacecraft and ground system requirements, necessary to achieve the major scientific opportunities from space-borne ocean color data, were determined. The following requirements, hopefully, allow significant scientific progress in limited well-defined programs, while still offering sufficient flexibility to satisfy a reasonable portion of the needs of other scientific and operational areas. The OCSWG believes these requirements provide the basis both for successfully executing the exciting nearer term shelf carbon/nitrogen flux experiment and for providing a basis for further development in color sensing science in other fields in the future. The minimum requirements for an ocean color system which could receive the support of a significant portion of the oceanographic community follows.

II.1 SPACECRAFT

The Tiros/NOAA-I spacecraft was identified as being a suitable vehicle, provided it was flying in a near-noon local orbit (12:30 - 2:00 PM).

Adding an OCI to the NOAA-I complement of sensors does require some modifications to the baseline CZCS, such as the elimination of the thermal channel and of its cooler. This is an acceptable modification since equivalent thermal information would be available from other NOAA-I sensors. Additionally, the need for a diffuser plate to provide an on-board solar and radiometric calibration is required.

II.2 MEASUREMENT CHANNELS

The Nimbus-7 CZCS program demonstrated the feasibility of determining ocean chlorophyll levels (and diffuse attenuation coefficients) from

multi-channel visible space-borne observations. To resolve the chlorophyll concentration to within 50 percent over a range of concentration from 0.1 to 10.0 micrograms chlorophyll per liter in the open ocean and outer continental shelf areas requires radiance observations to 10 bit accuracy.

The following are the eight recommended wavelengths of which six will be used for routine open ocean and/or continental shelf measurements.

443 nanometers (nm)	590
490	670
520	765
560	867

The 490 and 590 nm channels are useful under special circumstances to extend the observations into more turbid coastal waters. Since the technique is still experimental, these are considered to be research channels which need to be selectable in the place of two of the other channels under infrequent circumstances, arranged well in advance.

II.3 SPATIAL RESOLUTION

The chlorophyll distribution in the ocean is patchy on all scales down to the sub-kilometer level. Thus, to adequately map phytoplankton variation in high-concentration shelf areas, which is the major goal of the first group of MAREX studies, a satellite must be able to resolve about a kilometer of the ocean. This small spot size also allows measurements closer to the shore to resolve local outwelling and upwelling zones, which tend to be nearshore phenomena in many cases. Such a high data rate may be relaxed somewhat for wide area studies of open ocean phytoplankton where statistical rather than process experiments are more likely. In this case, a degradation to about a 4-kilometer resolution is accepted. Therefore, a satellite system is required that can operate in two modes, analogous to the present NOAA AVHRR infrared system: (1) local area coverage of high resolution to about one km and (2) global area coverage of lower resolution to about four km.

II.4 OBSERVATIONAL COVERAGE

Coverage is defined as the frequency at which a chlorophyll data set for a given extended experimental region is available, assuming ideal, cloud-free conditions. The data set may be composited from several OCI images taken at various resolutions over an extended time period. By their nature, satellites provide a high density of observations within their swath coverage; however, one or more passes must be composited to generate the field of data which the scientists require. The satellite coverage is, then, a function of swath size, orbit configuration, and cloudiness. The time it takes for some part of the satellite swath to revisit every spot within an experimental area defines the length of time it takes to generate a data field. Repeat coverage is the time it takes to generate another such field in the same area. For example, a small experimental area, less than one swath width in size, might be entirely covered in one pass, while repeated coverage may not be available for several days or weeks. Phytoplankton variability in the ocean has a time scale of less than a week depending on seasonal changes of wind events and algal growth. It would be desirable, then, to have worldwide chlorophyll observations at least every 3 or 4 days. This is impossible due to natural cloudiness, reasonable orbit, and swath configurations, so there must be an accompanying program of in situ moored observations in the experiments to allow interpolation of satellite observations.

To make even this possible, it is required that a satellite system's swath pass over any given spot at least weekly.

II.5 NAVIGATIONAL ACCURACY

Location of pixels in latitude-longitude coordinates is important for quantitative scientific use of color scanner data. In order to make these data useful for other than individual scene analyses, the scientists must be able to use observations from many passes to generate time series and do statistical analysis. This implies that location accuracy of data from different passes must be sufficiently precise to allow compositing. For these purposes, we require an absolute navigational accuracy of 5 km for high-resolution local data and 25 km for low-resolution global data.

II.6 DATA DELIVERY

The details of data processing and delivery are complex. For purposes of an overall requirement, satisfactory data processing and delivery is considered to be among the most vital concerns that the ocean science community have for a new satellite observing system. History of other ocean-oriented satellite data systems has not been encouraging in this respect. Timeliness of data processing is most important in that if data processing time does not keep pace with the data flow, backlogs quickly develop and it can become literally years before the data are made available to the research community. In that case, the data are often not widely used by scientists and a multi-million-dollar satellite is under-utilized. Further, satellite pictures by themselves are not satisfactory for quantitative ocean study. The observations must be presented as quantitative information products, specifically, navigated values of chlorophyll and of the diffuse attenuation coefficient. To this end, the data available to the user must meet the following requirements:

- a. For near real-time positioning of ships during MAREX field experiments, quick-look data must be available with 24 hours of observation, or direct satellite read-out for user ground stations must be available in selectable areas worldwide.
- b. For integration with cruise results, fully processed high-resolution data must be available to the user within 30 days of observation. This is "Level II" processing (which means cloud removed, atmospherically corrected, chlorophyll values within a pass, identified by latitude-longitude on computer-compatible tape). False color images or contoured maps of these passes are also desirable.
- c. The same information is needed for the low-resolution global data. However, since the global data will be primarily used in the study of larger scale, longer term variations, the observations should be integrated and composited before delivery. Level II low-resolution values should be stored on a monthly 100 km grid. After three months for processing, the mean values should be published monthly as contours on ocean-scale maps. There is no

requirement for imaging individual passes, although individual Level II tapes should be preserved for 6 months for selected processing on request.

- d. All high- and low-resolution Level I tapes should be preserved in an archive for 5 years. Users should have on-line, interactive access to a catalogue of the archived data.
- e. The difficulty and cost involved in handling the flow from a high-data-rate instrument such as this is recognized. Ideally, all the sunlit data from the satellite should be stored and processed at high resolution. A minimum requirement is the ability to process 30 minutes of stored high-resolution data per day to Level II chlorophyll values, and 150 minutes of stored low-resolution data. This would result in enough capacity to process the ocean areas near the USA to high resolution, and at least one hemisphere at low resolution on a continuing basis. It would be highly desirable to double the low-resolution capacity to be assured of worldwide coverage. Direct broadcasting of high-resolution data on at least a 50 percent duty cycle would fill in the gaps of recorded high-resolution stored data for those users with ground receivers. It is strongly recommended that the direct broadcast mode be designed so that there is minimum impact to existing ground receiver stations used by researchers outside NASA. The system should be similar enough to the existing NOAA infrared broadcast protocol that other users need only make minor or no changes to their hardware and software for data capture.

II.7 MISSION LENGTH

In order to conduct the in situ field work necessary to exploit the ocean color observations from space, experiments listed earlier must be staged in a variety of seasons and conditions. Logistically, this implies that the spacecraft mission must cover at least two years to specify a typical situation, i.e., the occurrence of El Niño phenomena. In addition, even the coarsest values for ranges in interannual productivity are not known for most ocean areas. An absolute minimum of two years of observation is

necessary to identify the scale of variability. Thus, a minimum mission length of two years is required, with any extension of that length highly desirable. That also implies that instrument calibration be constant, or identifiable, during the minimum two-year mission to allow valid comparisons of ocean observational values.

SECTION 1. INTRODUCTION

The potential of the carbon cycle of the sea to either yield fish or store atmospheric CO_2 is a subject of continuing controversy as man's ability to modify the marine environment increases. Because the actual amount of CO_2 fixed annually during marine photosynthesis is unknown, the fates of phytoplankton, serving as a precursor either to fish carbon or to sediment carbon, are also unknown. Debates over the amount of potential fish harvest (Ryther, 1969, Alversen et. al., 1970) and CO_2 storage capacity (Broecker et. al., 1979; Walsh et. al., 1981) of the ocean thus hinge on the amount and fate of marine primary production. Current estimates of annual marine primary production range from 20 to 55×10^9 tons of carbon per year (Ryther, 1969; Platt and Subba Rao, 1975; DeVoys, 1979; Walsh, 1981). This range accounts for ≈ 25 to 50 percent of the total net global carbon fixation (Woodwell et. al., 1978), and is 400 to 1000 percent of either present fish yield or fossil fuel emissions.

Over the last century, man's ability to extract nitrogen from the atmosphere has also begun to rival that of N_2 fixation by plants. Between 1950 and 1975 world production of agricultural fertilizers increased ten-fold. Nitrogen loadings from agrarian runoff, deforestation, and urban sewage have already impacted local streams and ponds, some large lakes, major rivers, and perhaps even the continental shelves. Nitrogen is now only routinely measured in 25 percent of the world's 240 largest rivers, however, and few biological time series are available to document the coastal zone's past response to fluvial nutrient transients on a decadal time scale. The annual primary production of the Dutch Waddensea, for example, has apparently increased threefold between 1950 and 1970 (Postma, 1978). Future measurements of ocean color by satellites and of in situ fluorescence by buoys are required to provide adequate chlorophyll time series to assess the fate of phytoplankton carbon and nitrogen, as well as their productivity in the sea. With this information, one can address present problems of overfishing, as well as the future and perhaps more ominous consequences of these linked

activities--man's accelerated extraction of nitrogen from the atmosphere and addition of carbon to the atmosphere.

Large areas of the ocean, such as the central gyres, have relatively low rates of production per unit surface area, but account for a major fraction of total carbon fixation because of their large areal extent (Table 1-1). In contrast, highly productive coastal and upwelling regions account for only 10 percent of the ocean by area and probably 25 percent of the ocean primary productivity; they provide more than 95 percent of the estimated fishery yield, however, and most of the proposed organic carbon sink of atmospheric CO_2 (Table 1-2). These various ocean provinces exhibit pronounced differences in their phytoplankton species assemblages as the evolutionary consequence of their physical habitat. They also have significant differences in spatial and temporal variability of algal biomass as a function of nutrient input grazing losses (Walsh, 1976) and have very different fates of the fixed carbon (Walsh et. al., 1981). Their contribution to global carbon fixation (Table 1-1) may be underestimated from two- to tenfold (Smith et. al., 1981).

There are two basic reasons for the large uncertainty in the estimates of marine carbon fixation (Table 1-1); both are of equal importance. First, the methodology used to estimate the rate of primary productivity (the ^{14}C method) may be in serious error (Geiskes et. al., 1979; Eppley, 1980). Secondly, the highly productive shelf regions exhibit a much wider range of spatial and temporal variability of biomass than the open ocean, on scales which have been very poorly sampled by classical ship-board programs. It is in the oligotrophic (gyre) regions, where the biomass variability is not pronounced, that the methodology errors are greatest. This is because the oceanic phytoplankton are thought to be more sensitive to stresses related to capture and prolonged enclosure. However, the long food chains and 90 percent recycling processes of the offshore regime (Table 1-2) provide insignificant fish harvest (Ryther, 1969) and little net biotic storage of CO_2 (Eppley and Petersen, 1980).

In the coastal regions where productivity is much higher, and the results of the ^{14}C methodology are probably more representative of the actual rate, the spatial extent and the temporal character are poorly

Table 1-1. Uncertainty of Carbon Fixation Within the Sea (after Ryther, 1969).

Province	Percent- age of ocean	Area (10^6 km^2)	Mean productivity ($\text{gm C m}^{-2} \text{ yr}^{-1}$)	Approx. range of chl. conc. (mg m^{-3})	Total productivity ($10^9 \text{ tons C yr}^{-1}$)	(%)	Degree to which actual production may exceed reported values
Open ocean	90.00	326	50	0.01-0.1	16.3	(82)	$\leq \times 3 - \times 10$
Coastal zone	9.83	36	100	0.1-1.0	3.6	(18)	$\leq \times 3$
Upwelling areas	0.17	0.6	300	1.0-10.0	0.18	(0.5)	$\leq \times 2 - \times 5$
Total		362.6			20	(100)	

Table 1-2. A Balanced Budget of Annual Net Fluxes ($\times 10^9$
tons C yr⁻¹) of the Global CO₂ Cycle (after
Walsh et al., 1981).

Sources	Fossil fuel emission	5.20
	Equatorial outgassing	1.00
	Volcanism	0.05
	Deforestation	<u>1.00</u>
	Total	<u>+7.25</u>
Abiotic Sinks	Atmospheric storage	2.60
	Reverine release of DOC	0.80
	Estuarine sediment	0.20
	Deep water formation	<u>2.00</u>
	Total	<u>-4.60</u>
Biotic Sinks	Open ocean fecal pellets	0.10
	Slope storage of phyto-detritus	<u>1.55</u>
	Total	<u>-1.65</u>

known. For example, within 30 km off the Peru coast, the surface chlorophyll biomass ranges from 0.4 to 40.0 $\mu\text{g chl l}^{-1}$ and the integrated primary production from <1 to $>10 \text{ gC m}^{-2} \text{ day}^{-1}$ (Walsh et. al., 1980). Approximately 25 percent of shelf production ($\sim 1.6 \times 10^9$ tons C yr^{-1} , see Table 1-2) is thought to be sequestered as organic carbon deposits on adjacent continental slopes. Although the anthropogenic input of nitrogen to the shelves may have increased tenfold over the last 50 to 100 years, a sufficient time series of phytoplankton data is not available to accurately specify changes in primary productivity or shelf export to continental slopes. This lack of a proper spatial and temporal perspective has hindered our understanding and, therefore, our ability to make accurate estimates of coastal productivity and subsequent carbon and nitrogen fluxes to the rest of the food web.

Understanding the coastal ecosystem processes has far greater significance than their areal extent or contribution to total marine carbon fixation would suggest because:

- a. The fate of carbon and nitrogen fixed in these highly productive shelf regions is quite different from the oceanic areas of the sea, sinking to slope depocenters instead of grazing within the water column (Walsh et. al., 1981; Eppley and Petersen, 1980).
- b. Impacts of human activity are greater in the coastal region.

Thus, there is a strong motivation to obtain, for the first time, synoptic biomass and productivity data required to study these highly dynamic oceanographic regions over both long periods at decadal time scales, and at the much higher Nyquist frequency for resolution of biological processes.

Preliminary investigations undertaken in the 1960s by Clarke, Ewing, Lorenzen, Yentsch, and others provided evidence that the quality of light reflected from the sea surface and remotely sensed by the aircraft instrumentation might be interpreted as phytoplankton biomass, i.e., chlorophyll, in the upper portion of the water column. These workers (e.g., Clarke et. al., 1970) were limited by their equipment to an altitude of 3

km. However, even at that altitude, the influence of the atmospheric backscatter was quite obvious as it began to dominate the color signal reflected from the ocean surface. This raised the question of whether the rather poorly reflected ocean could be sensed through the entire atmosphere from a spacecraft, and if the contributions of the Rayleigh backscatter and aerosol backscatter could be effectively removed from the signal seen by a spacecraft. Additional NASA-supported studies in 1971 and 1972 with Lear Jet and U-2 aircraft and a rapid scan spectrometer at altitudes of 14.9 and 19.8 km, demonstrated that this concept could be used to develop spacecraft equipment for the purpose of estimating ocean water column chlorophyll from earth satellites. This became possible through the realization that problems associated with the scattering properties of the atmosphere, as well as direct reflectance of the sun from the sea surface (glint), could be either avoided or corrected (Hovis and Leung, 1977).

The first satellite-borne ocean color sensor, the Coastal Zone Color Scanner (CZCS), was launched aboard Nimbus-7 in October 1978 (refer to Table 1-3). It has four visible and two infrared (one of which is thermal) bands, with a sensitivity about 60 times that of the Landsat-1 multispectral scanner. Unlike many satellite sensors of ocean properties (Table 1-3), the CZCS responds to more than the features of the mere surface of the sea and is sensitive to algal pigment concentrations in the upper 20 to 30 percent of the euphotic zone. A predictable relationship was established between the CZCS estimates of pigments and plankton chlorophyll measurements made aboard a ship in the Gulf of Mexico (Gordon et. al., 1980). Other shelf studies within the Southern California Bight (Smith and Baker, 1982) and coastal waters mouth of New England (Gordon et. al., 1982) have also compared ship track chlorophyll data and CZCS data. In all three coastal regions there was great spatial variability of in vivo chlorophyll, with a striking agreement between the two methods (+30 to 40 percent). The widespread evolution and dissipation of high and low chlorophyll features over a period of 13 days in the Southern California Bight (Frontispiece) was dramatically captured in these CZCS images (Smith

and Baker, 1981), demonstrating the potential power of this synoptic approach.

Table 1-3. Ocean-related NASA Spacecraft Activities: Previous Decade

Satellite	Sensor Complement	Launch	Status
Nimbus-5	Microwave radiometer (MR) + meteorological sensors	1972	Completed (9-years life)
Skylab	MR, altimeter (ALT), + scatterometer (SCAT)	1973	Completed (intermittent over 2 years)
Nimbus-6	MR + meteorological sensors	1975	Completed (6-year life)
Geos-3	ALT	1975	Completed (3-year life)
Seasat	ALT, MR, SCAT, + synthetic aperture radar (SAR)	1978	Completed (3-months life)
Nimbus-7	Coastal zone color scanner (CZCS), MR + meteorological sensors	1978	Operating

Satellite and aircraft remote-sensing techniques, as well as moored biological buoys, have matured rapidly in the last 3 to 5 years to now make such sampling feasible within a future Marine Resources Experiment (MAREX) program. As a consequence, the multiplatform (ship, buoy, aircraft, and satellite) sampling strategies of the proposed MAREX research offer an opportunity to significantly reduce the variance in estimates of shelf phytoplankton abundance, carbon fixation, consumption, deposition, and their concomitant nitrogen fluxes.

SECTION 2. PRESENT LIMITATIONS

Space and time domains of the relevant biological and physical processes controlling productivity are compared in Figure 2-1 with the present space-time sampling regimes of various measurement platforms. Individual phytoplankton, zooplankton, and fish have life cycles on the order of respectively 1 cycle day⁻¹, 0.1-0.01 cycles day⁻¹, and 0.01-0.001 cycles day⁻¹ (Walsh et. al., 1977), which are translated into longer time scales of the communities within which their birth and death processes take place. Phytoplankton communities, for example, experience major changes over periods on the order of 1 to 10 days and, as a result of shelf flow regimes, over areas of 10 to 100 square kilometers. Fish, because they are larger, swim faster and live longer, occupy the time domain between 10² to 10³ days and the space domain between 10³ to 10⁶ square kilometers. Comparing these domains for various physical processes and resultant biological distributions with the sampling regimes of the various measurement platforms (Table 2-1), one arrives at a major reason for the proposed MAREX program--the need to measure distributions of biological properties at frequencies which can resolve causally the sources of their variance.

2.1 SHIP IN SITU SENSING

Classical shipboard programs consist of productivity measurements made once a day over a spatial area limited by the usual 10-12 knot speed of the research vessel. At present, shipboard rate measurements, such as nutrient uptake, photosynthesis, respiration, grazing, excretion, and sinking, can only be made at a few points of the sea, to be later multiplied by some inadequate estimate of mean biomass in order to calculate fluxes of elements within the marine food web. However, phytoplankton species on the continental shelves can divide every 0.5 to 2 days; without losses, a population during the spring bloom could increase at the same rate. To resolve the temporal and spatial consequences of this resultant rate process, a sampling frequency of at least 0.25 day⁻¹ is required by sampling theory (Blackman and Tukey, 1957).

ORIGINAL PAGE IS
OF POOR QUALITY

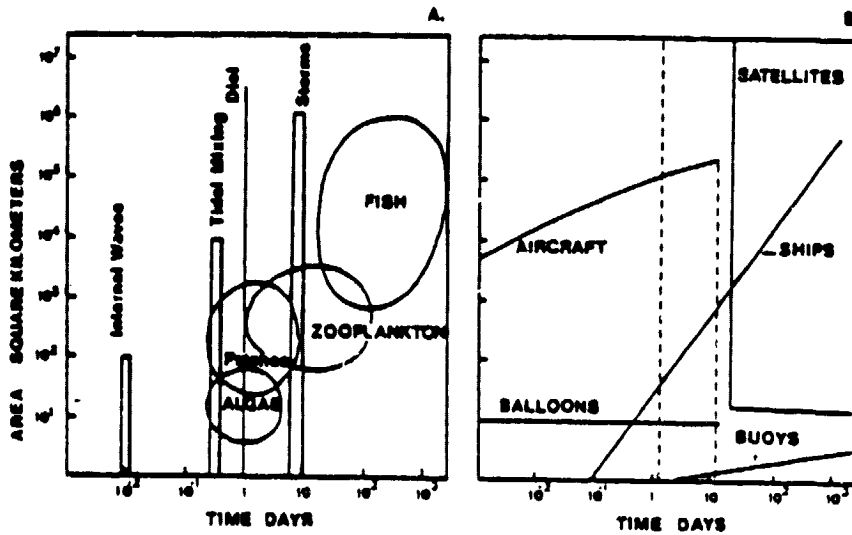
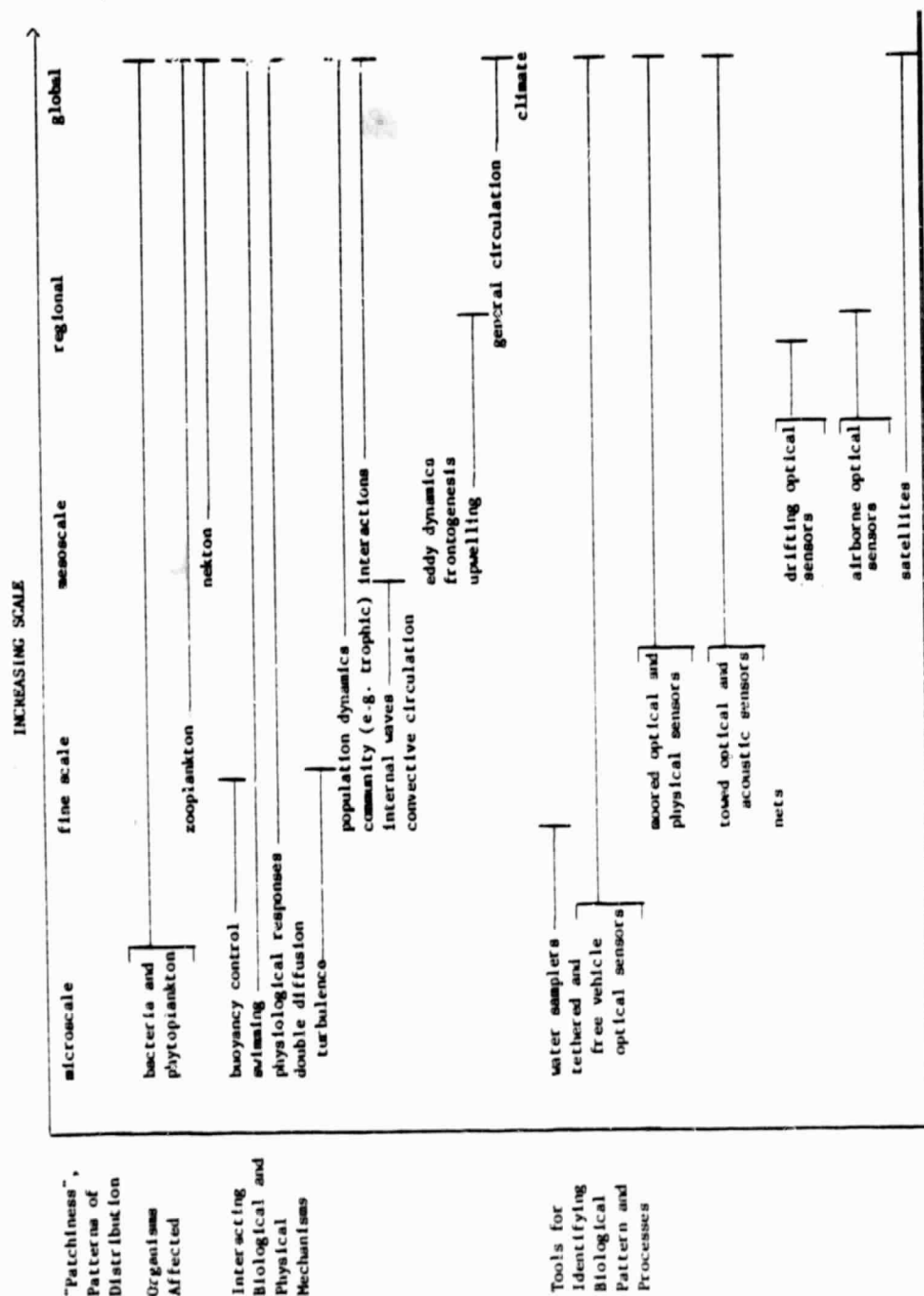


Figure 2-1. Simplified Space and Time Domains for Some Oceanic Processes and Sampling

Table 2-1. Scaled Biological Patterns in the Ocean and Their Driving Mechanisms



If one sampled every 4 hours in a typical longshore upwelling flow regime of 30 cm sec^{-1} to resolve this process, at least 5 ships would be required every 20 km^2 for the necessary biomass measurements (Kelley, 1976). To date, the closest realization of this sampling requirement was the Fladen Ground Experiment (FLEX), which involved sequential deployment of ~20 ships for 100 days over a 10 km^2 area. Extending such synoptic biomass measurements beyond the ship domain could serve as one definition of what is meant by remote sensing. Some biomass measurements previously made on a ship, for example, can now be made by buoys, but a combination of buoys and one ship, or even a fleet, cannot duplicate areal coverage by aircraft and satellites. In many respects, however, these different platforms collect mutually exclusive, but complementary data sets, all of which are required to properly assess the fate of shelf production.

2.2 SATELLITE REMOTE SENSING

The Coastal Zone Color Scanner (CZCS) on the Nimbus-7 satellite is the only satellite sensor in orbit (Table 2-2) for the purpose of assessing marine biomass (Hovis et al., 1980; Gordon et al., 1980). The CZCS was specifically designed to detect upwelling radiance in spectral bands selected for the purpose of detecting variations in the concentrations of phytoplankton pigments. The theoretical and experimental techniques for describing the bio-optical state of ocean waters and its relationship to optical parameters that can be remotely sensed have been discussed by a number of workers (Morel and Prieur, 1977; Smith and Baker, 1978a,b; Baker and Smith, 1981).

Simply stated, the CZCS radiance data can be utilized to estimate ocean chlorophyll concentrations by detecting shifts in sea color, particularly in oceanic waters. Clear open ocean waters have low chlorophyll concentrations ($0.01\text{-}1.0 \mu\text{g chl l}^{-1}$) and the solar radiation reflected from the upper layers of these waters is blue; conversely, waters with high concentrations of chlorophyll ($>1.0 \mu\text{g chl l}^{-1}$) are green (Morel and Smith, 1974). It has been demonstrated that this change in ocean color can provide a quantitative estimate of chlorophyll concentration (Gordon and Clark, 1980; Smith and Baker, 1981) for oceanic regions with an accuracy of 0.3 to 0.5 log C (where C is the chlorophyll concentration).

Table 2-2. Space-borne Ocean Sensing Techniques

Altimeter. A pencil beam microwave radar that measures the distance between the spacecraft and the earth. Measurements yield the topography and roughness of the sea surface from which the surface current and average wave height can be estimated.

Color Scanner. A radiometer that measures the intensity of radiation emitted from the sea in visible and near-infrared bands in a broad swath beneath the spacecraft. Measurements yield ocean color, from which chlorophyll concentration and the location of sediment-laden waters can be estimated.

Infrared Radiometer. A radiometer that measures the intensity of radiation emitted from the sea in the infrared band in a broad swath beneath the spacecraft. Measurements yield estimates of sea-surface temperature.

Microwave Radiometer. A radiometer that measures the intensity of radiation emitted from the sea in the microwave band in a broad swath beneath the spacecraft. Measurements yield microwave brightness temperatures, from which wind speed, water vapor, rain rate, sea-surface temperature, and ice cover can be estimated.

Scatterometer. A microwave radar that measures the roughness of the sea surface in a broad swath on either side of the spacecraft with a spatial resolution of 50 kilometers. Measurements yield the amplitude of short surface waves that are approximately in equilibrium with the local wind and from which the surface wind velocity can be estimated.

Synthetic Aperture Radar. A microwave radar similar to the scatterometer except that it electronically synthesizes the equivalent of an antenna large enough to achieve a spatial resolution of 25 meters. Measurements yield information on features (swell, internal waves, rain, current boundaries, and so on) that modulate the amplitude of the short surface waves; they also yield information on the position and character of sea ice from which, with successive views, the velocity of ice flows can be estimated.

Processing of the CZCS data, as well as all of the rest of the Nimbus data, proved to be far more of a problem than anticipated before launch. In order to handle the large volume of data that would be collected by an imaging sensor such as the CZCS with an operating time up to two hours per day, and a return signal rate of 800,000 bits per second, a special processing line was established at NASA/Goddard Space Flight Center (GSFC) using the latest in automatic data processing techniques. Unfortunately, these techniques were not at a state that they could handle such a large volume routinely, and only as a result of intense effort by the GSFC data processing staff was a routine flow of data finally accomplished approximately two years after launch. This delay in data availability forced a corresponding delay in analysis of the data comparison with measurements made shortly after the launch of the spacecraft. When data was finally available for such analysis, however, comparisons with ship measurements showed the correlation of derived and surface-measured pigment concentrations and diffuse attenuation coefficients were quite good in open oceans, with accuracy degrading in areas of high sediment suspension due to the limited number of spectral bands available.

Although the validation of the CZCS-derived pigment concentration, C , is still underway, the results up to this point in time are very encouraging. (A complete description of the CZCS algorithms is presented in Appendix B.) The initial comparisons between CZCS imagery and surface pigments measured continuously along ship tracks carried out by Gordon et al. (1980) and Smith and Wilson (1981) suggested that C could be retrieved from the imagery to within about a factor of two. Subsequently, Smith and Baker (1982) and Gordon et al. (1982) have shown that accuracies of the order of ± 30 percent in C are possible for Morel's Case 1 waters (Morel and Prieur, 1977; see also, Appendix B). An example of the Gordon et al. (1982) comparison between CZCS-derived (heavy line) and ship-measured (light line) pigments is presented in Figure 2-2. The ship track is from Georges Bank (left edge) to Delaware Bay (right edge) and the ship data were taken within ± 12 hours of the satellite overpass on Orbit 3240. Atmospheric correction was effected by applying the techniques described in Appendix B to a Warm Core Gulf Stream Ring centered about 150 km from

ORIGINAL PAGE IS
OF POOR QUALITY

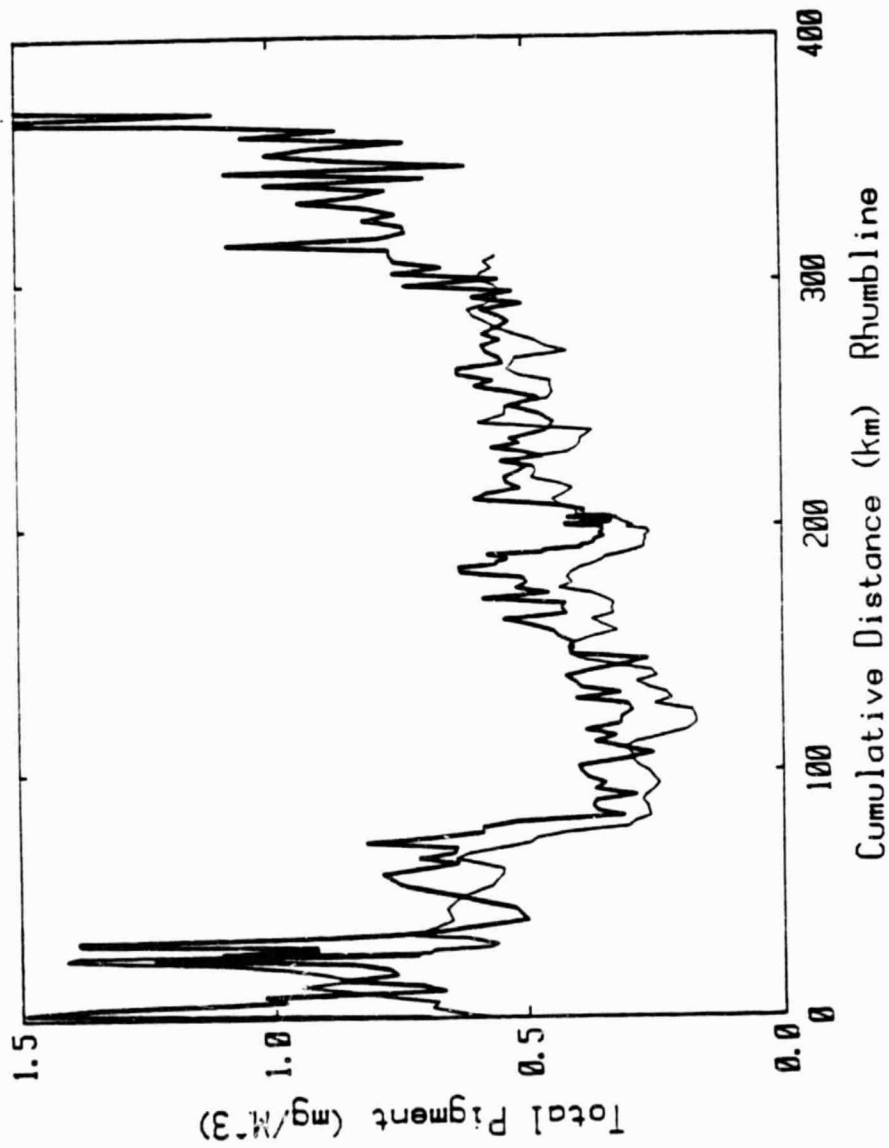


Figure 2-2. The Distribution of CZCS-derived (Heavy Line) and In Vitro Measurements (Light Line) of Chlorophyll Along a Ship's Track from Georges Bank to Delaware Bay

the middle of the track. CZCS-derived values of the water-leaving radiances were within 15 percent of those measured at the ship station (near the center of the track) at the time of the satellite overpass.

An example of pigment retrieval on the shelf at somewhat higher concentrations is provided in Figure 2-3. This track from the Gulf of Mexico is identical to that presented in Gordon et al. (1980), but was reprocessed using the current algorithms. It demonstrates that accuracies of ± 30 percent can be obtained with pigment concentrations as high as $5 \mu\text{g l}^{-1}$. Further improvements in the pigment retrieval accuracy over this range ($\sim 0\text{--}5 \text{ mg/m}^3$) are unlikely considering that the inherent error in the bio-optical algorithms for Case 1 waters appears to be about ± 30 percent.

Emphasis in algorithm development is now being placed on retrieval techniques for near-Case 2 waters. Preliminary retrievals in the Mississippi Delta have been within a factor of ± 2 using the algorithms described above. Considering their definition, one cannot foresee the existence of a universal Case 2 bio-optical algorithm, since phytoplankton do not dominate the optical properties of such waters. Instead, site-specific algorithms are to be expected. This poses no problem for MAREX since measurements from buoys are an integral part of the proposed program, and such measurements can be used to provide data to "update" the remotely sensed pigment concentrations if necessary. Also the assumption used in the atmospheric correction algorithm (see Appendix B) that the ocean is black at 670 nanometers is not valid in areas of high sediment suspension, indicating that another spectral band at longer wavelengths in the near infrared should be added to a follow-on CZCS.

Furthermore, in areas of little river runoff, Smith and Baker (1981) have presented a preliminary time series of CZCS imagery, along with a quantitative statistical analysis of each image, of the Southern California Bight, which clearly provide a synoptic view of this complex upwelling region. The sequence of qualitative images reveals significant temporal and spatial variation and a richness of detail which is impossible to obtain from shipboard data alone. These chlorophyll maps of the California upwelling regime from the Nimbus-7 CZCS were further used to develop an algorithm for estimating primary production from the satellite imagery (Smith, Eppley

ORIGINAL PAGE IS
OF POOR QUALITY

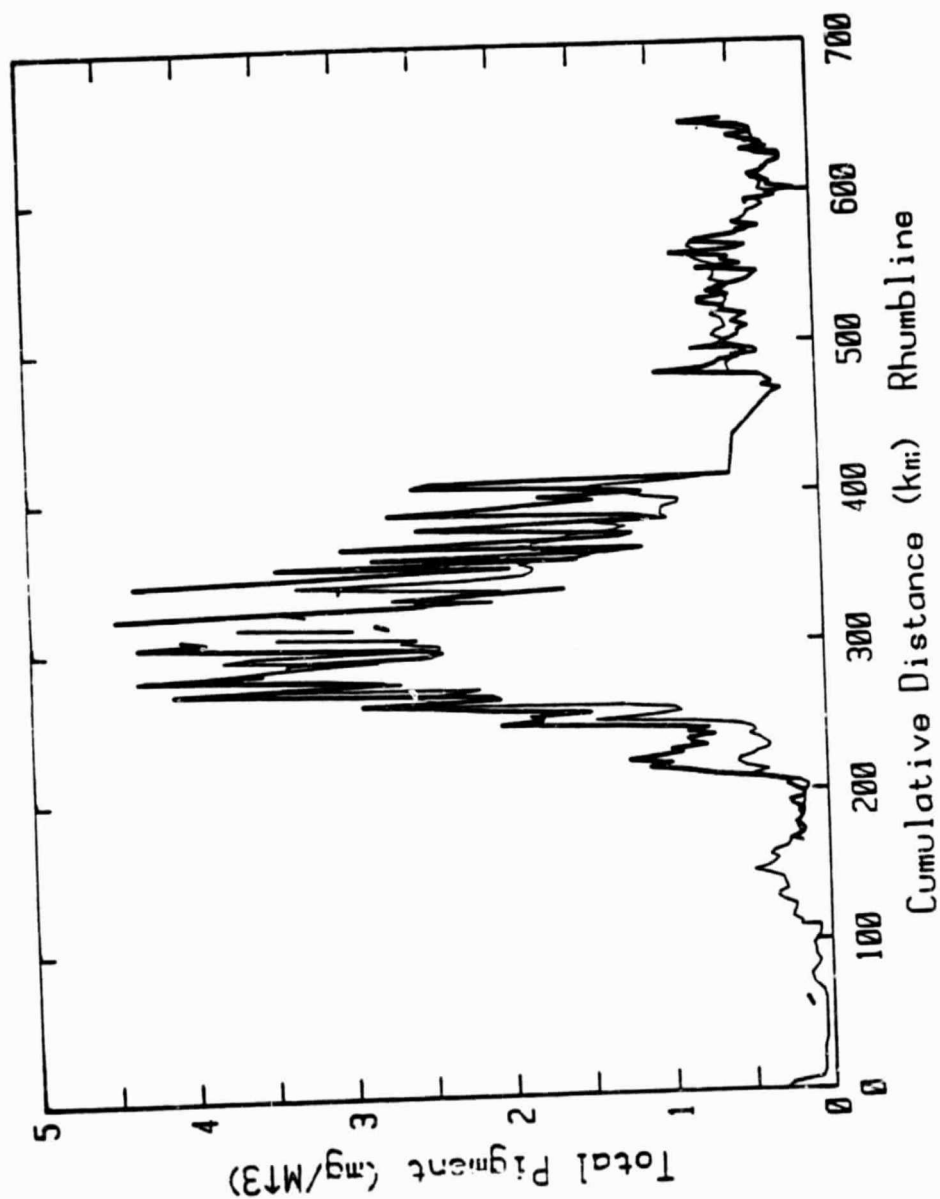


Figure 2-3. The Distribution of CZCS-derived (Heavy Line) and In Vitro Measurements (Light Line) of Chlorophyll along a Ship's Track from the Gulf of Mexico to the West Florida Shelf

and Baker, 1981) to be eventually extended to changes of fish populations (Smith and Eppley, 1982). Prediction of primary productivity from CZCS chlorophyll data is now limited by the high standard error or estimates associated with any attempt to link biomass to growth rates. Regression analyses are inherently non-causal (Walsh, 1971) and the same amount of productivity variance could be correlated with either changes in biomass or with changes in light and temperature.

The results of the CZCS program to date have been sufficiently convincing; however, a consideration is now underway for the flight of a newer generation instrument on the NOAA polar orbiting satellites in support of a large number of users. This early work clearly indicates that concurrent ship, buoy, airplane, and satellite data, with an appropriate sampling strategy, must be utilized to provide a more accurate assessment of coastal primary production on a regional basis. Once the algorithm for satellite sensing of chlorophyll on the shelf is updated, an extensive simultaneous time series of the world shelves can be obtained; during times of minimum phytoplankton loss, the satellite sensed time rate of change of surface chlorophyll can be used to estimate a lower bound of coastal primary production. Additional information is required, however, on both the depth distribution of phytoplankton and at time-space scales below the Nyquist frequency of satellite observations, i.e., ~2 to 10 days depending on cloud cover and ~2 km or twice the pixel length.

2.3 AIRCRAFT REMOTE SENSING

Restricted by cost and flight time to local areas, remote sensing by aircraft nevertheless fills a critical gap in the space-time sampling domain (Figure 2-1) between conventional measurements made from ships and those currently within the capability of satellite sensors. Parameters (Table 2-3) can be measured from aircraft platforms, such as salinity and chlorophyll fluorescence, that are at least a decade away from being technologically feasible from space. The two sensors that are particularly unique to aircraft platforms are laser (lidar) fluorosensors and microwave

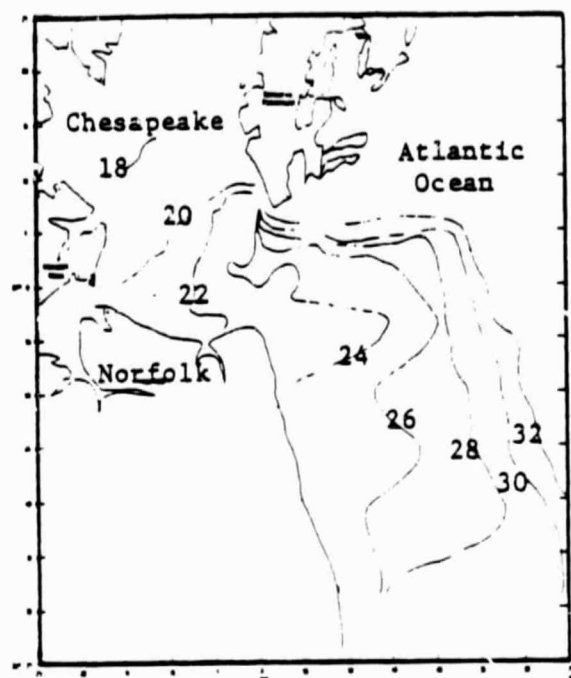
Table 2-3. Aircraft Remote Sensors Used in Marine Productivity Experiments

Name	Type of Sensor	Characteristics	Measurements
AOL	Laser (Lidar) Fluorosensor	Uses single-wavelength laser to induce fluorescence; measures emission in 40 channels; has vertical profiling capability	Fluorescence of chlorophyll <u>a</u> and other pigments; light attenuation; phytoplankton color group diversity
L-Band	Microwave Radiometer	Measures passive microwave radiation from water surface in single channel	Salinity (requires independent measurement of surface temp.)
PRT-5	Infrared Radiometer	Measures passive thermal radiation from water surface in single channel; commercially available	Surface temperature
MOCS	Multispectral Scanner	Measures backscattered sunlight in visible and near infrared spectral range; has 20 bands, 15 nm wide	Chlorophyll <u>a</u> in real time: suspended and dissolved matter that affects color
OCS	Multispectral Scanner	Has 10 bands in visible and near infrared spectral range; forerunner of CZCS instrument on NIMBUS 7 satellite; flown on NASA Lear Jet	Two-dimensional high-altitude imagery; maps of chlorophyll <u>a</u> and suspended sediments
IOS	Multichannel Spectrometer	Measures upwelling radiance spectra in 256 channels in the visible and near infrared range	Chlorophyll <u>a</u> by natural (sun-stimulated) fluorescence and broad band color effects; suspended sediments.

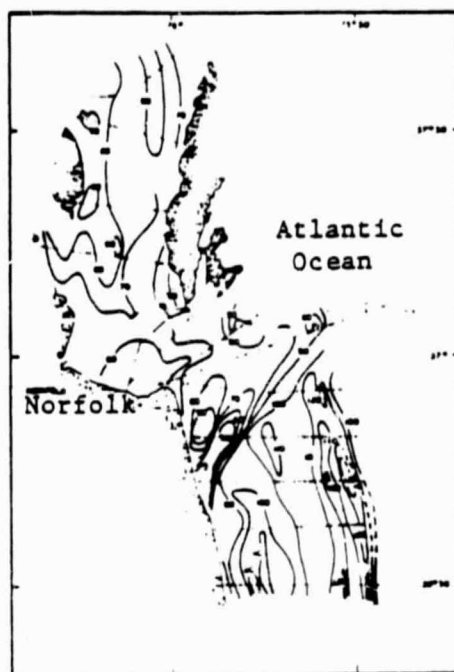
radiometers. Moreover, the resolution and spatial scales of these airborne sensors can provide ground truth and calibration data for the satellite sensors over wide areas, thus potentially extending the utility of the present generation of satellite instrumentation.

Laser fluorosensors are in a class known as "active" remote sensors because they provide their own source of energy. Laser pulses are fired into the water column from low flying aircraft and the induced emission spectrum is sensed in narrow spectral bands. The returning laser light varies as a function of backscatter from particulate matter within the ocean and as a function of absorption. Red shifted Raman backscatter from the water molecule itself is proportional to the number of water molecules accessed, or equivalently, to the penetration depth of the laser beam into the water. The Raman backscatter provides a direct measure of water clarity or turbidity. Further, the strength of the Raman signal can be used to correct fluorescent signals received from photopigments for spatial variations in optical transmission properties of water (Bristow et al., 1979; Hoge and Swift, 1981), thus eliminating the need for extensive surface truthing of water transmissivity. As with shipboard or moored fluorometers, the corrected chlorophyll a fluorescence signal centered at 685 nm is used to gauge chlorophyll a concentration.

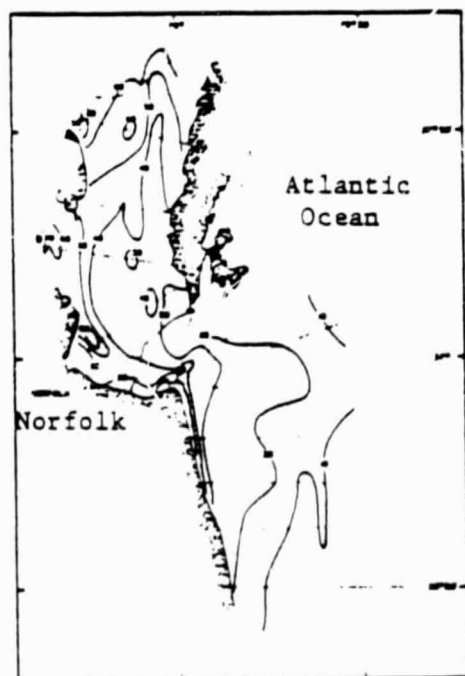
A measure of the relative abundance of different pigment classes or color groups of phytoplankton, such as the golden-brown species (diatoms and dinoflagellates), can also be made by using laser light of different frequencies to excite the photopigments (Figure 2-4). Through "time gating," the entire return emission spectra can be sampled separately in layers. Alternatively, a single band can be temporally measured providing detailed vertical distribution of a particular constituent. Unfortunately, chlorophyll a, the most useful photopigment in estimating phytoplankton dynamics, fluoresces at 685 nm in the red spectral region where the transmissivity in water is comparatively low. Therefore, the depth measurement of the 685 nm chlorophyll a fluorescence signal itself is especially limited to upper surface layer observations. Differential absorption of two or more laser wavelengths, however, has a good potential for allowing chlorophyll a measurements at depth throughout the optical layer of the ocean. Recently



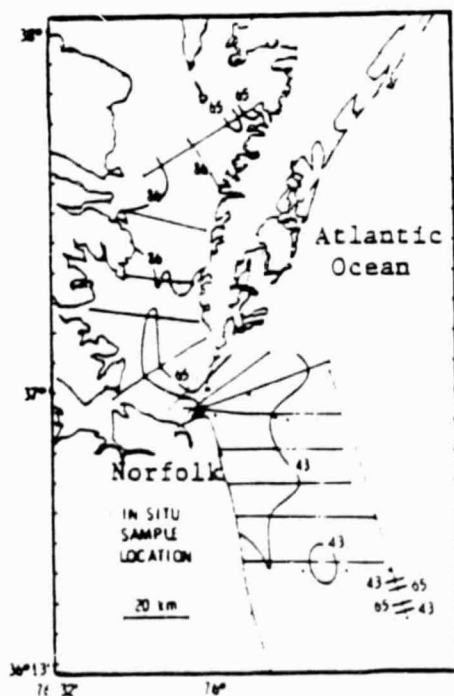
(a) Salinity



(b) Light Penetration



(c) Chlorophyll-a
Fluorescence



(d) Percent Golden-
Brown Species

Figure 2-4. Airborne Remote Sensor Mappings of the Lower Chesapeake Bay and Plume Made on June 23, 1980 (from NASA CP-2188, 1981)

reported temporal measurements of laser backscattered signals in connection with airborne hydrographic experiments (O'Neil, 1981; Hoge and Swift, 1980) have shown a reasonable capability of making these measurements with present state-of-the-art instrumentation and technology.

The microwave radiometers, classified as "passive" remote sensors, measure the natural microwave emission of the water surface. The emissivity of the water is a function of water temperature and conductivity, and hence, salinity. This technique has been developed to provide a remote measurement of water surface temperature and salinity with relative precisions on the order of 0.5°C and 0.5 part per thousand (ppt), respectively (Blume et al., 1981; Kendall and Blanton, 1981).

2.4 FLUOROMETER IN SITU SENSING

Over short time periods, spatial resolution of surface phytoplankton populations in local areas can now be reasonably well resolved by laser mapping of chlorophyll fluorescence in the path of an aircraft (Campbell and Thomas, 1981). The temporal resolution of this technique is poor, however. It lacks the ability to make routine biological measurements with depth, at time scales similar to physical variables currently measured with moored arrays of current, temperature, and conductivity sensors. As the first step towards a biological analog to a current meter (Carder, 1981), in situ fluorescence has been measured for a 2- to 3-week periods with Turner Designs model 10-005RU fluorometers, equipped with a high-pressure cuvette and housed in water-tight aluminum cases (Whitledge and Wirick, 1982).

These fluorometers were suspended within electromagnetic current meter arrays (Figure 2-5) on the shallow (30 m) shelf off Long Island, New York, during August 1977, September-October 1977, and April-May 1979. Water samples were continuously pumped through each fluorometer at approximately 0.6 min^{-1} , the fluorescence data were averaged for 20-minute periods, and telemetered in real-time ashore. Power to operate the fluorometers and reduce the output data was derived from the same large battery package and in situ data processor-telemetry system developed for the current meter arrays (Scott and Csanady 1976; Walsh et al., 1978; Beardsley et al., 1981).

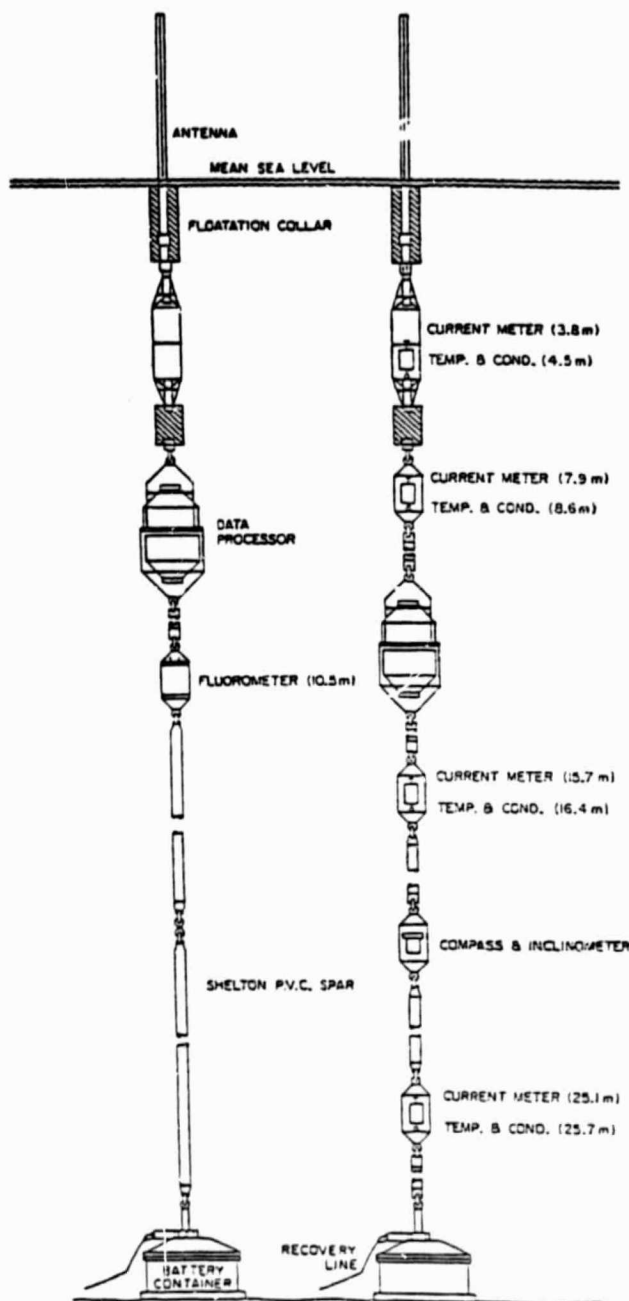


Figure 2-5. Initial Mooring Design for High-frequency Time Series of Chlorophyll from In Situ Fluorometers off Long Island

Chlorophyll concentrations were calculated from these time series (Figure 2-6), using shipboard calibration samples, collected with both sample bottles and pumps at each fluorometer depth. At the event time scale within these studies, chlorophyll biomass increased in response to wind-driven upwelling off the Long Island coast. With a seasonal change in stratification and prolonged nutrient addition by vertical mixing, diel variations of chlorophyll (Owens et al., 1980), shifted from a pattern dominated by tidal transport to one reflecting biological processes of nutrient uptake and grazing. This early work suggests that both resolution of the event scale (2 to 10 days) and the Nyquist sampling frequency required to resolve phytoplankton cell division can, in fact, be achieved with this approach.

The initial fluorometer arrays have been redesigned as self-contained units for taut-wire moorings to operate on the deeper shelf and in the waters of the upper continental slope. The large battery pack has been replaced with flash light batteries and the fluorometers now sample in a burst-mode to conserve power. The time-averaged fluorescence data is stored with an internal recording cassette logger for post retrieval analysis rather than line-of-sight telemetry ashore as in the past. With these new instruments, data collection could be continued for about 1 to 3 months unattended and may be extended for as much as one year with periodic battery and cassette changes.

Such an in situ fluorometry approach in either a moored or drifting mode, provides the necessary time-series records for comparison of long-term trends in the CZCS data set and for analysis of event responses within the shorter periods taken during combined aircraft-ship studies of areal distribution and rate processes. By incorporating all of these recent advances within a suitable MAREX sampling strategy (utilizing ships, buoys, aircraft, and satellites), it is now possible to significantly lower the variances in both estimates of phytoplankton abundance and population growth rates in the coastal zone. With the appropriate data sets, the future fluxes of carbon and/or nitrogen in the coastal and open ocean

ORIGINAL PAGE IS
OF POOR QUALITY

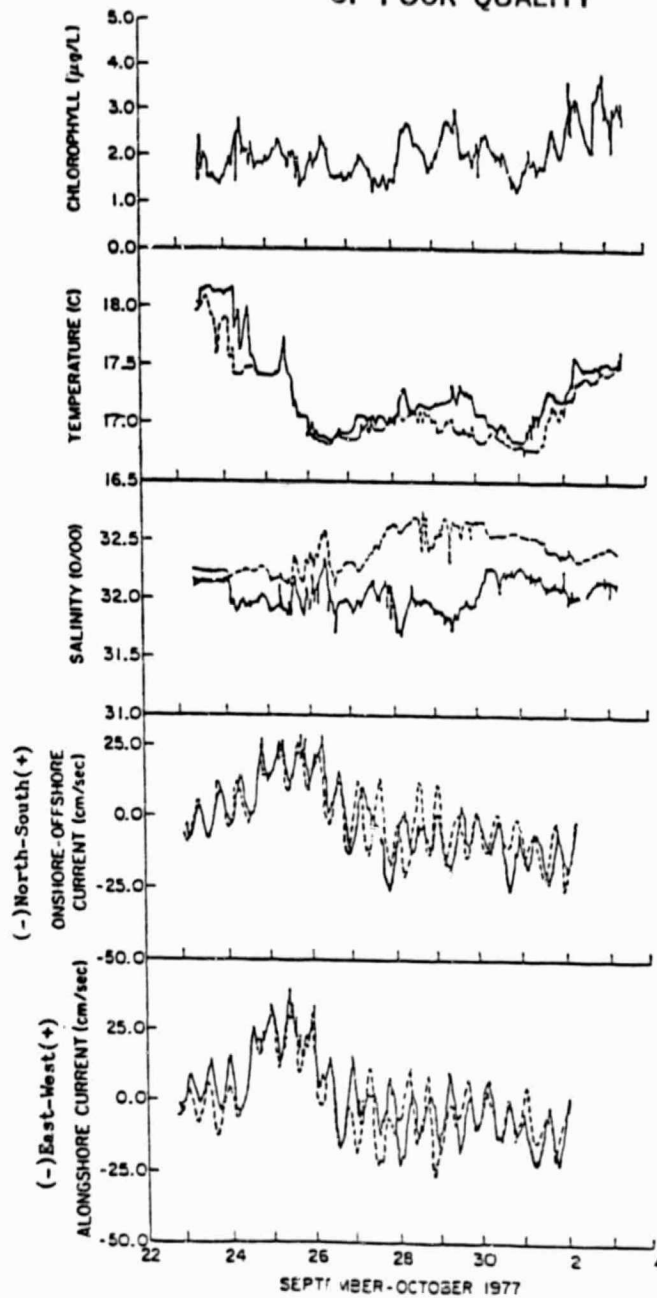


Figure 2-6. Time Series of Chlorophyll at 10.5 m between Temperature, Salinity, and Current Sensors at 8 m (---) and 16 m (- - -) During the 1977 Fall Bloom off Long Island

regions can then be addressed in the context of changes in coastal eutrophication, storage pools of CO_2 , and fishery yields at daily and decadal time scales.

SECTION 3. MAREX PROJECT PLAN OBJECTIVES

The objectives of the proposed MAREX project all center around processes controlling carbon and nitrogen fluxes in the sea, with particular emphasis on shelf transfer and recycling processes. Within this context questions can be grouped into three major areas of research:

- a. C/N waste disposal, which constitutes the necessary understanding for eventual applications of weather modification.
- b. Fisheries regulation.
- c. Specification of the assimilatory capacity of the sea.

3.1 C/N AND CLIMATE

Uptake of CO_2 during marine primary production (Table 1-1) is 10- to 20-fold that of the fossil fuel CO_2 released from anthropogenic sources each year, but not retained in the atmosphere (2.5×10^9 tons C yr^{-1}). Two major unknown questions exist:

- a. What areal and temporal changes of shelf production have occurred over the last 100 years since the industrial revolution?
- b. How much of the "missing" carbon of global CO_2 budgets is stored in ungrazed, slowly decomposing phytodetritus (Table 1-2)?

As a result of agricultural fertilizers, urban sewage, and deforestation, for example, the nutrient content of major rivers (e.g., Mississippi, Rhine, and Yantsze) is now 10-fold that of both the pre-industrial riverine condition and the presumably unmodified nutrient content found in slope waters.

In the form of fixed phytoplankton nitrogen, the ultimate fate of increasing loadings of anthropogenic dissolved nitrogen must be explored with an adequate time series of both satellite color sensors and moored fluorometers. Past measurement of nitrogen production, remineraliza-

tion, and exchange along food webs off Peru, the Mid-Atlantic Bight, in the Bering Sea, and within the Gulf of Mexico, suggest that large fractions of the organic matter produced on continental shelves must be exported to continental slopes (Walsh et al., 1981). The annual loss of organic matter from continental shelf ecosystems is far greater than in the open ocean (Table 1-2). If part of the loss of nearshore primary production has increased in those coastal zones where anthropogenic inorganic nutrient supplies have been consistently increasing since the industrial revolution, then burial and diagenesis of this material in slope depocenters, similar to the fate of particulate nitrogen in Lake Erie, could represent the missing BMTs of carbon in global CO₂ budgets.

As a result of colonial deforestation by 1850, subsequent farming, and present urban wastes, Lake Erie received an input of 1.6×10^5 tons N yr⁻¹ during 1966-67, of which a range of 5 to 50 percent was then thought to be of non-agricultural origin (Vollenweider, 1968; Sly, 1976). Between 1930 and 1970, moreover, the nitrogen content of western Lake Erie had increased by an order of magnitude to a winter-spring maximum of 30 to 60 $\mu\text{g-at N l}^{-1}$ (Burns, 1976), similar to the nitrogen content of the Mississippi River in 1970 (Walsh et al., 1981). By this time, phytoplankton numbers had increased 20-fold in the western basin (Leach and Nepszky, 1976) and the mean annual primary production of Lake Erie was $250 \mu\text{g C m}^{-2} \text{ yr}^{-1}$, over two- to four-fold that of the more oligotrophic Lakes Huron and Superior (Vollenweider et al., 1974), and similar to that of most continental shelves (Walsh, 1982).

The entire Lake Erie food web, from phytoplankton to fish species (Regier and Hartman, 1973), had changed as a result of this nutrient transient, yet as much as 1/3 of the annual carbon production was unconsumed and accumulating on the bottom of the lake in 1970-71 (Kemp et al., 1976). Estimates of sedimentation rate within Lake Erie at that time ranged as high as 1.50 cm yr^{-1} (Kemp et al., 1976), compared to a mean Holocene rate of 0.17 cm yr^{-1} (Sly and Lewis, 1972). Nitrogen loading to the sediments increased seven-fold between 1850 and 1970 (Kemp et al., 1974); between 1930 and 1970 the organic carbon and nitrogen content of the sediments doubled. Within the last decade, the amount of organic matter on the lake bottom may, in fact, have doubled

again (Fisher and Matisoff, 1982) as a result of additional nutrient loading.

Similarly, between 1850 and 1950, the nitrogen content of the Rhine River had only increased perhaps two-fold to $\sim 100 \mu\text{g-at N l}^{-1}$, with a second doubling by 1970. Over just the last decade, it has doubled again to $\sim 400 \mu\text{g-at N l}^{-1}$ (Van Bennekom and Salomons, 1981), for example, while that of the Seine (Y. Monbet, personal communication) also increased four-fold to $\sim 400 \mu\text{g-at N l}^{-1}$ from 1965 to 1975. The mean winter nitrate content of the North Sea shelf in the 1960s was also at least two- to four-fold higher off the Thames estuary, the Wash and the Rhine estuary than at the edge of the shelf (Johnston, 1973); the winter phosphate content off the Dutch coast has since doubled from 1961 to 1978 (Van Bennekom and Salomons, 1981). Indeed, as much as $350 \mu\text{g-at NO}_3 \text{ l}^{-1}$, ~ 10 -fold the concentration of NO_3 in deep slope water, is now found both in the Scheldt estuary and 10 km off the Belgian coast (Mommaerts et al., 1979). The annual production of the nearshore zone of the Waddensea has apparently increased from 80 to $240 \text{ g C m}^{-2} \text{ yr}^{-1}$ over 20 years (Postma, 1978) as a result of these nutrient inputs.

With respect to global impact of the changing nutrient input from these two boundaries of the shelf (land, shelf-break) and subsequent carbon fixation, the MAREX program would thus address the following questions:

- a. What is the relationship between estuarine outwelling and shelfbreak upwelling on the development, distribution and magnitude of the spring bloom of phytoplankton, both off an individual estuary and along an entire coastline?
- b. How far seaward and over what area does estuarine influence and contained pollutants extend? Are phytoplankton transported ungrazed across an entire shelf to the slope boundary?
- c. Can the land source of nutrients be distinguished from one estuary to the next with regard to degree of eutrophication of the estuary and consequent impacts on fishery resources in the estuary and on/over the adjacent shelf? (For example, as a result of flow and estuarine area, the Hudson estuary should

export more dissolved nitrogen and less chlorophyll than the Chesapeake.)

- d. What is the relative influence of shelf edge (upwelling) and other western boundary current intrusions (arm core eddies) on phytoplankton abundance, distribution, and metabolic activity; i.e., can the productivity of poorly sampled shelves be estimated from CZCS data and presumably known analogs of eastern and western boundary habitats?
- e. What is the evolution of a catastrophic event, such as the 1976 Ceratium tripos bloom in the Mid-Atlantic Bight? What is its origin, over what areas does it occur, and what are its impacts on the living marine resources? Would satellite temperature data have been useful in predicting the onset of the bloom?
- f. Are annual cycles of phytoplankton composition, distribution, abundance, and production generally repeated from year to year over a shelf area, e.g., from Cape Hatteras to Nova Scotia, within the southeast Bering Sea, or off Peru? Are changing patterns from one year to the next, e.g., the North Sea, representative of all seas? Has coastal production and organic carbon deposition increased over the last 10 years?
- g. What is the behavior of fish (avoidance or attraction) with respect to natural and eutrophic features? How much of the primary production is passed up the food web in a local area? Can chlorophyll accumulation at shelf fronts, e.g., the Irish and Bering Seas, be detected within CZCS overflights on a routine basis?
- h. How much of the primary production is composed of algal species, poorly used by higher trophic levels, e.g., Phaeocystis blooms? What is the effect of seasonal changes in cell size on chlorophyll retention time within the surface layer?
- i. How can the distribution of hydrographic and nutrient properties be related to phytoplankton abundance, distribution,

and type as indicated by winds, ice, and temperature data also derived from concurrent satellite observations?

3.2 FOOD WEBS AND FISHERIES

In recent years a number of statutory mandates concerning fisheries in the U.S. have been legislated for which ocean color information from the CZCS can play an important role. For example, (Public Law 94-265) the Fishery Conservation and Management Act of 1976 charges the Secretary of Commerce with the management of fishery resources within the contiguous fishery conservation zone beyond the territorial sea and within 200 nautical miles of shore. To effectively discharge management responsibilities under the Act, the Secretary must also conduct "a comprehensive program of fishery research," which must include reliable information on the status of living marine resources and their environment. In addition, the Marine Mammal Protection Act of 1972 (Public Law 92-522) involves improving understanding of the ecology of marine mammals, for which the importance of chlorophyll fronts has only recently been established.

The National Ocean Pollution Research, Development, and Monitoring Planning Act of 1978 (Public Law 95-273) has generated monitoring requirements for many marine environmental indices. Many of these indices are amenable to observation by ocean color change for investigation of fishery/pollution interactions and impact studies. There are also a number of existing and potential international fisheries agreements and commissions involving the U.S. which require that the U.S. provide reliable information of fishery resources and their environment. Selected examples of these are the International North Pacific Fisheries Commission, Inter-American Tropical Tuna Commission, International Whaling Commission, and International Council for Exploration of the Seas (ICES).

In addition, the U.S. is a leading participant in many international fisheries research programs. For example, the international Scientific Committee on Ocean Research (SCOR) Working Group-67 is proposing an international program on Ocean Science Related to Living Resources which is intended to study similar fishery complexes over a multi-year period

in areas as diverse as California, South Africa, Japan, New Zealand, Spain, Peru, and Argentina. The regions have fish specie complexes containing anchovy, sardine, mackerel, and hake, all contributing important fisheries which undergo unusual and drastic population crashes and expansions which have great economic effects. Fishery scientists need to understand the mechanisms involved in these changes, which are believed to be due to a combination of physical and biological environmental effects on fish survival.

CZCS data can play an important role in fishery research and fishery management by providing ocean color measurements for use in evaluating environmental effects on the distribution, abundance, and availability of fishes for use in the assessment of the status of fish populations. The greatest immediate success in the application of CZCS-type measurements to marine biology is in those cases where there is sufficient understanding of the biology and oceanic phenomena to identify key oceanographic processes (such as ocean fronts and upwelling) that substantially influence the well being, behavior, abundance, and distribution of biota. Ocean color data can also play a significant role in the resolution of subtle scientifically complex problems in marine ecosystems such as the long-term impact of pollution on resource populations. CZCS data are also utilized in fishery aid products for use by commercial and recreational fishermen and other users in the fishing community.

MAREX investigations for which CZCS measurements may provide essential oceanographic data are:

- a. The determination of year class strength and recruitment, where information is required on marine habitat characteristics, e.g., the distribution of phytoplankton and other prey items critical in the survival of early life stages of fishes.
- b. Migration studies of highly mobile species (such as tuna, billfish, and marine mammals) where migration patterns are linked to ocean features, such as color boundaries which may be monitored over vast areas remotely from space by the CZCS.

- c. Fishery forecasting efforts which utilize ocean color distribution to predict stock availability and fish stock assessment studies where models incorporate oceanographic/environmental conditions.
- d. Fishery/pollution interaction and impact investigations where color imagery shows waste disposal sites and estuarine outflows.
- e. Energy budget/ecosystem modelling approaches for estimating potential fish stock production in upwelling vs. outwelling systems where ocean color is correlated with ship primary production measurements.
- f. Fishery-related habitat management where quantitative environmental information is required, e.g., changes in wetland use as detected and quantified by color imagery.
- g. Marine mammal ecosystem studies, involving food web analyses as traced by color measurements of habitats.
- h. Temporal and spatial monitoring of areas of economic interest between cruises for following catastrophic events (e.g., exceptional cold or exceptional water runoff) where the response in phytoplankton can be seen by satellite color imagery.
- i. Studies where ocean color data are received in quasi real time by scientists at sea for use in planning research operations and by extrapolating in time and space the point source measurements made aboard ship, i.e., a combination of the other MAREX platforms in a field study.

3.3 WASTE DISPOSAL

Whether looking at long-term variability, short-term meteorological, or man-induced events, it is essential in terms of the MAREX objectives, to be able to identify principal water mass and frontal systems where biological populations interact in the sea. Characteristics such as

temperature, salinity, sediment, and chlorophyll concentrations assist in distinguishing one water mass from another. They are easily observed using satellite, moored, and airborne sensors, making it possible to monitor climatic change or seasonal development of the distribution and magnitudes of spring blooms of phytoplankton. Surface fronts concentrate both phytoplankton and pollutants (including those materials from oil spills and waste dumping--two currently controversial issues requiring documentation as to their concentration, dispersion, and impact on aesthetics, production, and value of resources).

Within a water mass, day-by-day assessments of the Lagrangian properties of the shelf or open sea are necessary for understanding the transport of organisms, pollutants, or their interactions between polluted water masses and nonpolluted water masses. For instance, in the case of dumping at the 106-mile Deep Water dumpsite, it would be desirable to follow the movement of the materials as they are mixed within the original water mass dumped material, sludge, acids, or spoils. Knowledge of frontal and eddy positions is also essential for determining the position of future dump sites. Access to high-resolution imagery will enable real-time inspection of the dynamic environment, biological character, and certain physical properties of a dumpsite. It will also aid dumpers (1) to target quadrants that, at the time, are not occupied by water having significant biological activity and (2) to avoid water masses such as warm core rings and other entrainment features, should that be desirable. Furthermore, use of the MAREX products will permit environmental managers to maintain a real time assessment of catastrophic events in which materials, detectable at the surface, can be tracked over large geographic areas through time. Immediate use of such information will make it possible to provide advice in regard to the effects of spills, determine directions that contaminated waters are moving in, and clean up spilled materials.

SECTION 4. EXPERIMENTAL DESIGN

4.1 PREVIOUS STUDIES

Recent oceanographic studies have utilized part of the proposed MAREX sensor array to address limited aspects of local marine productivity on the east coast of the United States. For example, Superflux, a joint NASA-NOAA study, was a prototype experiment at the mouth of the Chesapeake Bay to demonstrate the use of remote aircraft sensing in studying the effects of estuarine outwelling on shelf ecosystems (Figure 2-2). This project consisted of three interactive aircraft-ship deployments conducted during 1980 to study the Chesapeake Bay plume's seasonal interaction with the adjacent continental shelf region (Campbell and Thomas, 1981). A second nearshore experiment, conducted on Nantucket Shoals in May 1981, used the same set of remote sensors (Lidar and microwave radiometer) to investigate the coupling of biological and physical processes in a topographically controlled upwelling system. The aircraft, interfacing with ships, provided near real-time data to enable NASA-, NOAA-, and DOE-supported investigators to update sampling plans for the shipboard measurements of biological rate processes (primary production, grazing, etc.). A series of current meter moorings were deployed in both experiments to measure the advective and diffusive fluxes. The synopticity provided by the aircraft sensors, both of physical and biological properties, together with measurements of vertical properties, chemistry, and biological rates using conventional shipboard technique over the appropriate time scales, will permit a more complete analysis of the dynamics of both the Chesapeake Bay and Nantucket Shoals local system.

Off the U.S. west coast, fishery programs which now depend mainly on the Coastal Zone Color Scanner involve monitoring of the distribution of the pelagic fish spawn and correlating the spawn with temperature and color imagery of an 85,000 square mile region of the California Current. This research allows delineation of preferred habitats for anchovy spawning, survival, and recruitment. Color imagery shows areas of high productivity and convergence, and allows water type identification both

synoptically and over the entire spawning ground. Water clarity measured by the CZCS in conjunction with acoustic tracking investigation of albacore has also allowed fishery scientists to demonstrate causal mechanisms involved in the aggregations of albacore tuna associated with ocean fronts and boundaries. In an application mode, location of ocean color boundaries detected by the CZCS contributes a useful guide to fisherman. This information is now being distributed by NASA's Jet Propulsion Laboratory (JPL) in cooperation with the National Marine Fisheries Service and National Weather Service.

Farther offshore, an NSF-funded study of warm core eddies, shed from the Gulf Stream, is now using CZCS color imagery to monitor, before, during and after cruises, the positions, trajectories, and chlorophyll content of low-chlorophyll boluses within slope water. Another study of mid-Atlantic slope/shelf interactions, Shelf Edge Exchange Processes (SEEP) funded by DOE, involves the use of meters, thermistor chains, sediment traps, and in situ moored fluorometers to study the seasonal import of shelf organic carbon to the bottom of the continental slope. The MAREX experimental design will be the first, however, to use a combination of shipboard rate measurements and moored fluorometer-aircraft time series to interpret the CZCS imagery as a data set of dynamic biological variables from each major continental shelf rather than as a corroborative snapshot of the physical properties of a local water mass.

4.2 MAREX SHELF STUDIES

As a function of latitudinal changes in wind forcing, and geographic differences in shelf width, bottom topography, and human population centers, both the anthropogenic and natural nutrient inputs, as well as the annual primary production, of U.S. shelves exhibit a wide range (Table 4-1). Within North America, the nitrate content of the Mississippi River has at least doubled to $\sim 150 \mu\text{g-at NO}_3\text{l}^{-1}$ during spring floods over the past 10 years, while mean concentrations have increased from $\sim 40 \mu\text{g-at Nl}^{-1}$ in 1905 (Gunther, 1967), in 1935 (Riley, 1973), and in 1965 to $\sim 80 \mu\text{g-at Nl}^{-1}$ in 1980 (Walsh et al., 1981). Data for other eastern U.S. rivers which drain heavily populated areas, such as the Ohio (Wolman, 1971), Potomac and Susquehanna (Carpenter et al., 1969), Delaware (Kiry, 1974), and Hudson (Deck, 1981), suggest that their

Table 4-1. Variability in Nitrogen Inputs and Subsequent Primary Production on American Shelves

U.S. Shelf Region	Shelf Width (km)	N Source Anthropogenic or (Natural)	Primary Production ($\text{g C m}^{-2} \text{ yr}^{-1}$)
West Florida	150	(Loop Current)	30
Texas	125	Mississippi	100
Georgia	100	Altamaha/Savannah	150
Alaska	600	(Bering Slope)	200
California-Oregon	15	(Upwelling): Sewage outfalls	250
New York-New Jersey	100	Hudson/Delaware	300
Massachusetts	125	(Georges Bank)	450

nitrogen content ($<70 \mu\text{g-at NO}_3\ell^{-1}$) has also increased over the past 25 to 50 years from sewer inputs, agricultural fertilizers, and nitrate release to groundwater after deforestation (Likens et al. 1978). The White's Point Sewage outfall off Los Angeles, for example, has a daily discharge to the Southern California Bight, which is 1 percent of the flow of the Rhine and contains $\approx 2500 \mu\text{g-at NH}_3\ell^{-1}$. Other U.S. rivers which drain areas of low populations in the south and west (e.g., the Columbia (Park et al., 1972), the Yukon (W. Reeburgh, personal communication), and the MacKenzie (Van Dennekorn and Salomons, 1981) rivers) contained 10-fold less inorganic nitrogen ($<7\text{-}10 \mu\text{g-at N}\ell^{-1}$) before 1970 than the rivers discussed in previous sentences. However, the nitrate content of at least the southern region rivers, e.g., the Altamaha (Walsh et al., 1981) and Pamlico (Hobbie et al., 1975), is now $\geq 30 \mu\text{g-at NO}_3\ell^{-1}$. Primary production within the Altamaha River plume is as high as $550 \text{ g C m}^{-2} \text{ yr}^{-1}$ e.g., more than Georges Bank (Table 4-1), while those of the Mississippi (Thomas and Simmons, 1960; Fucik, 1974) and Hudson (Malone and Chervin, 1979) river plumes ($250\text{-}350 \text{ g C m}^{-2} \text{ yr}^{-1}$) are more than the Bering Sea.

To specify the areal extent and fate of production from anthropogenic and natural sources of nutrients, the MAREX program proposes to assess the increase in phytoplankton biomass per unit area over a specific increment of time as one measure of primary productivity, i.e., the rate of change of biomass on these shelves (Table 4-1). This approach assumes that there is no competing process, such as the removal of newly produced phytoplankton biomass by herbivore grazing or the dispersal of a unit or patch of phytoplankton by advective currents. In most parts of the ocean this assumption is rarely met, with perhaps the shelf spring bloom as an exception; hence, additional experimental and modeling techniques will also be used within MAREX to determine and predict regional primary production.

The experimental approach, of course, entails subsampling a parcel of water from a ship (and, hence, include the errors associated with plankton patchiness previously discussed) and incubating the water sample with ^{14}C to determine instantaneous rates of photosynthesis per unit phytoplankton biomass. These rates are then extrapolated to give

daily rates of primary production. As discussed, the accuracy of the ^{14}C method for measuring primary productivity in nutrient-poor, open-ocean regions recently has been questioned; research on assessing error for these regions is currently ongoing. In coastal waters, the ^{14}C method is representative of the actual rate of carbon fixation. Due to the great spatial and temporal variability, however, large errors in primary production estimates exist in these waters where undersampling in a heterogeneous environment exists. This situation will be resolved with the MAREX biomass data set.

A second historical approach for determining primary productivity has been through mathematical models, ranging from single process models of photosynthesis through ecosystem simulation with complex coupled biological-physical numerical modes. These models all share a common parameterization of primary production as some function of an initial concentration of phytoplankton biomass. Early models of primary production over Georges Bank, an important commercial fishing ground, included the concept of regulation of photosynthesis by light and nutrients; these models were limited by the state-of-the-art view of photosynthetic regulation (Riley, 1946).

The utility of the more sophisticated recent models in predicting regional primary productivity is still largely hindered by the current meager knowledge of the coupling of physical dynamics with biological processes on the appropriate time and space scales. MAREX proposes to measure the temporal change of biomass and productivity at 1 km intervals over at least two years, as frequently as possible on those continental shelves within the Mid-Atlantic Bight, the Georgia Bight, the Gulf of Mexico, the California Current, and the Bering Sea (Table 4-2). With this comparative information, the fate of nitrogen and carbon on U.S. and perhaps world shelves can be specified, with respect to the MAREX objectives involving CO_2 sinks, fish yields, waste disposal, and anthropogenic nutrient stimulation.

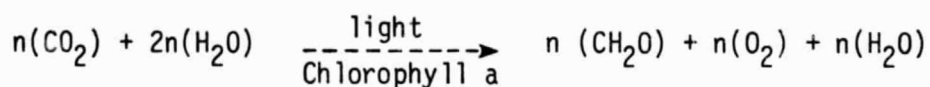
4.3 RELIABILITY OF INDIVIDUAL MEASUREMENTS

Recent advances in the basic understanding of photosynthesis and the modulating role of environmental parameters on phytoplankton

Table 4-2. MAREX Biomass/Productivity Experiments in 1987-89

	Ship Measurements	Moored Fluorometer	Drifting Fluorometer	Aircraft Sensor	Ocean Color Imagery
Local Area-Shelves					
Mid-Atlantic Bight	X	X	X	X	X
Georgia Bight	X	X	X	X	X
Gulf of Mexico	X	X	X	X	X
California Current	X	X	X	X	X
Bering Sea	X	X	X		
Local Area-Slopes					
Northeast Atlantic	X		X	X	X
Gulf of Mexico	X		X	X	X
Northwest Pacific	X		X		
Global Area-Shelves					
North Sea	X				X
Barents Sea					X
S. China/Japan Seas	X				X
Arabian Sea					X
West African Shelf					X
Patagonian Shelf	X				X
Peru-Chile Shelf	X				X
Timor/Arafura Seas					X
Global Area-Slopes					
Southern Ocean	X		X		X

photosynthetic rates, now make feasible the extrapolation of rates of primary production, with confidence limits, from shelf phytoplankton biomass. The most commonly used measure in oceanography of phytoplankton biomass is chlorophyll a concentration. The photosynthetic process, the basis of primary production can be specified by



where CO_2 is carbon dioxide, H_2O is water, (CH_2O) represents a primary unit of photosynthetically fixed organic carbon, and O_2 is molecular oxygen. Photosynthesis is comprised of two basic components: a photochemical (or so-called light) reaction in which light energy is trapped by chlorophyll and converted into biochemical reducing potential; and an enzymatic (or so-called dark) reaction in which the biochemical reducing potential is used to synthesize organic carbon.

The process of photosynthesis is characterized by a three parameter functional response to light intensity (Figure 4-1) where α describes the light-limited photochemical portion of the reaction, P_m describes the light-saturation or enzyme rate-limited portion, and β describes a photo-inhibition effect experienced at very high light intensities.

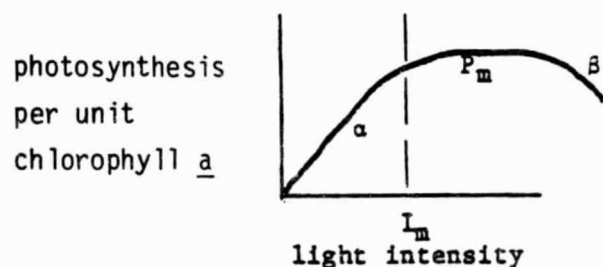


Figure 4-1. Functional Response of Photosynthesis to Light Intensity

Recently, theoretical upper limits have been determined for the two major components of photosynthesis: α and P_m . Both parameters can be specified as functions of chlorophyll a with α as carbon fixed per chlorophyll a per unit light intensity per time, and P_m as a maximal rate of carbon fixed per chlorophyll per time. Based on the well-specified maxima quantum yield (amounts of energy fixed in carbon bonds per quantum of light energy absorbed by chlorophyll), the theoretical

upper limit for α is $0.115 \text{ g carbon [g chlorophyll]}^{-1} \text{ h}^{-1} [\mu\text{E m}^{-2} \text{ s}^{-1}]^{-1}$ (Platt and Jassby, 1976). A theoretical upper limit for P_m of $24 \text{ g carbon g chlorophyll}^{-1} \text{ h}^{-1}$ has been calculated based on the turnover rates of photosynthetic units (Falkowske, 1982). A large suite of both laboratory and field data for phytoplankton and higher plants document empirical confirmation of these values as upper limits (cf., Malone and Neale, 1981).

These theoretical maxima are important for remotely sensed determinations of marine primary productivity because they place an upper bound on primary production calculations based on color scanner chlorophyll concentrations. Specific environmental conditions including temperature, nutrients, light intensity, and light history set the actual lower values for computing instantaneous primary productivity rates from biomass. Results of research over the last several years on phytoplankton physiology have advanced our understanding of the effects of temperature, nutrients, and both present light intensity and recent light history on photosynthesis. These results provide mechanisms for assigning realistic values within the theoretical maximal rates for primary productivity per unit of chlorophyll biomass sensed by buoys, aircraft, and satellites.

With the availability of other remotely sensed environmental data, e.g., ocean temperature, incident light intensity arriving at the sea surface, wind stress (Tables 2-2 and 2-3), the precision for resolving instantaneous rates of primary productivity can be further enhanced. Biological, enzyme-mediated reactions exhibit a temperature dependency which is often expressed by the Arrhenius equation for temperature regulation of a chemical rate reaction

$$\ln k = -E (RT)^{-1} + C$$

where k is a rate constant in units of t^{-1} , t is time, E is a temperature characteristic $(\text{calories mole})^{-1}$, R is the universal gas constant $(\text{calories } ^\circ\text{K}^{-1} \text{ mole})^{-1}$, T is absolute temperature (degrees Kelvin), and C is a constant. The maximal photosynthetic rate, P_m , is enzymatically determined, and hence, is affected by temperature; this contrasts with

the light-limited reaction, which is temperature independent. Figure 4-2 shows an Arrhenius plot for temperature dependence of P_m ; the dramatic decrease in photosynthesis at extremely high temperatures depicts high-temperature inactivation of enzyme activity. The genetic composition of the phytoplankton assemblage in a subregion of the ocean will affect the specification of a particular environmental effect, but the general functional form and direction (sign) of an environmental effect is universal. Information on temperature will thus provide empirical limits for primary productivity. Simultaneous remote sensing of ocean temperature will obviously increase the accuracy and precision of remotely sensed primary productivity estimates.

Nutrient availability, specifically of nitrogen, modulates primary production in two ways: a lack of nitrogen causes a decrease in chlorophyll concentration per cell and, hence, decreases the potential of a phytoplankton assemblage to increase in biomass; nitrogen limitation also causes a decrease in the efficiency of both α and P_m for the persisting chlorophyll. In some U.S. coastal areas dominated by upwelling events (Table 4-1) and in open ocean regimes with strongly divergent circulation, surface temperature is highly correlated with nutrient concentration. Figure 4-3 shows a relationship between surface temperature and nitrate in 10° longitudinal bands along the west coast of North and South America. For these regions the empirical relationship between low surface temperature and high nutrient provide limits for specifying the magnitude of the nutrient modulation of primary productivity. In other regions of coastal outwelling, shipboard information on nutrient inputs will still be required in conjunction with salinity information from aircraft over flights; within the next decade it may be feasible to measure nutrients from moored sensors as well, e.g., with specific ion electrodes, lasers, or wet chemistries.

Vertical mixing in the upper ocean affects the distribution of phytoplankton in context of both nutrient resupply and the vertical light intensity gradient. Vertical mixing thus has an additional impact on primary production by determining the amount of time that a cell resides at light intensities greater than I_m (e.g., P_m) and at intensities less than I_m (α). Figure 4-4 shows the results of a Markov

ORIGINAL PAGE IS
OF POOR QUALITY

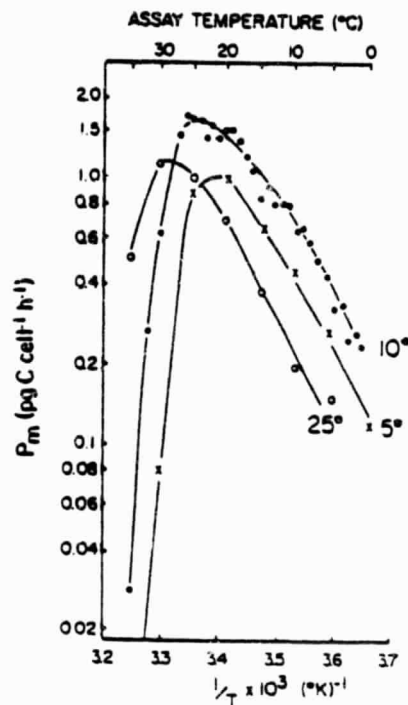


Figure 4-2. Arrhenius Plots of Light-Saturated Photosynthetic Rate of *Phaeodactylum tricornutum* Previously Grown at 5°C (x), 10°C (●) and 25°C (o), from Li (1981)

ORIGINAL PAGE IS
OF POOR QUALITY

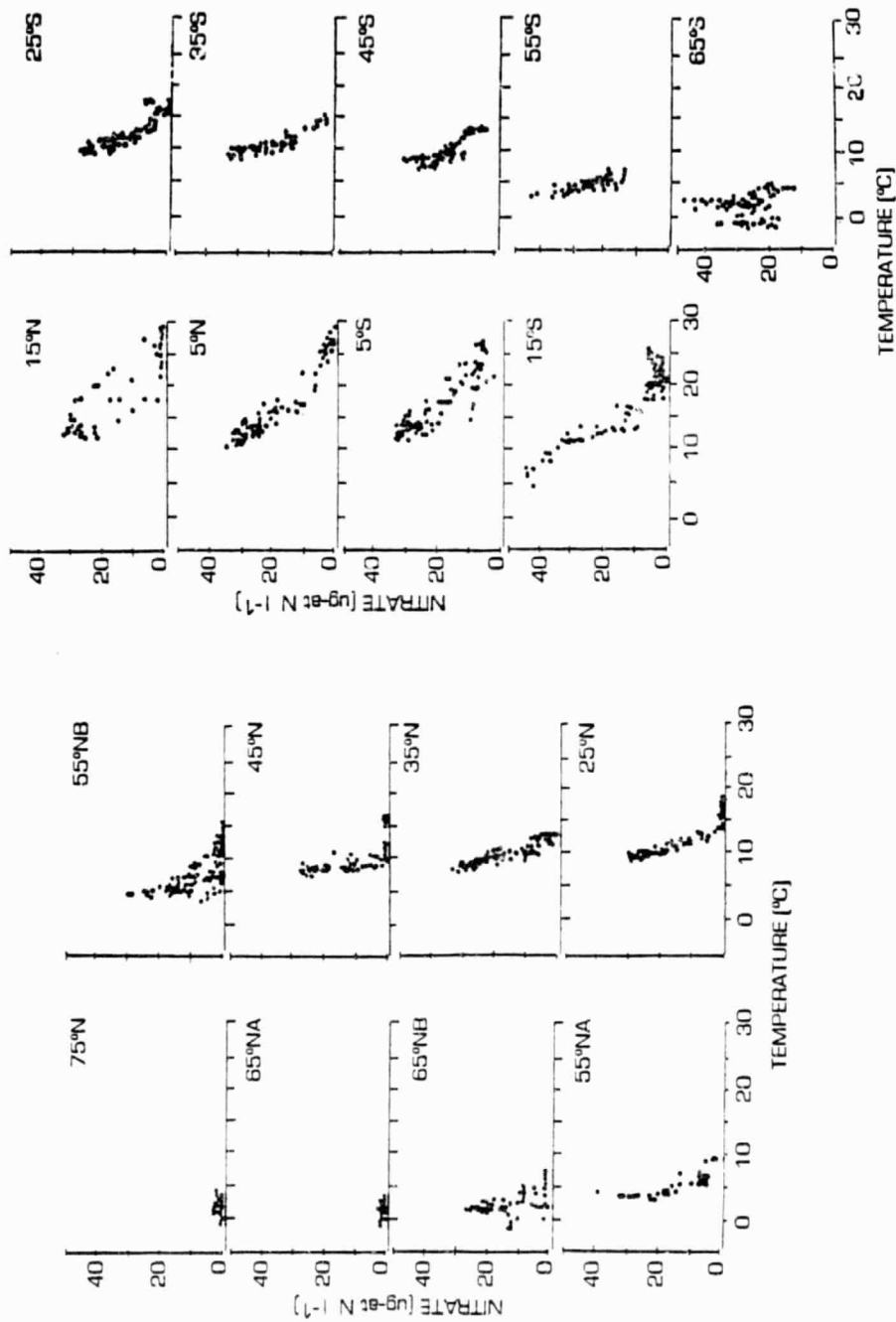


Figure 4-3. Scatter Diagrams of Temperature Versus Nitrate along the West Coast of America, from Zentara and Kamykowski (1977)

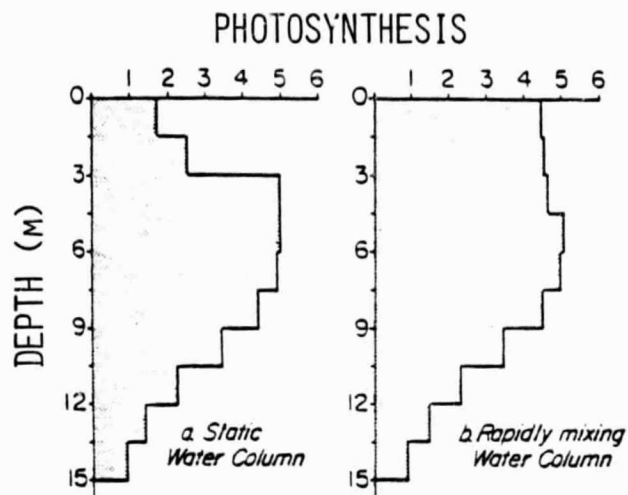


Figure 4-4. Depth Profiles of Instantaneous Photosynthesis Simulated by Random Walk Model of Phytoplankton Circulation With Time-Dependent Photosynthetic Rate at High Irradiance

simulation of primary production for a static water column vs. a dynamic rapidly mixing water column. Phytoplankton following a complex trajectory and experiencing a wide range of light intensities in the mixing water column are capable of a high level of primary productivity. Scatterometer wind stress measurements, coupled with increasing sophistication in turbulence models for the upper mixed layer, will provide information on the intensity and effect of vertical mixing.

Finally, the rates of vertical mixing have a third implication for calculating primary productivity from chlorophyll a concentrations: specifically by the influence of light history on the molecular organization of chlorophyll into discrete functional photosynthetic units. Phytoplankton grown at low light intensities (less than I_m) tend to have large functional photosynthetic units with 800 to 1400 chlorophyll molecules, while cells grown at high light intensities (greater than I_m) tend to have smaller units of 400 to 600 chlorophyll molecules. Although the larger units are more efficient per unit at low intensities than the smaller units, the individual chlorophyll molecules are actually less efficient in the larger units. Figure 4-5 indicates the trend in the value of α as a function of the size of the functional photosynthetic unit. Changes in the size of these units and concomittant changes in values of α are predictable as a function of varying light intensities with time (Falkowski, 1981; Marra, 1980).

The results of recent research on the control of photosynthesis by these environmental parameters--temperature nutrients, light intensity, and light history--all give improved accuracy to primary production models. Ongoing research in these areas will continue to improve our abilities to determine instantaneous shelf primary production from single measurements of remotely sensed data on phytoplankton chlorophyll concentration, oceanic optical properties, temperature, and wind stress. Because the wind event source of habitat variability is present on the shelves and not the open ocean (Walsh, 1976), however, the MAREX experimental design must certainly resolve the wind event frequency (3 to 5 days) and hopefully that of cell division (0.25 days) in order to detect causal changes in primary production.

ORIGINAL PAGE IS
OF POOR QUALITY

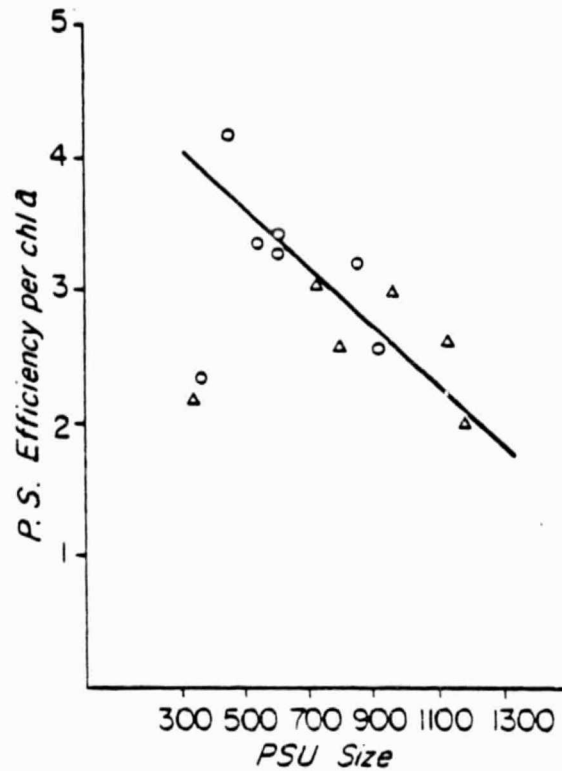


Figure 4-5. Photosynthetic Efficiency (α) Per g Chlorophyll as a Function of PSU (Photosynthetic Unit) Size for Marine Phytoplankton, from Perry et al. (1981)

4.4 FREQUENCY OF SAMPLING

U.S. fishery needs for future ocean color measurements are primarily in the productive coastal waters within the 200 mile economic zone surrounding the continental U.S., islands, and territories (Table 4-1). Mid-ocean regions, where U.S. distant water fisheries are located, and through which highly migratory fish and mammals move during migration to coastal waters are also important. The frequency of required satellite coverage and information will vary depending on location and perhaps to some extent on season. Generally 2-day coverage will be required in coastal/local waters and 3- to 5-day coverage for most mid-ocean applications. Global coverage may be needed on the order of every 15 to 30 days. In addition to measurements made from satellites, fishery research studies will generally require oceanographic data measured from ships, buoys, and aircraft.

Unfortunately, it has not been possible to obtain CZCS-type measurements of the global oceans on anything close to a daily basis. On any given day, the major fraction of our watery planet is obscured by clouds. A qualitative idea of realizable sampling characteristics has been gleaned by the MAREX working group members from screening a few time sequences of CZCS data for which regular sampling was attempted. This experience suggests that in a month of data collection, useful data will be obtained on several days within randomly distributed clear-sky domains which are a few hundred km in extent, and less frequently >1000 km in extent. Of the nominal 2 hours of Nimbus-7 CZCS coverage taken and recorded per day, an average of approximately 30 to 40 percent is rejected and not processed due to total cloud cover (no significant open water areas).

In sum, our experience to date suggests that global CZCS coverage would yield, on average, between 10 (at the equator) and 20 (at 40 degrees N) usable images per month. This figure represents the required sampling interval of every 1.5 days, for a given 1000 km x 1000 km ocean domain, with the majority of usable data in patchy subscenes of typically a few hundred km in extent, and with an occasional clear view of most of the domain in one image. Coverage frequencies will assuredly fluctuate seasonally (and regionally) around these nominal estimates; coverage

gaps of 2 to 3 weeks are likely to occur several times per year, with less frequent gaps of longer duration. In winter, low sun elevations will cause sampling voids of several weeks to a few months (increasing with latitude) at latitudes above 40 degrees. These characteristics assume that a single CZCS-type instrument is operated in a Nimbus-7 orbit on a global basis (for the approximately 25 percent of each orbit with suitable solar elevation).

Clearly the present data base collected with the Nimbus-7 CZCS is inadequate to apply to the global mapping of primary productivity, except in a qualitative sense. It is limited both in terms of sampling frequency and in terms of concurrent oceanographic experimental data necessary to bridge the interpretive gap from phytoplankton pigment distributions to net primary production. Adequate data do exist in certain shelf regions (Table 4-1), however, to develop a sampling methodology for a global productivity assessment program (Table 4-2) utilizing a follow-on CZCS-type sensor. It is intended to deploy moored in situ fluorometers, as discussed previously, and drifting fluorometers, similar to the meteorological sensors of the 1979 Global Weather Experiment, in defined 1987-89 MAREX shelf experiments to allow interpretation of time-space composite descriptions of at least parts of the ocean. With global sampling, CZCS-type images will permit instantaneous resolution of the shapes of shelf synoptic-scale patterns of phytoplankton pigment distribution from any domain. These images will also permit interpolation rather than extrapolation from this data set (Table 4-2).

In general, phytoplankton standing stock and pigment concentration levels at a fixed time within a particular pattern feature are the result of a complicated set of biological, chemical, and physical processes with time scales ranging from seconds to seasonal, and space scales ranging from global to microscopic (Table 2-1). The shapes and locations of patterns delineating meso- and synoptic-scale shelf features are dominated, however, by physical-dynamical processes transporting the plankton populations. Therefore, meso-scale patterns ($10 < x < 100$ km) tend to evolve over time scales ranging from several hours to a few days (i.e., at the time scale of a moored or drifting fluorometer array), while the synoptic-scale patterns ($100 < x < 1000$ km) tend

to evolve over time scales of order a few weeks to a month, i.e., at the probable CZCS time scale. Considering these scales and CZCS sampling characteristics together, long-term global sampling with a CZCS-type instrument can adequately resolve synoptic-scale phytoplankton standing stock distributions, while higher frequency data gaps could be covered within the five specific shelf areas by CZCS in situ instrumentation (Table 4-2) and judicious use of ships and aircraft.

4.5 ADDITIONAL OCEANIC STUDIES

Oceanic systems are more tractable than shelf systems for understanding certain aspects of biological-physical coupling because they are freed from some of the high-frequency fluctuations of coastal systems (Walsh, 1976), from effects of local bottom topography, and from complex color patterns produced by river-borne organics and suspended sediments. Because of these simplifications compared to coastal regions and the more reasonable expectation of isotropy in the background signals of oceanic systems, oceanic regions are logical natural laboratories for investigation of selected biological and physical processes. Eddies, for example, are relatively easily tracked over the open ocean in studies of eddy formation and evolution. Frontal evolution similarly may be more easily followed than near-shore phenomena. Areas homogeneous in space are logical regions in which to monitor evolution in time.

The upcoming ODEX (Optical Dynamics Experiment) study, for example, will evaluate the effects of autumn mixing on oceanic optical properties. A site has been selected between Hawaii and San Diego to exclude major advective "noise" from its time-course "signal." The primary goal of ODEX is to develop and field test a two-dimensional physical-biological optical model of the upper ocean that predicts the diffuse attenuation coefficient, $K(Z, t, \lambda)$, in those regions where advective effects are small. (Here, two dimensions mean depth and time.) Additional goals are to assess the feasibility of a four-dimensional model (x, y, z , and time) and to predict other optical properties such as spectral beam attenuation and the volume scattering function.

ODEX and will take place about 1000 miles west-southwest of Monterey, California, where horizontal variability will be minimal during October and November 1982. The time was chosen to overlap the change from the summer to winter chlorophyll regimes. The biological-optical model will be merged with an upper-layer model based on the Level 2-1/2 Mellor-Yamada Turbulence Closure Scheme. This model is being modified to permit the inclusion of realistic vertical profiles of the relevant parameters such as the downwelling solar irradiance and chlorophyll. Preliminary versions of the new model have been used to demonstrate the diurnal response of the upper ocean. Comparison with measurements have shown that the upper ocean is sensitive to solar irradiance and (optical) water type. Ships in the ODEX experiment will be R/V FLIP and the R/V ACANIA. Both will be fully instrumented with a complete range of chemical, physical, meteorological, and optical instruments.

For any large-scale ($x \geq 1000$ km) oceanic domain, oceanographic applications of measurements made with a CZCS-type sensor are constrained by the same sampling considerations discussed in the preceding shelf studies; sampling frequency, as governed by orbit parameters and cloud cover, will still vary with latitude and season. In general, we expect to adequately resolve synoptic scale phenomena and obtain statistical descriptions of embedded meso-scale structure, in any given oceanic domain. Near surface optical properties are indirectly related to two prime foci of modern physical oceanography, ocean circulation and mixed layer dynamics/thermodynamics, in several ways, including:

- a. The vertical irradiance attenuation coefficient, k , governs the vertical distribution of heating by incident sunlight. Zaneveld et al., 1981, review the influence of k on vertical density stratification in the mixed layer; they document that, under light winds, vertical temperature structure is significantly sensitive to k over its range of variability in global water masses. CZCS has been demonstrated to be capable of mapping the distributive patterns of k both in open ocean and coastal waters. Preliminary examination of CZCS imagery suggests that a rich structure in synoptic-scale and meso-scale patterns of horizontal k distributions may pervade nearly all

ocean regimes. Research should be undertaken to determine and quantify the sensitivity of horizontal distributions of sea surface temperature and of mixed layer structure to k distributive patterns.

- b. If meso-scale and smaller individual patches of k and phytoplankton pigments can be positively identified in several CZCS images over periods of several days, then the trajectories of those patches can be used as Lagrangian estimates of synoptic-scale ocean currents. This application would be directly analogous to the use of cloud drift winds, derived from GOES VISSR data, in meteorological analyses. The NSF Warm Core Rings Experiment is now using CZCS-derived products to augment thermal imagery for ring translation studies. Initial scrutiny of a few CZCS image sequences shows the data to be provocative and promising, but results to date are too preliminary and tentative to draw conclusions about the general utility of this method as a tool in future oceanic studies.
- c. Over synoptic-length scales, significant changes in ocean optical properties are frequently (perhaps usually) associated with changes in temperature and salinity. This occurs because separate water masses frequently have different chemical, biological, optical, temperature, and salinity characteristics. Optical contrast between water mass, therefore, causes many synoptic-scale ocean circulation features to be visualized as two-dimensional patterns of ocean color (and therefore k and pigments) in CZCS images. Examples of CZCS-observed color patterns which have clear (albeit as yet qualitative) dynamical interpretations, are warm core rings, the Gulf Stream front (Mueller and LaViolette, 1981), and synoptic-scale eddies and frontal features in the California Current System. A similar, and even more direct, case may be made for Sea Surface Temperature (SST) patterns in infrared images measured from space. Taken together, infrared SST and optical patterns can hypothetically provide empirical sets of time-varying horizontal interpolation/extrapolation functions applicable to

near-surface density structure, at least in some oceanic regimes. Downward continuation of these patterns, when and if feasible, will require other information (perhaps a mix of climatological and concurrent in situ data) and mathematical models. In at least some instances (e.g., warm core rings), the feasibility of downward continuation of such interpolation functions to infer subsurface density and flow structure is particularly promising and warrants near-term research emphasis.

Other examples are available such as frontal studies off the Grand Banks (Mueller and La Violette, 1981) and off the Somali coast, but the foregoing ones are sufficient to illustrate prospective applications of CZCS-type data to problems in oceanic regions. In summary, possibilities include use of k distributions in mixed layer models, Lagrangian estimation of synoptic scale currents from color patch trajectories, and downward continuation of combined SST and ocean color patterns pursuant to three-dimensional analyses of dynamical oceanic features. Clearly, time sequences of Nimbus-7 CZCS data which correspond to open ocean experiments must be studied to refine the above generalities into specific hypotheses to be tested using the MAREX data sets. As the results of present oceanic experiments (Warm Core Rings, Optical Dynamics Experiment, and other, smaller individual experiments/analyses) become available, other open ocean studies will take advantage of the proposed MAREX sensor package and data capability.

SECTION 5. REQUIREMENTS

The Ocean Color Science Working Group (OCSWG) spent a considerable amount of time attempting to specify the limitations and compromises of a MAREX satellite monitoring system. From this background, a set of minimum spacecraft and ground system requirements were identified in order to accomplish the major scientific opportunities from space-borne ocean color data. To propose a system which would satisfy all possible users, research and operational, is beyond the scope of this report and also is unrealistic to expect. As a result, only the experiments (Table 4-2) discussed earlier in the report are being considered in framing requirements. Thus, this provides the focus for the requirements allowing significant scientific progress in limited well-defined programs, while still offering sufficient flexibility to satisfy a reasonable proportion of the needs of other scientific and operational areas. This report will provide the basis for further development in color sensing science in other fields in the future as well as execute an exciting nearer term shelf carbon/nitrogen flux experiment. The minimum requirements for an ocean color system which could receive the support of a significant portion of the oceanographic community are discussed in this section. While there are a number of possible system scenarios, it is recommended that NASA proceed with a formal study of a system to meet minimum data requirements.

5.1 SPACECRAFT

At the present time, the only polar orbiting spacecraft operated by the United States civilian space program that can support the CZCS mission is one of the advanced TIROS-N (ATN) series (Table 5-1). Two NOAA satellites, NOAA-6 and NOAA-7, are in near polar sun synchronous orbits crossing the equator at 7:30 a.m. and 7:30 p.m. for NOAA-6, and 2:30 p.m. and 2:30 a.m. for NOAA-7. In order for the CZCS to be most effective, the desired crossing time at the equator is near noon, so that the sun is either ahead or behind the spacecraft to minimize the effect of sun reflection (glint) directly into the sensor during the ± 40 degree side scan. The OCSWG addressed the question of whether the spacecraft could orbit with a 1:30 p.m. and 1:30 a.m. equatorial crossing time with an ascending node orbit

Table 5-1. Ocean-Related Spacecraft Activities: Next Decade

Satellite	Sponsor	Sensor Complement	Launch	Status
DMSP	USAF NASA	MR + meteorological sensors MR data processing facility	1984	Approved Proposed (7-yr coverage planned for MR)
GEOSAT	USN	ALT	1984	Approved (some data to be classified)
MOS-1	JAPAN	CZCS, IR, MR	1985	Approved
MOSS	USN/NOAA/NASA	ALT, CZCS, MR, SCAT	1986	Cancelled
ERS-1	ESA NASA	ALT, SAR, SCAT, IR SAR data receiving/processing facility	1987	Approved Proposed (essentially)
NOAA-H	NOAA NASA	Meteorological sensors (including IR) Contribute piggyback CZCS	1987	Approved Proposed (essentially)
SPOT-2	CNES	Terrestrial sensors + piggyback ALT	1987?	Proposed
TOPEX	NASA	ALT + option for SCAT	1988?	Proposed
ROSS	USN NOAA NASA	ALT, MR, SCAT Contribute bus (NOAA-D spacecraft) Contribute SCAT	1988?	Proposed Proposed Proposed
ERS-1	JAPAN NASA	SAR Utilize SAR data facility (noted above)	1988?	Proposed Proposed
GRAVSAT	NASA	Accurate tracking between two satellites	1989?	Proposed
ERS-2	ESA	ALT, SAR, SCAT, ?	1989?	Tentative
RADARSAT	CANADA NASA	SAR Contribute launch + piggyback SCAT	1990?	Proposed Proposed
MOS-2	JAPAN	ALT, CZCS, MR, SCAT	1990?	Tentative

(that is, whether the spacecraft could fly from the South Pole toward the North Pole on the daylight side of its orbit). The study showed: that the spacecraft can, indeed, operate successfully in such an orbit; that the CZCS, less the radiation cooler, can fit on the spacecraft; and that the present data system could be enlarged to accommodate data transmission from the CZCS to the ground.

The parameters of an orbit under consideration for the series of Advanced Tiros-N (ATN) satellites that could carry a CZCS are summarized in Table 5-2. The inclination of the orbit is necessary in order to preserve the sun synchronous characteristic so that the orbit plane may precess at the same rate as the earth rotates around the sun. NASA/GSFC also addressed the question of whether the necessary space was available on the earth-viewing portion of the ATN in order to accommodate a future CZCS (see Appendix A) and the necessary data processing system to support it. Figure 5-1 shows the bottom, or earth-viewing side, of the ATN and a location which can accommodate the CZCS and the color data processor needed to support the instrument. Unfortunately, the end of the spacecraft where radiation coolers may be utilized is fully occupied by the AVHRR, the SSU, and the HIRS; therefore, the CZCS will have to fly without a radiation cooler, eliminating the 10.5 to 12.5 micrometer band. This is not a serious problem in that the AVHRR, which operates continually, provides thermal measurements in the split window of 10.5 to 11.5, and 11.5 to 12.5 micrometers over the ocean. There will be some problems registering the thermal data with the color data since the AVHRR will not have the tilt mechanism of the CZCS and the mirrors are not synchronized. Nevertheless, the CZCS fits fairly comfortably into the bottom of the ATN.

Table 5-2. NOAA-I/CZCS Orbit Parameters

Parameter	Nominal Value
Altitude (km)	870
Inclination (degrees)	98.899
Nodal period (minutes)	102.368
Nodal regression (degrees/revolution)	25.592
Nodal precession (degrees/day)	0.9856
Orbits per day	14.067
Sun angle range limits (degrees)	46-80

P-2 MISSION
NOAA-I/CZCS

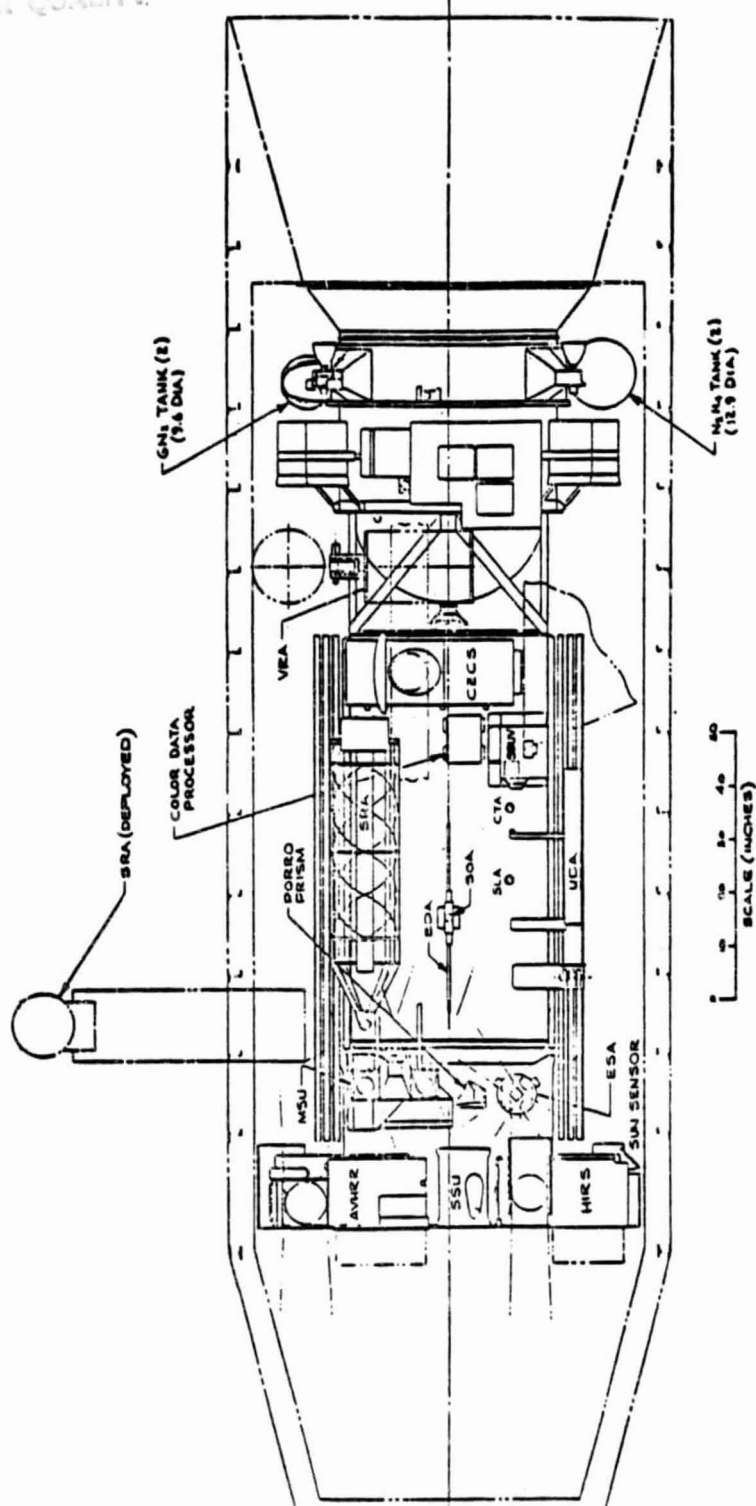


Figure 5-1. Possible Location of CZCS on NOAA-I Satellites

The question of whether the diffuser plate for calibration can be mounted on the ATN spacecraft is now under study. In summary, the OCSWG found that a quite acceptable CZCS program could be carried out from the ATN, that there are no insurmountable technical problems in moving the orbit closer to noon, and that there are no serious problems in mounting the CZCS on the ATN.

5.2 MEASUREMENT CHANNELS

The Nimbus-7 CZCS program demonstrated the feasibility of determining ocean chlorophyll levels (and diffuse attenuation coefficients), from multi-channel visible space-borne observations (see Appendix B for discussions of the algorithms). The OCSWG requirement is to resolve the chlorophyll concentration to within 50 percent over a range of concentration from .05 to 10.0 $\mu\text{g chl}\ell^{-1}$ in the open ocean and outer continental shelf areas. Radiance observations to 10 bit accuracy are required at a minimum of six of the following eight wavelengths, dependent on water-mass type:

<u>Wavelength (nm)</u>	<u>Bandwidth (nm)</u>
443	20
490	20
520	20
560	20
590	20
670	20
765	40 (Notched for O2 A band 759-770nm)
867	45

The 490 and 590 nm channels are useful under special circumstances to extend the observations into more turbid coastal waters.

5.3 SPATIAL RESOLUTION

The chlorophyll distribution in the ocean is patchy on all scales down to the sub-kilometer level (Table 2-1). Thus, to adequately map phytoplankton variation in high-concentration shelf areas, which is the major goal of the first MAREX studies, a satellite must be able to resolve about a kilometer of the ocean. This small spot size also permits measurements

closer to the shore, allowing resolution of local outwelling and upwelling zones, which tend to be nearshore phenomena in many cases. Such a high data rate may be relaxed somewhat for wide area studies of open ocean phytoplankton where statistical rather than process experiments are more likely. In this case, a degradation to about 4-kilometer resolution can be accepted. Therefore, a satellite system is required that can operate in two modes, analogous to the present infrared system: (1) local area coverage of high-resolution to about one km and (2) global area coverage of lower resolution to about four km (Table 4-2).

5.4 OBSERVATIONAL COVERAGE

Coverage here is defined as the frequency at which a field of chlorophyll data is available (barring cloud cover interference) which completely covers an experiment area at some density and composited over some length of time. Typically in meteorology, this means the entire earth, at varying density of some hundreds of kilometers every 3 or 6 hours. By their nature, satellites provide a high density of observations within their swath coverage; however, one or more passes must be composited to generate the field of data which the scientist requires. The satellite coverage is, then, a function of swath size, orbit configuration, and cloudiness. The time it takes from some part of the satellite swath to revisit every spot within an experimental area defines the length of time it takes to generate a data field. Repeat coverage is the time it takes to generate another such field in the same area. For example, a small experimental area, less than one swath width in size, might be entirely covered in one pass, but wait for several days or weeks for repeat coverage. Phytoplankton variability in the ocean has a time scale of less than a week depending on seasonal changes of wind events and algal growth. It would be desirable, then, to have worldwide chlorophyll observations at least every 3 or 4 days. This is impossible due to natural cloudiness and reasonable orbit and swath configurations, so there must be an accompanying program of in-situ moored observations in the experiments to provide temporal sampling below the Nyquist period and thereby to allow interpolation of satellite observations (Table 4-2). To make even this possible, it is required that a satellite system's swath pass over any given spot at least weekly.

5.5 NAVIGATIONAL ACCURACY

Location of pixels in latitude-longitude coordinates is important for quantitative scientific use of color scanner data. In order to make these data useful for other than individual scene analyses, the scientist must be able to use observations from many passes to generate a time series and do statistical analysis. This implies that location accuracy of data from different passes must be sufficiently precise to allow compositing. For these purposes, an absolute navigational accuracy of 10 km for high resolution local data and 25 km for low resolution global data is required.

5.6 DATA DELIVERY

The details of data processing and delivery are complex and are discussed in more detail later in Appendix C. For purposes of an overall requirement, the OCSWG considers satisfactory data processing and delivery to be the most vital concerns that the ocean science community have for a new satellite observing system. History of other ocean-oriented satellite data systems has not been encouraging in this respect. Timeliness of data processing is most important in that if data processing time does not keep pace with the data flow, backlogs quickly develop and it can become literally years before the data are made available to the research community. In that case the data are often not widely used by scientists and a multi-million-dollar satellite is under utilized. Further, satellite pictures by themselves are not satisfactory for quantitative ocean study, but the observations must be presented as quantitative, navigated values of chlorophyll and diffuse attenuation coefficient. To this end, the data available to the user must meet the following requirements:

- a. For near real-time positioning of ships during MAREX field experiments, quick-lock data must be available within 24 hours of observation or direct satellite read-out for user ground stations must be available in selectable areas worldwide.
- b. For integration with cruise results, fully processed high-resolution data must be available to the user within 30 days of observation. This is "Level II" processing which means cloud removed,

atmospherically corrected, chlorophyll values within a pass, identified by latitude-longitude, on computer-compatible tape. False color images or contoured maps of these passes are also desirable.

- c. The same information is needed for the low-resolution global data. However, since the global data will be primarily used in the study of larger scale, longer term variations, the observations should be integrated and composited before delivery. Level II low-resolution values should be stored on a monthly 100 km grid and the mean values published monthly, after allowing three months for processing, as contours on ocean scale maps. There is no requirement for imaging individual passes, although individual Level II tapes should be preserved for 6 months for selected processing on request.
- d. All high- and low-resolution Level I tapes should be preserved in an archive for 5 years. Users should have on-line, interactive access to a catalogue of the archived data.
- e. The difficulty and cost involved in handling the flow from a high-data-rate instrument such as this is realized. Ideally, all the sunlit data from the satellite should be stored and processed at high resolution. As a minimum, though, the ability to process 30 minutes of stored high resolution data per day to Level II chlorophyll values, and 150 minutes of stored low resolution data is required. This would result in enough capacity to process the ocean areas near the USA to high resolution and at least one hemisphere at low resolution on a continuing basis (Table 4-2). It would be highly desirable to double the low-resolution capacity to be assured of worldwide coverage. Direct broadcasting of high-resolution data on at least a 50 percent duty cycle would fill in the gaps of recorded high-resolution stored data for those users with ground receivers. It is strongly recommended that the direct broadcast mode be designed so that there is minimum impact to existing ground receiver stations used by researchers outside NASA (see Appendix D). The system should be similar enough to the existing NOAA infrared broadcast protocol

that other users need only make minor or no changes to their hardware and software for data capture (see Appendix D).

5.7 MISSION LENGTH

In order to conduct in the in situ field work necessary to exploit the ocean color observations from space, experiments listed earlier must be staged in a variety of seasons and conditions. Logistically, this implies that the spacecraft mission must cover at least two years to specify atypical situations, e.g., the occurrence of El Nino phenomena. In addition, even the coarsest values for ranges in interannual productivity are not known for most ocean areas. An absolute minimum of two years of observation is necessary to identify the scale of variability. Thus, a minimum mission length of two years is required, with any extension of that length highly desirable. That also implies that instrument calibration be constant, or identifiable, during the minimum two-year mission to allow valid comparisons of ocean observational values.

APPENDIX A. SENSORS

One difficulty in interpreting remotely sensed ocean color measurements arises from the fact that the thermocline and the chlorophyll maximum often occur at depths in excess of three to four optical attenuation lengths, depending upon season, weather and location. Thus, to provide physical and biological interpretation of the information contained in the CZCS images, it is important to understand the dynamic three-dimensional ocean processes that create them, including, for example, the effects of local upwelling on phytoplankton productivity, the effects of internal waves on the variability of the chlorophyll maximum, and the complex interaction of wind events on nutrient, phytoplankton, and zooplankton relationships.

Such measurements can best be made by sensing from in situ instruments which have the capability of eventually examining the vertical, physical, and biological structure of the euphotic zone of the ocean. Improved accuracy and interpretation of Ocean Color Imager (OCI) data will therefore result if additional satellite, airborne, in situ, and in vitro measurements are taken coincidently with satellite ocean color measurements. A summary of various satellite ocean sensor performance characteristics is presented in Table A-1 (After Stewart, 1981).

A.1 OCEAN COLOR IMAGER

Since the development of a new sensor always involves some risk, the modification of an existing design is often preferable with respect both to cost and probability of success. The Nimbus-7 CZCS has proved to be an excellent system with a useful life of over 3 years and is therefore the leading candidate for a system designed to measure global oceanic chlorophyll concentration.

The modifications to the CZCS design necessary to generate the required sensor system are as follows:

- a. Remove the thermal (10.5 - 12.5 m) channel and its associated passive cryogenic cooler.

Table A-1. Satellite Instrument Performance

Instrument	Spacecraft	Geophysical Observable	Best Estimate of Measurement Accuracy	Remark
Altimeter (ALT)	Seasat	Surface topography	+ 7 cm rms *(precision)	20-30 cm absolute accuracy with laser tracking of spacecraft
Scatterometer (SCAT)	Seasat	Significant wave height	+5% or 0.5 m	5-24 m/s range; directional ambiguity
Synthetic-Aperture Radar (SAR)	Seasat	Wind velocity	+ 1.6 m/s rms, speed + 16 deg. rms, direction	50-1,000 m range, rough estimate of height
Color Scanner (CZCS)	Nimbus-7	Surface waves	+ 3% wavelength + 2 deg. direction (precision)	No clouds; low suspended sediment concentration
		Sea ice boundaries	+ 250 m absolute positioning accuracy	Same as above
		Chlorophyll concentration	+ 30%	No rain, heavy clouds, sunglint, or RFI**
		Diffuse attenuation coefficient	+ 15%	Same as above 0-2 m/s
Microwave Radiometer (SMR)	Seasat Nimbus-7	Surface temperature	+ 1 deg. C	No clouds
		Wind speed	+ 2.5 m/s, no direction	
		Fractional ice cover	+ 15%	
		Ice age	New or multi-year	
Infrared Radiometer (VIRR)	NOAA-6	Surface temperature	0.6 deg. C	

*root mean square

**radio frequency interference

- b. Locate four spectral channels in the chlorophyll absorption bands between 440 and 590 nm with characteristics similar to those of the present CZCS and two atmospheric correction bands between 670, 765, and 865 nm.
- c. Develop a data system capable of averaging 4-pixel by 4-line groups of data points, thereby reducing the data rate by 16 and enabling the on-board storage of global data.
- d. Maintain the present 820 m IFOV at the lower NOAA orbit (830 km) and increase the digitizer from 8 to 10 bits to accommodate the increased signal-to-noise.
- e. Provide for direct broadcast of the high resolution (1 km) data stream while in sight of properly equipped ground stations.
- f. Speed up the tilt mechanism in order to minimize the loss of data incurred while changing from the full aft to full forward position.

Application of the atmospheric correction algorithm requires a high degree of consistency between the calibration of the sensor and the extraterrestrial solar irradiance $F_0(\lambda)$ (Gordon, 1981). The sensor calibration and F_0 have independent errors, so trying to reduce this effect through very careful calibration and careful measurements of $F_0(\lambda)$ will be very difficult. One way of circumventing this problem directly is the addition of the capability of the sensor to view the sun in diffuse reflection as suggested by Yates (Gordon, 1981). The addition of this capability on the Ocean Color Imager is recommended.

In the present atmospheric correction algorithm the assumption that $S(\lambda, \lambda_0)$ be independent of position is required (except over Case 1 waters for which $C < 0.25 \text{ mg/m}^3$). Spatial variations in aerosol 'type' (APPENDIX B) will induce spatial variations in S . In the case of the present CZCS there is no direct way to detect such a change in S . However, if there were a band in one of the near IR windows at 765 and 865 nm, for which $L_w \approx 0$ in most waters, the detection of a variable S could easily be effected by looking for spatial variations in $S(670, 765)$ or $S(670, 865)$,

and adjusting $S(\lambda, \lambda_0)$ in the visible accordingly. For turbid coastal waters, for which $L_w(670) \neq 0$, the addition of both of these bands would also facilitate correction. The minimal set of bands suggested for the Ocean Color Imager are: 443nm, 520nm, 560nm, 670nm, 765nm, and 865nm. The visible bands should be 20nm wide and the I.R. bands 50nm wide. In addition, spectral bands at 490nm and 590 nm could be valuable in the retrieval of C in the coastal regime. Also, it is expected that some fine-tuning of the precise positions of the above bands will be necessary.

These changes together with several minor modifications will result in a system that will provide data from which global oceanic chlorophyll maps with a resolution of a few kilometers can be generated.

A.2 ANCILLARY INSTRUMENTS

Perhaps the most important ancillary satellite sensor for shelf primary productivity studies is the Advanced Very High Resolution Radiometer (AVHRR), an improved VHRR infrared radiometer. It is part of the standard complement of sensors presently flown on the NOAA series of polar-orbiting environmental satellites on which the OCI is a candidate for inclusion. It can provide sea surface temperature with an accuracy of about 0.6°C if no clouds contaminate the field of view, and if atmospheric effects are carefully removed. Horizontal temperature gradients of about 0.2°C can also be resolved. Acquiring such data concurrently with ocean color measurements will allow upwelling and frontal processes to be more accurately described and will help in identifying certain water masses and in locating boundaries of currents.

Two other satellite sensors which could be flying in the same time frame as the OCI are the altimeter and the scatterometer. Using a highly accurate altimeter (nadir radar with ± 2 cm precision) on a satellite with a well-known orbit allows the measurement of major surface current velocities; with an accurate geoid, slower currents (especially their variability) can be determined. Surface current measurements can be made by altimetric determinations of the slope of the sea surface since the slope increases with the speed of the current. Thus, with the TOPEX (dynamic TOPography EXperiment) satellite (see Wunsch, 1981), the current field will be better

understood. This will permit estimates of current shear, convergence, and divergence as well as nutrient and plankton transport for various oceanic regions. These processes all affect the productivity of the oceans and are impractical to measure globally by conventional means.

The third ancillary satellite sensor which can significantly improve our understanding of the processes affecting the productivity of the oceans is the scatterometer. It measures the off nadir backscattered radar return, largely from capillary waves which respond in height directly with the surface wind stress or wind speed. Wind-driven divergence zones can produce upwelling of cool, nutrient-rich water to initiate and sustain phytoplankton blooms, and wind-driven convergence zones can concentrate bouyant food resources (e.g. phytoplankton, detritus, seaweed), attracting fish. Since the surface currents are primarily wind-driven, a better understanding of the wind field will also improve models of the current field and of the density structure in the euphotic zone (depth of the mixed layer, thermocline stability, etc.), affecting the vertical distribution of shelf phytoplankton and productivity in response to wind events (Walsh, 1976).

The prospects of a scatterometer flying in the last part of this decade are good. One is scheduled to be aboard ERS-1 (a European Space Agency satellite), and NASA is studying the feasibility of flying a scatterometer "piggyback" on an available polar orbiter. A dedicated altimetric satellite (TOPEX) is a prospective mission of the Environmental Observation Division of NASA, with a possible launch date late in the decade. The footprint (pixel size) of passive microwave radiometers, which provide sea surface temperature measurements through the clouds is generally too large (e.g., 100 km) to be of much utility to ocean productivity studies. These sensors also suffer from inaccuracies within 600 km of land (sidelobe returns), where the most dynamic productivity processes (e.g., coastal upwelling) occur.

APPENDIX B. ALGORITHMS

The CZCS provides estimates of the near surface concentration of phytoplankton pigments (defined to be chlorophyll *a* and its associated phaeopigments) by measuring the spectral radiance backscattered out of the ocean. This radiance scattered out of the ocean and reaching the top of the atmosphere comprises only a small portion of the total radiance measured at the sensor. In general, the sensor radiance $L_t(\lambda)$ (λ is the wavelength) can be decomposed into $L_1(\lambda)$, the radiance due to photons that never penetrated the sea surface, and $t(\lambda)L_w(\lambda)$, the radiance due to photons which were backscattered out of the water (the water-leaving radiance) and diffusely transmitted to the top of the atmosphere, i.e.,

$$L_t(\lambda) = L_1(\lambda) + t(\lambda)L_w(\lambda). \quad (1)$$

All of the information relating to the oceanic constituents such as the chlorophyll concentration is contained in $L_w(\lambda)$.

Schemes for extracting $L_w(\lambda)$ from $L_t(\lambda)$ are referred to as 'atmospheric correction' algorithms, and empirical relationships used to derive the pigment concentration from the extracted $L_w(\lambda)$ are called 'bio-optical' algorithms.

B.1 BIO-OPTICAL

Most early studies concerning the remote sensing of ocean color (Clarke et al., 1970; Arvesen et al., 1973) were directed toward the extraction of the surface chlorophyll concentration from the spectral radiance upwelling above the sea surface. Chlorophyll a is the pigment present in living plants responsible for photosynthesis. In the ocean, this pigment is present in microscopic organisms called phytoplankton, which form the first link in the marine food chain. In productivity studies, chlorophyll a is usually taken as a measure of phytoplankton 'biomass' (Platt et al., 1975).

In the ocean, degradation products of chlorophyll a, the phaeopigments, are also present. These are produced upon acidification of chlorophyll a as would happen for example in the gut of zooplankton feeding on phytoplankton. The phaeopigments have absorption characteristics which are so similar to chlorophyll a in the blue that separation of these pigments with an instrument with as few spectral bands as the CZCS is impossible. Therefore, for CZCS studies it is necessary to consider chlorophyll a and the phaeopigments together. The sum of the concentrations of chlorophyll a and the phaeopigments will henceforth be called the phytoplankton pigment concentration or just the pigment concentration and will be denoted by C.

To establish algorithms for retrieval of the pigment concentration from CZCS imagery a field program was initiated by NOAA/NESS in 1975. This program consisted of measurements of vertical profiles of upwelled (traveling toward the zenith) spectral radiance (L_u) and pigment concentration along with other optical, physical, and biological parameters of importance for the interpretation of ocean color remote sensing data (Gordon and Clark, 1980a; Clark et al., 1980; Clark, 1980). These measurements were made at the over 60 locations shown in Figure B-1. The measurements of chlorophyll a and its associated phaeopigments were made fluorometrically using the technique described by Yentsch and Menzel (1963) with the modifications given by Holm-Hansen et al. (1965). The upwelled spectral radiance measurements were made at 5 nm increments with a submersible radiometer covering a spectral range from 400 to 700 nm. The spectral resolution of the instrument was 4 nm.

From profiles of $L_u(\lambda, z)$, where z is depth, the attenuation coefficient of upwelled spectral radiance $K_u(\lambda)$ defined by

$$K_u(\lambda) = -d \ln(L_u(\lambda, z)) / dz \quad (2)$$

was computed. This allowed determination of the upwelled spectral radiance just beneath the surface $L_u(\lambda, 0)$ from

$$L_u(\lambda, 0) = L_u(\lambda, z) \exp +K_u(\lambda)z . \quad (3)$$

ORIGINAL PAGE IS
OF POOR QUALITY

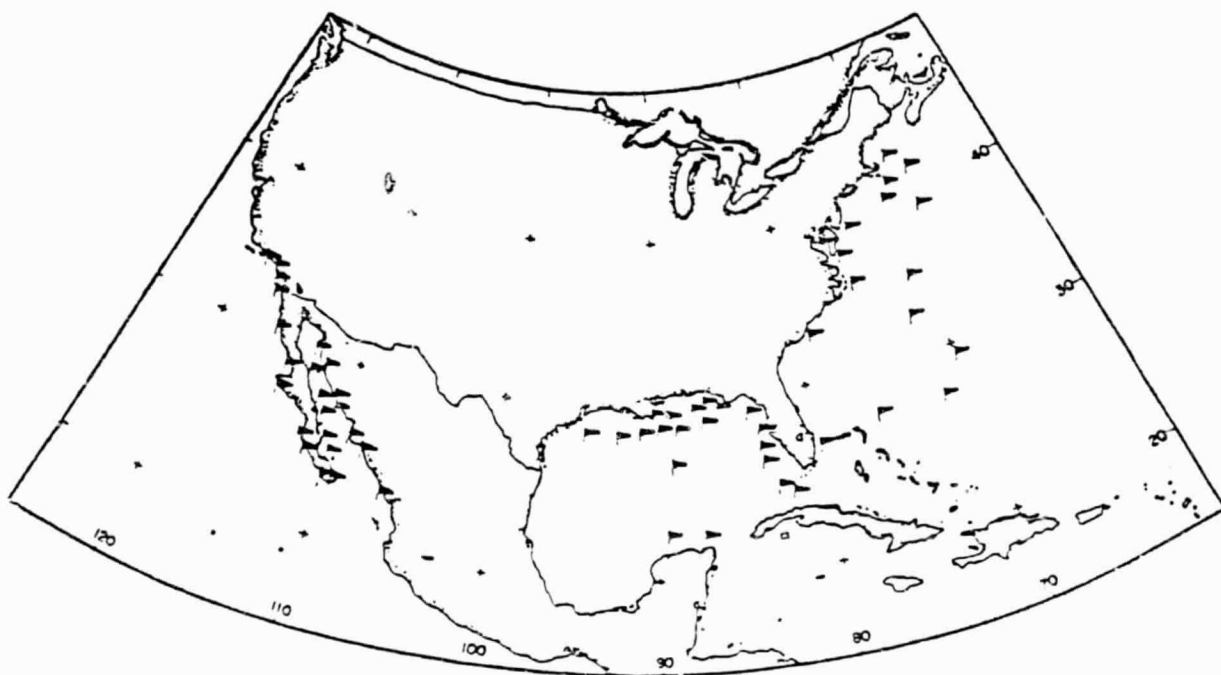


Figure B-1. In situ Chlorophyll Measurements for Validation of CZCS Imagery

$L_u(\lambda, 0)$ was then transmitted through the interface as described by Austin (1974) yielding the water-leaving spectral radiance $L_w(\lambda)$. An example of four such L_w spectra and their associated chlorophyll concentrations is presented in Figure B-2. Note that the main effect on the color of the ocean of increasing the chlorophyll concentration is a depression of $L_w(\lambda)$ in the blue region of the spectrum, i.e., a shift in color from blue to green. The actual enhancement of L_w in the green at high chlorophyll concentrations is due to scattering by detrital material which covaries with phytoplankton.

Finally, $L_w(\lambda)$ was weighted by the spectral responses of the CZCS (spectral resolution of about 20 nm) to provide $\langle L_w(\lambda) \rangle$, the CZCS weighted water-leaving radiance. This is the component of the upwelling radiance just above the sea surface which carries information concerning subsurface constituents. As discussed in the previous section, the goal of the atmospheric correction algorithm is the retrieval of $\langle L_w(\lambda) \rangle$ from the CZCS measured radiance $L_t(\lambda)$.

Since the solar irradiance backscattered out of the ocean may have actually penetrated to significant depths in the ocean, the relationship between C and the water-leaving radiance must depend on the vertical distribution of the phytoplankton. Gordon and Clark (1980b) have shown that the pigment concentration $\langle C \rangle$ for an optically homogeneous ocean which would produce the same water-leaving radiance as an optically stratified ocean with pigment concentration $C(z)$ is

$$\langle C \rangle = \int_0^{z_{90}} f(z) C(z) dz / \int_0^{z_{90}} f(z) dz, \quad (4)$$

where

$$f(z) = \exp[-2 \int_0^{z_{90}} K_d(z') dz'], \quad (5)$$

$K_d(z')$ is the attenuation coefficient for downwelling irradiance (given by Eq. 2 with L_u replaced by E_d), and z_{90} is the 'penetration depth' defined to be the depth at which E_d falls to $1/e$ of its value just beneath the surface. It is the depth above which 90 percent of the radiance contributing to

ORIGINAL PAGE IS
OF POOR QUALITY

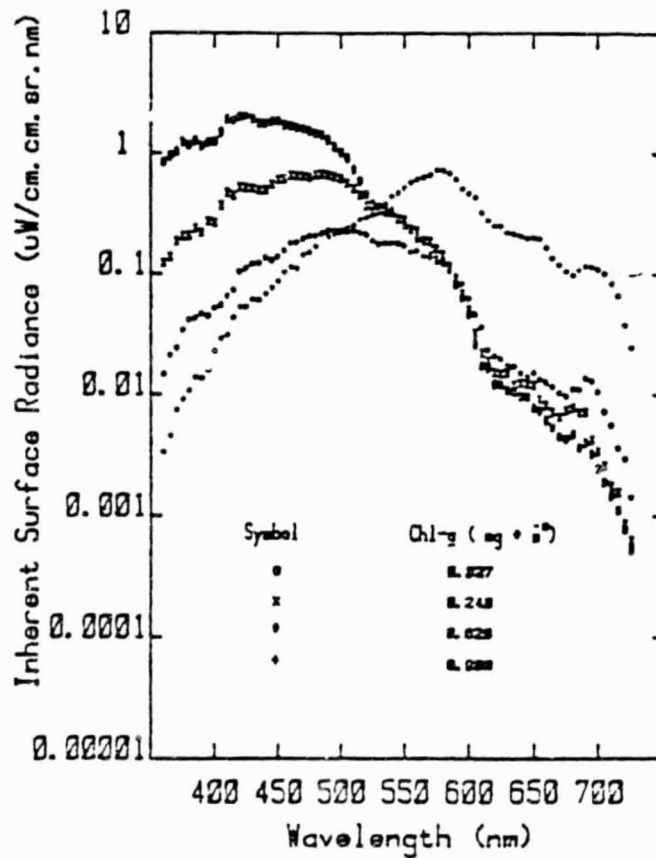


Figure B-2. Inherent Sea Surface Water--Leaving Spectral Radiance for Several Chlorophyll a Concentrations

L_w originates in a homogeneous ocean (Gordon and McCluney, 1975). Since K_d depends on wavelength, $\langle C \rangle$ should as well; however, direct computation (Clark, 1981) of $\langle C \rangle$ from the data acquired at the locations in Figure B-1 show that $\langle C \rangle$ is the same in all the visible CZCS spectral bands. Furthermore, these computations show that there is no statistical difference between $\langle C \rangle$ and the surface phytoplankton pigment concentration. This indicates no significant variation of C within z_{90} , suggesting that z_{90} was usually above the depth of the mixed layer. In all of the bio-optical algorithms discussed here, $\langle C \rangle$ was evaluated at 520 nm.

Morel and Prieur (1977) have optically classified sea water according to the constituents chiefly responsible for determining their optical properties. Those waters for which phytoplankton and their covarying detrital material play the dominant role in determining the optical properties are called Case 1 waters, while those for which inorganic suspended material (such as that which might be resuspended from the bottom in shallow areas), which do not covary with phytoplankton, play an important role are referred to as Case 2 waters. Most of the open ocean waters are near Case 1. These waters are the easiest to treat from a remote sensing point of view. Figure B-3 shows the relationship between $R(13) = \langle L_w(443) \rangle / \langle L_w(550) \rangle$ and the pigment concentration $\langle C \rangle$ for the waters in Figure B-1 believed to qualify as Case 1, while Figure B-4 gives the same quantities using the data from all of the Figure B-1 locations. The lines on these figures are linear regressions on data. Note the significantly tighter fit for the Case 1 waters, especially for $\langle C \rangle > 1 \text{ mg/m}^3$.

At high pigment concentration, $\langle L_w(443) \rangle$ usually becomes too small to be retrieved from $L_t(443)$ with sufficient accuracy to be useful. In this case it is necessary to employ the ratio $R(23) = \langle L_w(520) \rangle / \langle L_w(550) \rangle$ to extract the pigment concentration. This ratio and the associated regression for all of the data (Case 1 and Case 2) with $C \geq 1.5 \text{ mg/m}^3$ is shown in Figure B-5. $R(23)$ is less sensitive than $R(13)$ to variations in $\langle C \rangle$. Both the ratios $R(13)$ and $R(23)$ (but derived from a much smaller data base) were used in processing the imagery presented by Gordon et al. (1980) yielding two pigment displays for each scene: one

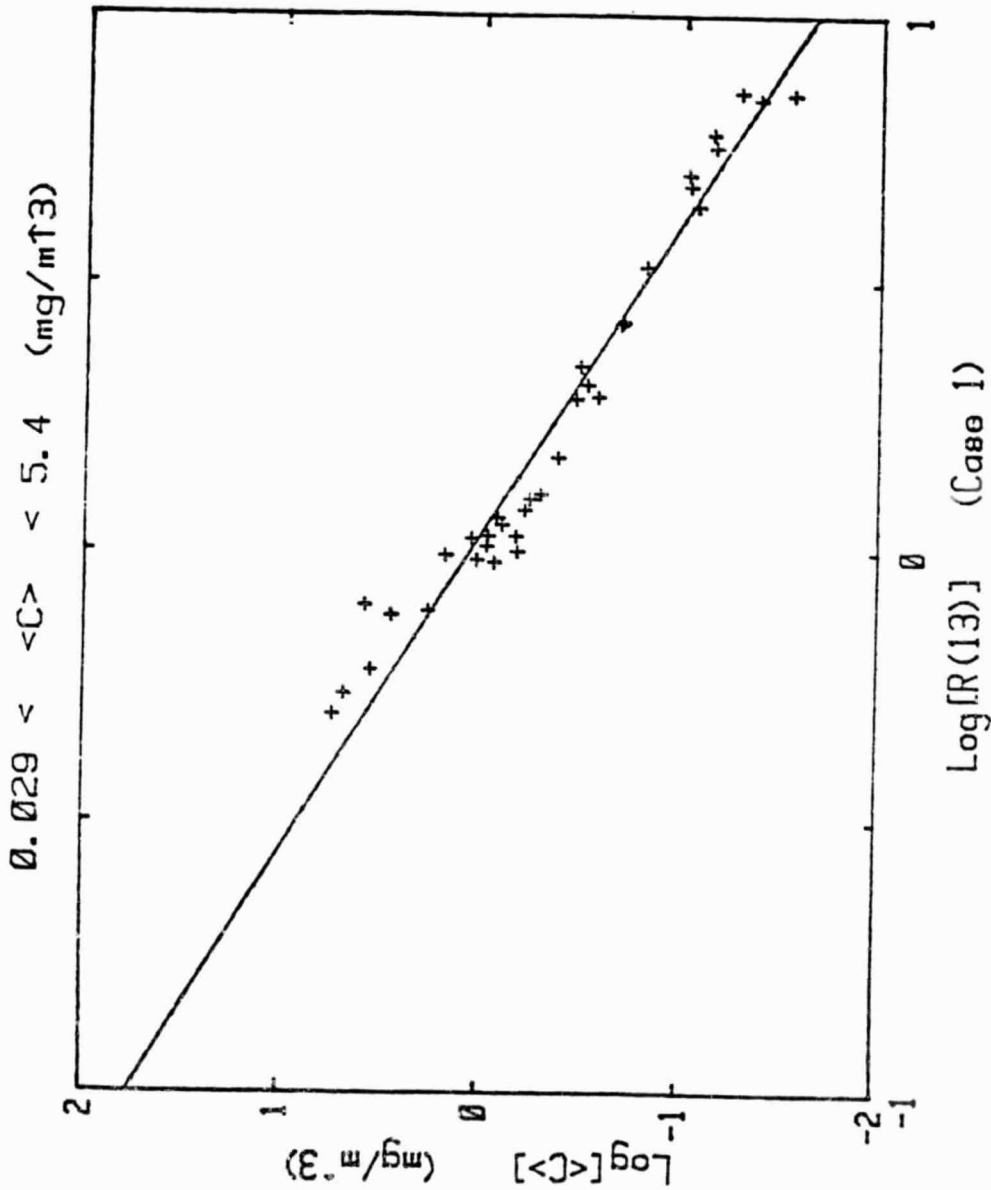
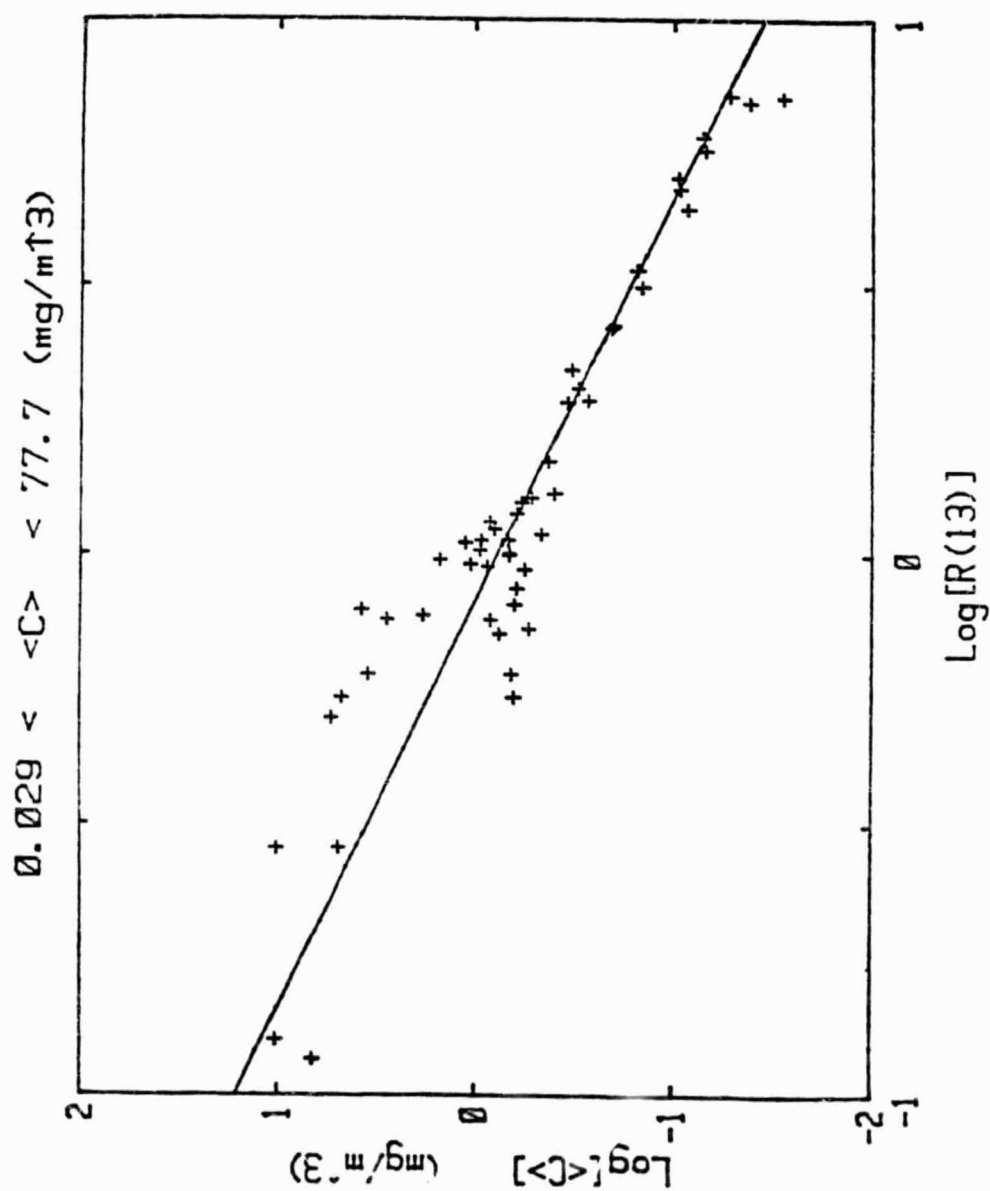


Figure B-3. The 443/550 Algorithm for Oceanic Case 1 Waters

ORIGINAL PAGE IS
OF POOR QUALITY



for $\langle C \rangle > 1 \text{ mg/m}^3$ [R(13)] and one for $\langle C \rangle > 1 \text{ mg/m}^3$ [P(23)]. A similar approach is still being used to process CZCS imagery: the regression line in Figure B-3 being used for $\langle C \rangle > 1.5 \text{ mg/m}^3$, and the regression line in Figure B-5 for $\langle C \rangle > 1.5 \text{ mg/m}^3$. The rationale for these choices is that low pigment applications would usually involve mostly Case 1 waters, while the higher concentrations are likely to be a mixture of Case 1 and Case 2 waters.

All of the linear regressions shown in these figures are of the form

$$\text{Log}\langle C(i,j) \rangle = \text{Log } A(i,j) + B(i,j) \text{Log } R(i,j). \quad (6)$$

The values of A , B , r^2 , the standard error of estimate, s , and the number of samples in the regression, N , for the various algorithms are presented in Table B-1. The relative error in $\langle C \rangle$ is approximately $10^5 - 1$. The specific algorithm now being used by NASA to compute $\langle C \rangle$ is:

$$\begin{aligned} \langle C \rangle &= \langle C \rangle_1 \text{ if } \langle C \rangle_1 < 1.5, \\ \langle C \rangle &= \langle C \rangle_1 \text{ if } \langle C \rangle_1 > 1.5 \text{ but } \langle C \rangle_3 < 1.5, \\ \langle C \rangle &= \langle C \rangle_3 \text{ if } \langle C \rangle_1 > 1.5 \text{ and } \langle C \rangle_3 > 1.5, \end{aligned}$$

where $\langle C \rangle_1$ is in mg/m^3 and $\langle C \rangle_1$ and $\langle C \rangle_3$ refer to algorithms 1 and 3 in Table B-1.

B.2 ATMOSPHERIC

To understand the physics of atmospheric correction, consider a physical setting wherein solar irradiance $F_0(\lambda)$ at a wavelength λ is incident on the top of the atmosphere at a zenith angle θ_0 and azimuth ϕ_0 and the scanner is detecting radiance $L_t(\lambda)$ at a nadir angle θ and azimuth ϕ . $L_t(\lambda)$ consists of radiance which has been scattered by the atmosphere and sea surface, and radiance generated by Fresnel reflection of the direct (unscattered) solar irradiance from the rough ocean surface (sun glint), as well as radiance which has been backscattered out of the water $t(\lambda)L_w(\lambda)$. The goal of the atmospheric correction is to estimate $t(\lambda)L_w(\lambda)$ on a pixel by pixel basis from measurement of $L_t(\lambda)$. This requires removal of the radiance added by interactions with the

ORIGINAL PAGE NO
OF POOR QUALITY

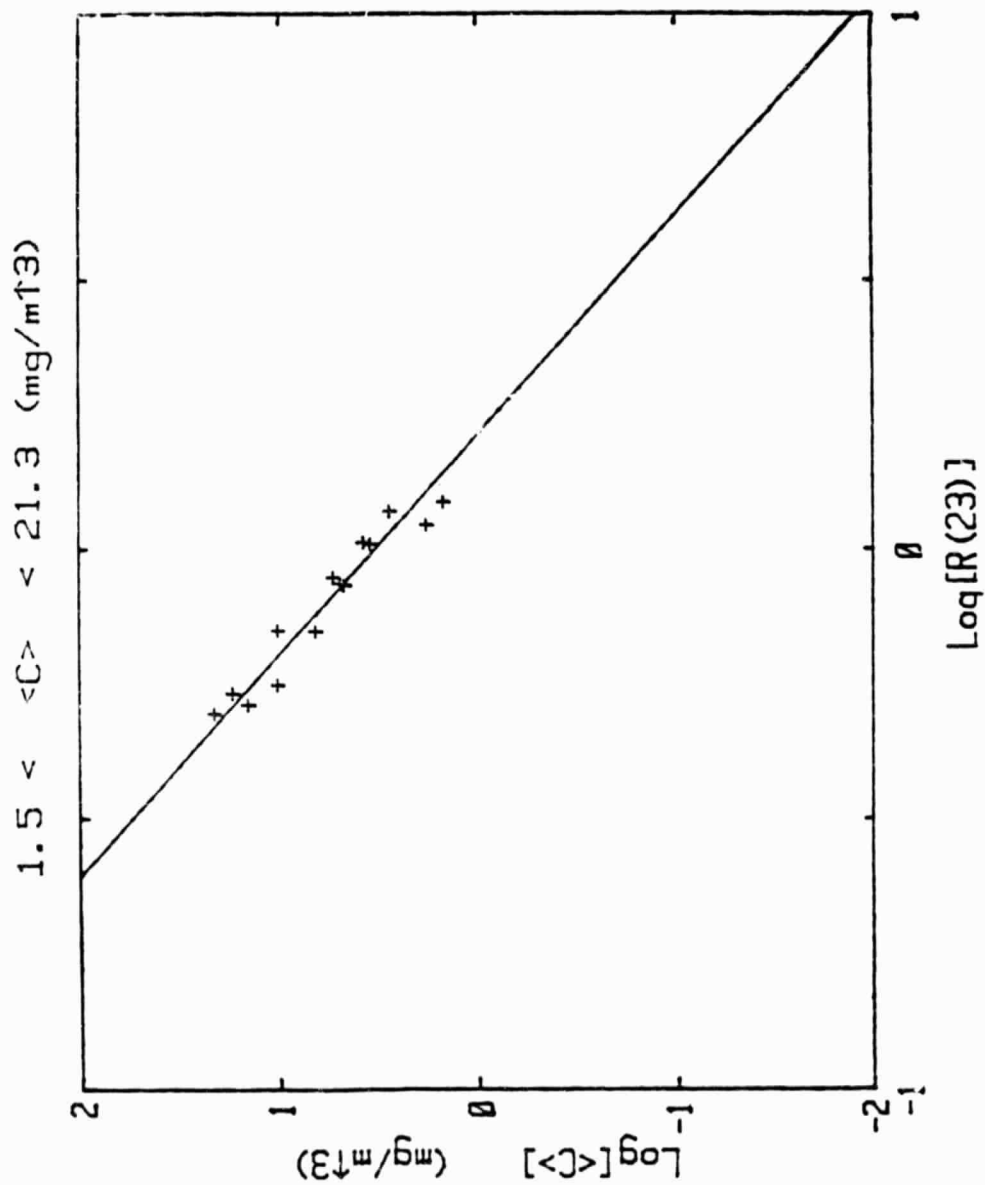


Figure B-5. The 520/550 Algorithm for Case 1 and 2 Waters at Higher Chlorophyll Concentrations (1.5 mg m^{-3})

Table B-1. Bio-Optical Algorithm Summary

	R(ij)	Case	C-Range	LogA	-B	r^2	s	N
1	R(13)	1	0.029- 5.4	+0.053	1.71	0.96	0.130	35
2	R(13)	1+2	0.029-77.7	-0.116	1.33	0.91	0.223	55
3	R(23)	1+2	1.5 -21.3	+0.522	2.44	0.93	0.098	14

atmosphere and sea surface ($L_1(\lambda)$ in Eq. 1). The interactions within the atmosphere consist of scattering by the air (Rayleigh scattering) and by microscopic particles suspended in the air (aerosol scattering). In principle this added radiance could be removed if the concentration and optical properties of the aerosol were known throughout an image. The aerosol, however, is highly variable and, unlike the Rayleigh scattering component, its effect on the imagery cannot be predicted a priori. Thus, only very general aspects of the aerosol properties can be used in estimating its contribution.

The basic approach to atmospheric corrections used in Gordon et al. (1980) involves knowing the inherent sea surface radiance $L_w(\lambda)$ at one position in the image. Briefly, the sensor radiance $L_t(\lambda)$ is divided into its components: $L_r(\lambda)$, the contribution arising from Rayleigh scattering, $L_a(\lambda)$, the contribution arising from aerosol scattering, and $t(\lambda)L_w(\lambda)$, the inherent sea surface radiance diffusely transmitted (Tanre et al., 1979) to the top of the atmosphere, i.e.,

$$L_t(\lambda) = L_r(\lambda) + L_a(\lambda) + t(\lambda)L_w(\lambda). \quad (7)$$

Note that it has been implicitly assumed that there is not direct sun glitter in the field of view of the sensor. Also, photons reflected from the sea surface (without penetrating) have been included in the term

$$L_r(\lambda) + L_a(\lambda). \quad (8)$$

Given $L_w(\lambda)$ at one position, $L_a(\lambda)$ can be found there from Eq. 7. Then if the normalized size frequency distribution and refractive index of the aerosol (which define an aerosol 'type') are independent of horizontal position over a significant portion of an image, the ratio of aerosol radiances at two wavelengths λ and λ_0 ,

$$S(\lambda, \lambda_0) = L_a(\lambda)/L_a(\lambda_0) \quad (9)$$

will be position independent over the same portion of the image, even though both $L_a(\lambda)$ and $L_a(\lambda_0)$ may vary. Gordon (1981a) has demonstrated

from CZCS imagery that $S(\lambda, \lambda_0)$ can in fact remain essentially constant over scales of hundreds of km, even in atmospheres with strong horizontal inhomogeneities. When the aerosol phase function is approximately independent of wavelength, the single scattering approximation shows that S is related to the optical properties of the aerosol through

$$S(\lambda, \lambda_0) = \epsilon(\lambda, \lambda_0) \frac{F_0(\lambda)}{F_0(\lambda_0)} \times \exp[-\tau_{0z}(\lambda) - t_{0z}(\lambda_0)] [1/\mu + 1/\mu_0], \quad (10)$$

where τ_{0z} is the ozone optical thickness, μ and μ_0 are, respectively, the cosines of the viewing angle and the solar zenith angle, and (λ, λ_0) is related to the aerosol optical thickness τ_a and single scattering albedo ω_0 through

$$\epsilon(\lambda, \lambda_0) = \frac{\omega_0(\lambda) a(\lambda)}{\omega_0(\lambda_0) a(\lambda_0)}. \quad (11)$$

Thus, $L_w(\lambda)$ can be found from

$$L_w(\lambda) = t(\lambda)^{-1} [L_t(\lambda) - L_r(\lambda) - S(\lambda, \lambda_0) \times [L_t(\lambda_0) - L_r(\lambda_0) - t(\lambda_0)L_w(\lambda_0)]] \quad (12)$$

If λ_0 is chosen such that

$$L_w(\lambda_0) = 0 \quad (13)$$

or

$$t(\lambda_0)L_w(\lambda_0) < \text{one digital count},$$

Equation 12 can be solved directly; however, if such a λ_0 does not exist (as for example in Case 1 waters with $\langle C \rangle \geq 1-2 \text{ mg/m}^3$) a further relationship among the various L_w 's is required. Smith and Wilson

(1981) use an empirical relationship derived by Austin and Petzold (1981) for Case 1 waters;

$$L_w(670) = 0.0829 L_w(443) [R(13)]^{-1.661} \quad (14)$$

and solve the resulting set of nonlinear equations iteratively.

As mentioned previously, in Gordon et al. (1980) $S(\lambda, \lambda_0)$ was determined from the water-leaving radiance measured at one position in the image from a ship. It is, however, desirable to be able to determine $S(\lambda, \lambda_0)$ without resorting to any surface measurements. The key to effecting a solution to Equations 12 and 13 or 14 is the determination of $S(\lambda, \lambda_4)$ or equivalently $\epsilon(\lambda, \lambda_4)$. This is accomplished using the concept of 'clear water radiances.' Gordon and Clark (1981) have shown that, for phytoplankton pigment concentrations less than about 0.25 mg/m^3 , the water-leaving radiance in the green, yellow, and red CZCS bands can be written

$$L_w(\lambda) = L_w(\lambda) N^{\cos \theta_0} \times \exp[-(\tau_r/2 + \tau_{0z})/\cos \theta_0], \quad (15)$$

where $[L_w]_N$, the normalized water-leaving radiance, is 0.498, 0.30, and less than 0.015 $\text{mW}/(\text{cm}^2 \text{ m ster})$ for 520, 550, and 670nm, respectively. Thus, if a region of image for which $C < 0.25 \text{ mg/m}^3$ can be located, Equations 7 and 10 can be used to determine $\epsilon(520,670)$, $\epsilon(550,670)$, and $\epsilon(670,670)$. $\epsilon(443,670)$ can then be estimated by extrapolation. An important aspect of this algorithm is that no surface measurements of either $\langle L_w(\lambda) \rangle$ or of any properties of the aerosol are required to effect the atmospheric correction with this scheme.

APPENDIX C. DATA REDUCTION

Experience with the present NIMBUS-7 CZCS shows that an ocean color data delivery system must have several general attributes. In particular such a system must be capable of processing all cloud-free scenes, be fast enough to accomplish processing without backlog, have methods of delivering scientific outputs quickly, and provide near real-time methods of sensor control, data indexing, and validation. Since an integral part of the proposed experiment is concerned with global assessment it also assumed that adequate capability must exist in the system to accomplish global coverage.

This scientific data delivery section is meant to give an overview of the proposed paths for ocean color data from sensor to user. An outline of a processing model is provided as well. These descriptions are not meant to explicitly specify each component required, but rather to illustrate data pathways, implicit assumptions concerning coverage, data availability, and processing methodology. As such, this is a series of recommendations and needs additional studies for optimization before implementation.

General Assumptions:

- Global real-time digital downlink of original data with house-keeping data is provided.
- Global reduced resolution non-real-time data is available.
- Tape recorded coverage is selectable in blank areas at full resolution.
- All data is archived.
- A facility is provided to produce derived products.
- On-line catalog of ocean color data is provided.
- Users can submit request for alteration of tape recorded coverage.

Figure C-1 presents a diagram of the proposed data flow. It mimics the present NOAA spacecraft data distribution system; consequently, it can be implemented with presently available technology and services.

Specific Assumptions:

- a. Tape recorder capacity for limited high-resolution and low-resolution non-real-time imaging (12 minutes high resolution plus 2 full orbits low-resolution coverage capacity).
- b. Ocean color data is separated from the satellite data stream at a central facility and routed with less than a three-orbit delay via DOMSAT link for general distribution and to an Ocean Color Processing Facility (OCPF), if possible.
- c. OCPF processes data at rates commensurate with data flow and routes results via DOMSAT link (if required) to a USER INTERFACE Facility (UIF).
- d. User Interface Facility has the capacity to maintain 4-day coverage online (1/2 real-time, 1/2 archive in origin).
- e. UIF is the sole scientific user interface for Ocean Color Data.

The central, ocean color, archive, and user interface facilities need not be separate; for cost reasons, one may wish to combine parts of them. They have been separated to illustrate the spectrum of functions required for scientific utilization of ocean color data. The dashed line connecting the user interface and the satellite command data acquisition site is the reverse conduit for user requests concerning satellite coverage changes. In fact, this may have to be routed through a satellite/sensor control facility before going to the CDA. A summarization of these four activity functions follows.

- a. Central Data Decommuration Facility. This facility exists for the satellite bus chosen, e.g., NESS-Suitland for ATN, FNOC-Monterrey for DMSP. Additional equipment is required to separate ocean color data from the parent spacecraft data stream and route

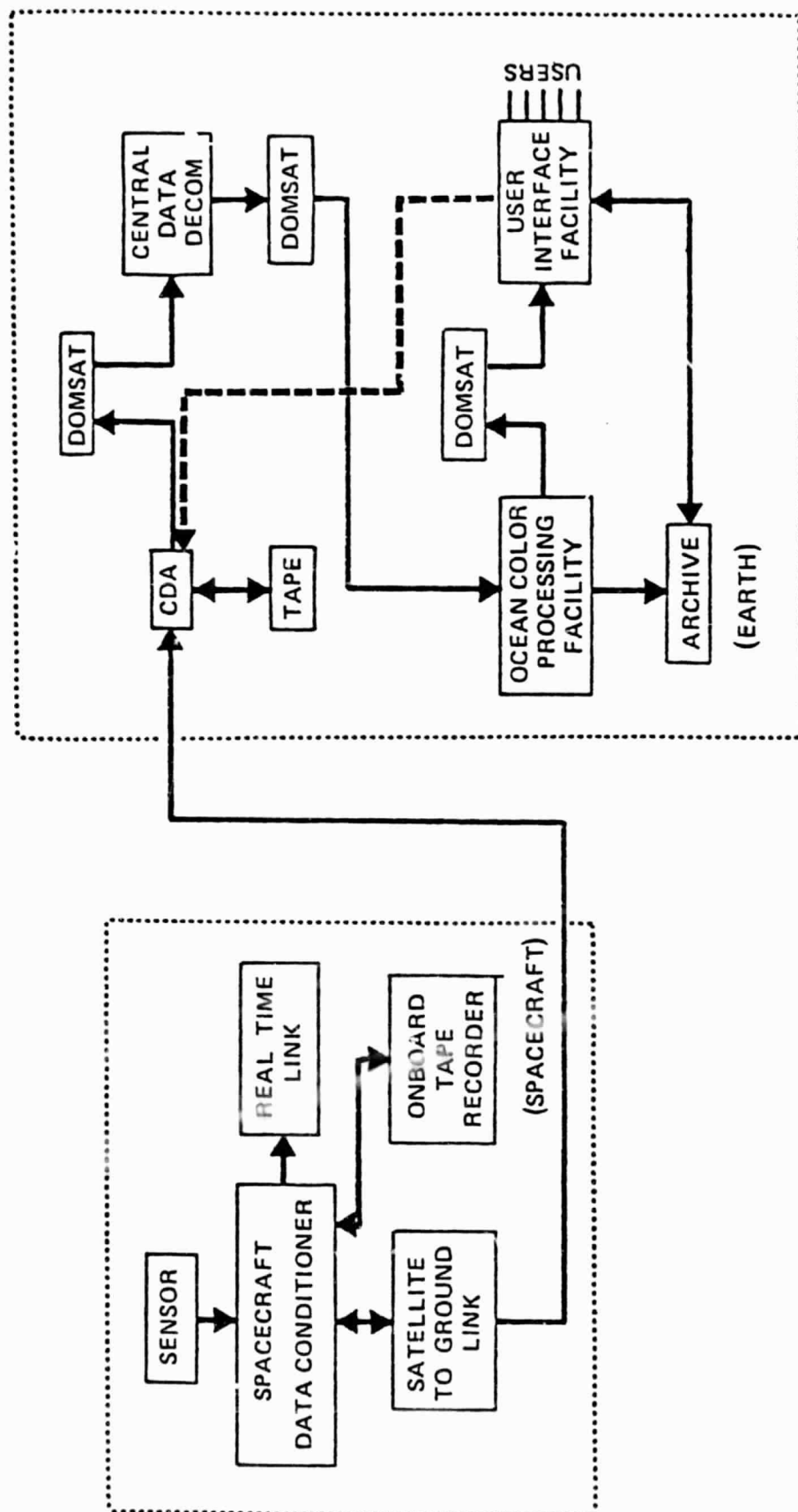


Figure C-1. Proposed Data Flow of MAREX Satellite Sensors

this data to the Ocean Color Processing Facility. Data rate is a standard NOAA channel at 1.33 mbits/second. A low-speed command channel, NOAA vice 9.6 kbits/second, is provided for communication of sensor command information back to the spacecraft.

- b. Ocean Color Processing Facility (OCPF). The OCPF will take raw telemetry stream data from the Central Processing Facility and convert it to computer-compatible form. This form, along with time, location, calibration, and cloudiness data attached will be archived. Note that this function requires a human, "M1," in Figure C-2, to perform cloud screening; the remainder is automatic. "Users" in Figure C-2 refers to the UIF. The atmospheric correction procedure is schematized on the right hand side of Figure C-2. Another human, "M2," has been included to locate "clear water" to serve as base areas for atmospheric correction. "Derived parameters" include chlorophyll and diffuse attenuation coefficient.
- c. Archive. Primary data and processed data is located in the archive. At a minimum it is assumed the archive will contain time, location, spacecraft altitude and health, calibration, raw data, processed data, and derived products. Users will not have direct access. This could be part of an existing archive.
- d. User Interface Facility (UIF). The UIF is envisaged to be the information server for individual scientists. The UIF would provide located, calibrated imagery in pictorial or digital format to interested investigators after processing at the OCPF. It would maintain catalogues of image availability, cloudiness, and proposed satellite coverage. These catalogues would be user accessible and, in the case of proposed coverage, subject to alteration/qualification by the interested investigators. User communication with the UIF would be via telephone circuits at rates of 4800 baud.

CZCS ALGORITHM

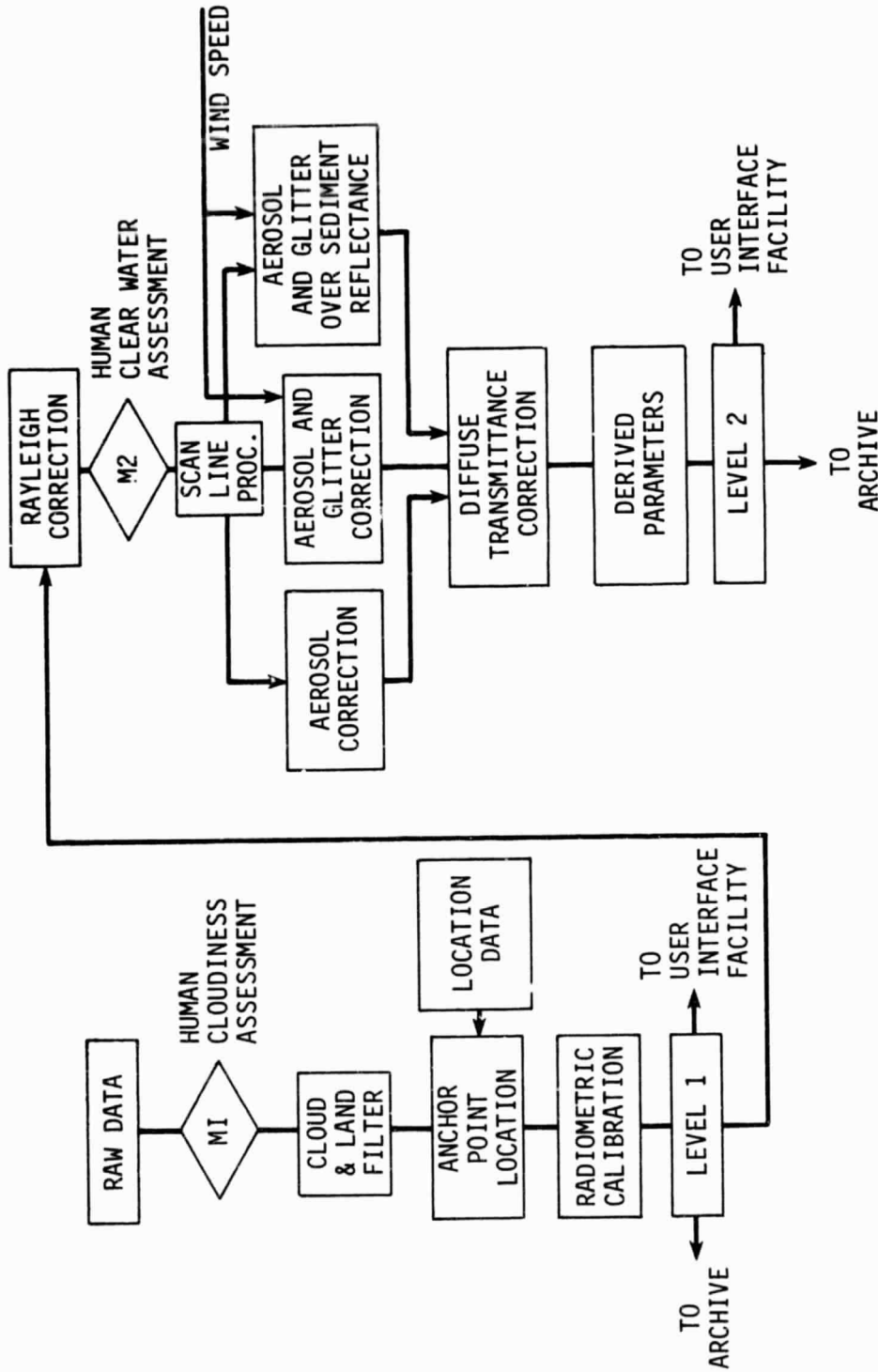


Figure C-2. Proposed Data Stream Within an Ocean Color Processing Facility

APPENDIX D. DEFENSE AND COMMUNICATION APPLICATIONS

Within the context of the proposed MAREX studies, the information gained would also be of value in the following ways.

- a. Non-acoustic ASW activities establish the requirement for a Navy capability to map bioluminescence potential on a global basis. The long-range scientific objective, therefore, is to apply satellite remote sensing technology to the problem of determining the occurrence and intensity of oceanic bioluminescence on a global scale. It is a generally accepted hypothesis that the geographical distribution of bioluminescence is associated with surface oceanic waters that are highly productive, but at present, there is no way to relate chlorophyll concentrations to bioluminescence potential. The few simultaneous in situ measurements of chlorophyll and bioluminescence are insufficient to answer this basic question and knowledge concerning the distribution and nature of bioluminescence in the surface ocean is based primarily on anecdotal reports from the main shipping lanes. Thus, the proposed program could supply Navy scientists with data for the first systematic investigation of oceanic bioluminescence utilizing satellite data and would result in techniques to permit extrapolation on a global scale.
- b. Fronts and eddies in the ocean have a significant impact on acoustic propagation because they contain density fluctuations which reflect and refract acoustic energy. Infrared satellite data is routinely analyzed to permit delineation of these features in support of ASW operations. However, IR sensing of sea surface temperature patterns is limited to certain areas and/or seasons because of the amount of water vapor in the atmosphere over the world's oceans. Because the CZCS is not as adversely affected by atmospheric water vapor as are IR sensors, it offers the potential for mapping ocean surface features based on color in geographical areas where satellite data has never been useful.

before. Another CZCS in orbit would certainly benefit the Naval community from this point of view.

- c. CZCS type data would benefit the Navy and DMA in optimizing use of conventional and advanced (airborne laser - HALS) systems for updating bathymetric charts and detection of navigational hazards. Multispectral visible data could be used to develop regional planning guides for operations. The objective would be to provide information relative to water and atmospheric transmission and bottom reflectance characteristics as a function of location and season.
- d. Backscatter from biological organisms in the ocean hinders active ASW sonars to varying degrees depending on the local biological environment. In some cases it can make the use of active sonar counter productive. The Fleet would, therefore, benefit from synoptic information on the geographical distribution and strength of acoustic volume scattering characteristics. The proposed MAREX experiment would be suitable for Naval research into the feasibility of satellite-derived ocean color data to provide this information.
- e. It is anticipated that both predictive models and real-time satellite remote sensing of the communications channels are required. The primary physical parameters of interest are: a) water column irradiance attenuation coefficients, b) cloud cover geometrical thickness, c) cloud cover optical thickness (attenuation lengths), and d) cloud height. While current technology cannot provide these primary parameters, they may be considered as goals for current development.
- f. Development of CZCS-type algorithms for removing atmospheric effects from measurements of ocean optical properties has indicated the potential for atmospheric measurements per se. Specifically, delineation of aerosol concentration, constituents, and variability is addressable by satellite multispectral visual and infrared data. Real-time and forecast data of this type could be used to improve performance of airborne E-0 weapon and sensor

systems and in the development and application of reconnaissance systems.

APPENDIX E. MAREX (MARINE RESOURCES EXPERIMENT)WORKING GROUP

John Walsh (Chairman)	Brookhaven National Laboratory
William Barnes	Goddard Space Flight Center
Otis Brown	University of Miami
Kendall Carter	National Aeronautics and Space Administration
Dennis Clark	National Environmental Satellite Service
Wayne Esaias	Langley Research Center
Howard Gordon	University of Miami
Ronald Holyer	Naval Ocean Research and Development Activity
Warren Hovis	National Environmental Satellite Service
Robert Kirk	Goddard Space Flight Center
Reuben Lasker	National Marine Fisheries Service
James McCarthy	Harvard University
Michael McElroy	Harvard University
James Mueller	Naval Postgraduate School
Mary Jane Perry	National Science Foundation
Raymond Smith	University of California at Santa Barbara

APPENDIX F. LITERATURE CITED

- Alversen, D.L., A.R. Longhurst, and J.A. Gulland. 1970. How much food from the sea? Science 168: 503-505.
- Arvesen, J., and Weaver, E.C., 1973. Remote sensing of chlorophyll and temperature in marine and fresh waters. Astronaut. Acta., 18, 229-239.
- Austin, R.W., 1974. The remote sensing of spectral radiance from below the ocean surface. Optical Aspects of Oceanography, N.G. Jerlov and E.S. Nielsen eds., Academic Press, London. Ch. XIV, 317-344.
- Austin, R.W., and Petzold, T.J., 1981. The determination of the diffuse attenuation coefficient of sea water using the coastal zone color scanner. Oceanography from Space, J.R.F. Gower ed., Plenum Press, New York, p. 239-256.
- Baker, K.S. and R.C. Smith. 1981. Bio-optical classification and model of natural waters II. Limnol. Oceanog. (in press).
- Beardsley, R.C., W.C. Boicourt, L.C. Huff, J.R. McCullough, and J. Scott. 1981. CMICE: A near-surface current meter intercomparison experiment. Deep-Sea Res. 28: 1577-1604.
- Blackman R.B. and J.W. Tukey. 1957. The Measurement of Power Spectra. Dover Press, pp. 1-190.
- Blume, H.J.C., B.M. Kendall, and J.C. Fedors. 1981. Multifrequency radiometer detection of submarine freshwater sources along the puerto rican coastline. J. Geophys. Res. 86: 5283-5291.
- Bristow, M.F., Bundy, B., Furtek R., and Baker, J., 1979, Airborne Laser Fluorosensing of Surface Water Chlorophyll a. Report EPA-600/4-79-048, EPA, Las Vegas.
- Broecker, W.S., T. Takahashi, H.J. Simpson, and T.H. Peng. 1979. Fate of fossil fuel carbon dioxide and the global carbon budget. Science 206: 409-418.
- Burns, N.M. 1976. Temperature, oxygen, and nutrient distribution patterns in Lake Erie, 1970. J. Fish. Res. Board Can. 33: 485-511.
- Campbell, J.W. and J.P.. Thomas. 1981. Chesapeake Bay plume study: super-flux 1980. Proc. NASA Conf. 2188, Wash. D.C., pp. 1-515.
- Carder, K.L. 1981. Oceanic lidar. Proc. NASA Conf. 2194, Wash D.C., pp. 1-33.

- Carpenter, J.H., D.W. Pritchard, and R.C. Whaley. 1969. Observations of eutrophication and nutrient cycles in some coastal plain estuaries. Eutrophication: Causes, Consequences, Correctives, Nat. Acad. Sci., Washington, D.C. pp 210-221.
- Clark, D.K., Baker, E.T., and Strong, A.E., 1980. Upwelled spectral radiance distribution in relation to particulate matter in sea water. Boundary Layer Meteorology, 18, 287-298.
- Clark, D.K., 1981. Phytoplankton algorithms for the Nimbus-7 CZCS. Oceanography from Space, edited by J.R.F. Gower, Plenum Press, New York, pp. 227-238.
- Clarke F.W. 1924. The data of geochemistry. U.S. Geol. Bull. 770: 1-841.
- Clarke, G.K., Ewing G.C., and Lorenzen, C.J., 1970. Spectra of back-scattered light from the sea obtained from aircraft as a measure of chlorophyll concentration. Science, 167, 1119-1121.
- Deck, B.L. 1981. Nutrient-Element Distribution in the Hudson Estuary. Ph.D. dissertation Columbia Univ., New York, pp. 1-396.
- Delwiche, C.C. and G.E. Likens. 1977. Biological response to fossil fuel combustion products. Global Chemical Cycles and Their Alterations by Man, W. Stumm ed., Dahlem Konferenzen, Berlin, pp. 89-98.
- De Vooy, C.G.N. 1979. Primary production in aquatic environments. B. Bolin, E.T. Degens, S. Kempe, P. Ketner eds., The Global Carbon Cycle, 259-92, Scope 13. Wiley, New York.
- Emery, K.O., W.L. Orr and S.C. Rittenberg. 1955. Nutrient budgets in the ocean. Essays in Honor of Captain Allan Hancock, Univ. S. Cal. Press, Los Angeles, pp. 299-309.
- Emery, K.O. 1979. Hypsometry of the continental shelf off Eastern North America. Estuar. Coastal Mar. Sci. 9: 653-658.
- R.W. Eppley. 1972 Temperature and phytoplankton growth in the sea. Fish. Bull. 70:1063-1085.
- Eppley, R.W. 1980. Estimating phytoplankton growth rates in the central oligotrophic oceans. Primary productivity in the sea. Envir. Sci. Res. 19, P.G. Falkowski, ed. 19, Plenum, New York, pp. 231-42.
- Eppley, R.W. and B.J. Peterson. 1980. Particulate organic matter flux and planktonic new production in the deep ocean. Nature 282: 677-680.
- Fisher, J.B. and G. Matisoff. 1982. Downcore variation in sediment organic nitrogen. Nature 296: 345-347.
- Falkowski, P.. 1981. Light-shade adaptation in marine phytoplankton. Primary Productivity in the Sea, P.G. Falkowski ed., Plenum Press, N.Y., pp. 99-119.

- Fucik, K.W. 1974. The Effect of Petroleum Operations on the Phytoplankton Ecology of the Louisiana Coastal Waters. Msc. Thesis, Texas A&M Univ., pp. 1-82.
- Garrels, R.M., F.T. MacKenzie, and C. Hunt. 1973. Chemical cycles and the global environment. Kaufmann, Los Altos, pp. 95-109.
- Geiskes, W.W.C., G.W. Kraay, and M.A. Baars. 1979. Current ^{14}C methods for measuring primary production: gross underestimates in oceanic waters. Neth. J. Sea Res. 13:58-78.
- Gordon, H.R., 1981a. A preliminary assessment of the Nimbus-7 CZCS atmospheric correction algorithm in a horizontally inhomogeneous atmosphere. Oceanography from Space, J.R.F. Gower, ed., Plenum Press, New York, pp. 257-266.
- Gordon, H.R., 1981b. Reduction in error introduced in the processing of coastal zone color scanner-type imagery resulting from sensor calibration and solar irradiance uncertainty. Applied Optics, 20, 207-210.
- Gordon, H.R., and Clark, D.K., 1980a. Atmospheric effects in the remote sensing of phytoplankton pigments. Boundary Layer Meteorology 18, 299-313.
- Gordon, H.R., and Clark, D.K., 1980b. Remote sensing optical properties of a stratified ocean: an improved interpretation. Applied Optics, 19, 3428-3430.
- Gordon, H.R., and Clark, D.K., 1981. Clear water radiances for atmospheric correction of coastal zone color scanner imagery. Applied Optics, 20, 4175-4180.
- Gordon, H.R., Clark, D.K., Brown J., Brown O.B., Evans, R.H., and Broenkow W.W., 1982. Phytoplankton pigment concentrations in the Middle Atlantic Bight: comparisons of ship determinations and satellite estimations. Applied Optics (to be submitted).
- Gordon, H.R., Clark, D.K., Mueller, J.L., and Hovis, W.A., 1980. Phytoplankton pigments derived from the Nimbus-7 CZCS: initial comparisons with surface measurements. Science 210, 63-66.
- Gordon, H.R., and McCluney, W.R., 1975. Estimation of the depth of sunlight penetration in the sea for remote sensing. Applied Optics, 14, 413-416.
- Gunter, G. 1967. Some relationships of estuaries to the fisheries of the Gulf of Mexico. Estuaries, G.H. Lauff, ed., Amer. Assoc. Adv. Sci. No. 83, Wash., D.C., pp. 621-638.
- Hobbie, J.E., B.J. Copeland, and W.G. Harrison. 1975. Nutrient cycling within the Pamlico Estuary. Estuarine Res., Vol. I, L.E. Cronin ed., Academic Press, New York, pp. 287-305.

- Hoge, F.E., Swift, R.N., and Frederick E. B., 1980, Water depth measurement using an airborne pulsed neon laser system. Applied Optics, Vol. 19, No. 6, 871-833.
- Hoge, F.E. and Swift, R.N., 1981, Airborne spectroscopic detection of laser-induced water raman backscatter and fluorescence from chlorophyll a, and other naturally occurring pigments. Appl. Opt., Vol. 20, No. 18, 3197-3205.
- Holm-Hansen O.G., Lorenzen G.J., Holmes, R.W., Strickland, J.D.H. 1965. Fluorometric determination of chlorophyll. J. Cons. Perm. Int. Explor. Mer., 30, 3-15.
- Hovis, W.A., Forman, M.L., and Blaine, L.R., Detection of Ocean Color Changes from High Altitudes, NASA X-652-73-371, Nov. 1973.
- Hovis, W.A., and Leung, K.C., Remote sensing of ocean color. Optical Engineering, 16, 158 (1977).
- Hovis, W.A., D.K. Clark, F. Anderson, R.W. Austin, W.H. Wilson, E.T. Baker, D. Ball, H.R. Gordon, J.L. Mueller,, S.Z. El-Sayed, B. Sturm, R.C. Wrigley, and C.S. Yentsch. 1980. Nimbus-7 Coastal Zone Color Scanner systems: description and initial imagery. Science 210: 60-63.
- Johnston R. 1973. Nutrients and metals in the North Sea. North Sea Science, E.D. Goldberg ed., MIT Press, Cambridge, pp. 293-307.
- Kelley, J.C. 1976. Sampling the sea. Ecology of the Seas, D.H. Cushing and J.J. Walsh, Blackwell eds., pp. 361-387.
- Kendall, M. and J.O. Blanton. 1981.. Microwave Radiometer Measurement of Tidally Induced Salinity Changes off the Georgia Coast. 86: 6435-6441.
- Kemp, A.L.W., T.W. Anderson R.L. Thomas, and A. Mudrochova. 1974. Sedimentation rates and recent sediment history of Lakes Ontario, Erie, and Huron. J. Sediment. Petrol. 44: 207-218.
- Kemp, A.L.W., R.L. Thomas, C.I. Dell, and J.M. Jaquet. 1976. Cultural impact on the geochemistry of sediments in Lake Erie. J. Fish. Res. Board Can. 33: 440-462.
- Kiry, P.R. 1974. An historical look at the water quality of the Delaware River estuary to 1973. Contrib. Dept. Limnol., Acad. Nat. Sci. Phil. 4: 1-76.
- Koblentz-Mishke,, O.J., V.V. Valkovsinky, and J.C. Kabanova. 1970. Plankton primary production of the world ocean. Scientific exploration of the South Pacific, W.S. Wooster ed., Nat. Acad. Sci., Washington D.C. pp. 189-193.
- Leach, J.H. and S.J Nepszy. 1976. The fish community in Lake Erie. J. Fish. Res. Board Can. 33: 622-638.

- Li, W.K.W. 1980. Temperature adaptation in phytoplankton: cellular and photosynthetic characteristics. Primary Productivity in the Sea, P.G. Falkowski ed., Plenum Press, N.Y., pp. 259-280.
- Likens, G.E., F.H. Bormann, R.S. Pierce, and W.A. Reiners. 1978. Recovery of a deforested ecosystem. Science 199: 492-496.
- Malone, T.C. and M.B. Chervin. 1979. The production and fate of phytoplankton size fractions in the plume of the Hudson River, New York Bight. Limnol. Oceanogr. 24: 683-696.
- Malone, T.C., and P.J. Neale 1981. Parameters of light-dependent photosynthesis for phytoplankton size fractions in temperate estuarine and coastal environments. Mar. Biol. 61: 289-297.
- Marra, J. 1981. Vertical mixing and primary productivity. Primary Productivity in the Sea, edited by P.G. Falkowski, Plenum Press, N.Y., pp. 121-137.
- Morrmmaerts, J.P., W. Baeyens, and G. Decadt. 1979. Synthesis of research on nutrients in the Southern Bight of the North Sea. Actions de Recherche Concertees, Bruxelles, pp. 215-234.
- Morel, A., and Prieur, L., 1977. Analysis of variations in ocean color, Limn. Ocean. 22: 708-722.
- Morel, A. and R.C. Smith. 1974. Relation between total quanta and total energy for aquatic photosynthesis. Limnol. Oceanogr. 19: 591-600.
- Mueller, J.L. and P.E. LaViolette. 1981. Color and temperature signatures of ocean fronts observed with the Nimbus-7 CZCS. Oceanography from Space, Gower, J.F.R. ed., Plenum, NY 295-302.
- O'Neil, R.A., 1981, Field trials of a lidar bathymeter in the Magdalen Islands. Proceedings of the Fourth Laser Hydrography Symposium, Penny M.F., and Phillips, D.M., eds., Defense Research Center Salisbury, Special Document ERL-0193-5D.
- Owens, T.G., P.G. Falkowski, and T.E. Whitledge. 1980. Diel periodicity in cellular chlorophyll content in marine diatoms. Mar. Biol. 59: 71-77.
- Park, K.H., C.L. Osterberg, and W.D. Forster. 1972. Chemical budget of the Columbia River. The Columbia River Estuary and Adjacent Ocean Waters, A.T. Pruter and D.L. Alverson eds., Univ. Wash Press, Seattle, pp. 123-134.
- Perry, M.J. M.C. Talbot, and R.S. Alberts. 1981. Photoadaptation in marine phytoplankton: response of the photosynthetic unit. Mar. Biol. 62: 91-101.
- Perry, M.J. M.C. Talbot, L. Welschmeyer, and J.C. Smith. Nitrogen limitation in marine phytoplankton: response of the photosynthetic apparatus. (submitted to Plant Physiology).

- Platt, T. and D.V. Subba Rao. 1975. Primary production of marine microphytes. Photosynthesis and Productivity in Different Environments, J.P. Cooper ed., Cambridge Univ. Press, p. 249-80.
- Platt, T., Denman, K.L., and Jassby, A.D., 1977. Modeling the productivity of phytoplankton, The Sea, vol. 6 Goldberg, E.D., McCave, I.N., O'Brien, J.J., and Steele, J.H. eds., Ch. 21, 807-856.
- Platt T. and C.L. Gallegon. 1980 Modelling primary production. Primary Productivity in the Sea, P.G. Falkowski ed., Plenum Press, N.Y., pp. 339-362.
- Postma, H. 1978. The nutrient contents of North Sea water: changes in recent years, particularly in the Southern Bight. Rapp. R.-V. Reun.. Cons.. Int. Explor.. Mer 172: 350-352.
- Regier, H.A. and W.L. Hartman. 1973. Lake Erie's fish community: 150 years of cultural stresses. Science 180: 1248-1255.
- Riley, G.A. 1946. Factors controlling phytoplankton populations on Georges Bank. J. Mar. Res. 6: 54-73.
- Riley, G.A. 1937. The significance of the Mississippi River drainage for biological conditions in the northern Gulf of Mexico. J. Mar. Res. 1: 60-74.
- Ryther, J.H. 1969. Photosynthesis and fish production in the sea. Science 166: 72-76.
- Ryther, J.H., D.W. Menzel, and N Corwin. 1967. Influence of the Amazon River outflow on the ecology of the western Tropical Atlantic. I. Hydrography and nutrient chemistry. J. Mar. Res. 25: 69-83.
- Ryther, J.H. and W.M. Dunstan. 1971. Nitrogen, phosphorus, and eutrophication in the coastal marine environment. Science 171: 1008-1013.
- Scott, J.T. and G.T. Csanady. 1976. Nearshore currents off Long Island. J Geophys Res. 81: 5401-5409.
- Segar, D.A. 1982. Contamination of Polluted Estuaries and Adjacent Coastal Ocean - a Global Review. MESA New York Bight Spec. Rept. Ser. (in press).
- Sly, P.G. 1976. Lake Erie and its basin. J. Fish. Res. Board Can. 33: 355-370.
- Sly, P.G. and C.F.M. Lewis. 1972. The Great Lakes of Canada - quaternary geology and limnology. Int. Geol. Congr. Montreal Que. Guideb. Trip A43: 1-92.
- Smith, P.E. and R.W. Eppley. 1982. Primary production and the anchovy populations in the Southern California Bight: comparison of time series. Limnol. Oceanogr. 27: 1-17.

- Smith, R.C. and K.S. Baker. 1978a. the bio-optical state of ocean waters and remote sensing. Limnol. Oceanogr. 23: 247-259.
- Smith, R.C. and K.S. Baker. 1978b. Optical classification of natural waters. Limnol. Oceanogr. 23: 260-267.
- Smith, R.C. and K.S. Baker. 1981. Oceanic chlorophyll concentrations as determined using Coastal Zone Color Scanner imagery. Mar. Biol. (in press).
- Smith, R.C., R.W. Eppley and K.S. Baker. 1981. Correlation of primary production as estimated from satellite chlorophyll images and as measured aboard ship in Southern California Coastal Waters. Mar. Biol. (in press).
- Smith, R.C., J.S. Campbell, W.E. Esaias, and J.J. McCarthy. 1981. Primary productivity in the ocean. Proc. Workshop on Life from a Planetary Perspective: Fundamental Issues in Global Ecology (in press).
- Smith, R.C., and Wilson W.H., 1981. Ship and satellite bio-optical research in the California Bight, Oceanography from Space, J.R.F. Gower ed., Plenum Press, New York, p.. 281-294.
- Steeman Nielson E. 1952. The use of radioactive carbon (^{14}C) for measuring organic production in the sea. J.J. Cons. Prm. Int Explor.. Mer 18, 117-40.
- Stewart, R.H. 1981. Satellite oceanography: the instruments. Oceanus 24: 66-74.
- Tanre, D., Herman, M., Deschamps, P.Y., and de Lefte, A., 1979. Atmospheric modeling for space measurements of ground reflectances, including bidirectional properties, Applied Optics, 18, 3587-3594.
- Thomas, W.J, and Simmons, E.G. 1960. Phytoplankton production in the Mississippi Delta. I Recent Sediments, Northwest Gulf of Mexico, F.P. Shepard, F.B. Phleger, and T.H. van Andel eds., Amer. Assoc. Petrol Geol., Tulsa, pp. 103-116.
- van Bennekom, A.J., G.W. Berger, W. Helder, and R.T.P. deVries. 1978. Nutrent distribution in the Zaire estuary and river plume. Neth J Sea Res 12: 296-323.
- van Bennekom, A.J and W. Salomons. 1981. Pathways of nutrients and organic matter from land to ocean through rivers. River Inputs to Ocean Systems, UNESCO, Switzerland,, pp. 33-51.
- Vollenweider,, R.A. 1968. Scientific fundamentals of the eutrophications of lakes and flowing waters, with particular reference to nitrogen and phosphorus as factors in eutrophication. OECD Tech. Rep. DAS/CS1/68-27: 1-95.

- Vollenweider, R.A., M. Munawar, and P. Stadlemann. 1974. A comparative review of phytoplankton and primary production in the Laurentian Great Lakes. J Fish. Res. Board Can. 31: 739-762.
- Walsh, J.J. 1971. Relative importance of habitat variables in predicting the distribution of phytoplankton at the ecotone of the antarctic upwelling ecosystem. Ecol. Monogr. 41: 291-309.
- Walsh, J.J. 1976. Herbivory as a factor in patterns of nutrient utilization in the sea. Limnol. Oceanogr. 21: 1-13.
- Walsh, J.J. 1981a. Concluding remarks: marine photosynthesis and the global CO₂ cycle. Primary Production in the Sea, P.G. Falkowski ed., 497-506, Academic Press, New York.
- Walsh, J.J. 1981b. Shelf-sea ecosystems. Analysis of Marine Ecosystems. A.R. Longhurst ed., Academic Press, New York, pp. 159-196.
- Walsh, J.J. 1982. Death in the sea: enigmatic phytoplankton losses. Prog. Oceanogr. (in press).
- Walsh, J.J., T.E. Whitledge, J.C. Kelley, S.A. Huntsman, and R.D. Pillsbury. 1977. Further transition states of the Baja California upwelling ecosystem. Limnol. Oceanogr. 22: 264-280.
- Walsh, J.J., T.E. Whitledge, F.W. Barvenik, C.D. Wirick, S.O. Howe, W.E. Esaias, and J.T. Scott. 1978. Wind events and food chain dynamics within the New York Bight. Limnol. Oceanogr. 23: 659-683.
- Walsh, J.J., T.E. Whitledge, W.E. Esaias, R.L. Smith, S.A. Huntsman, H. Santander, and B.R. DeMendiola. 1980. The spawning habitat of the Peruvian anchovy, Engraulis ringens. Deep-Sea Res. 27: 1-27.
- Walsh, J.J., G.T. Rowe, R.L. Iverson and C.P. Mcroy. 1981. Biological Export of Shelf Carbon is a Neglected Sink of the Global CO₂ Cycle. Nature 291: 196-201.
- Whitledge, T.E. and C.D. Wirick. 1982. Observations of chlorophyll concentrations off Long Island from a moored in situ fluorometer. Deep-Sea Res. (in press).
- Wolman, M.G. 1971. The nation's rivers. Science 174: 905-918.
- Woodwell, G.M., R.H. Whittaker, W.A. Reiners, G.E. Likens, C.C. Delwiche, and D.B. Botkin. 1978. The biota and the world carbon budget, Science 199: 141-146.
- Yentsch, C.S., and Menzel, D.W., 1963. A method for the determination of phytoplankton chlorophyll and phaeophytin by fluorescence. Deep Sea Res., 10, 221-231.

Zaneveld, J.R.V., J.C. Kitchen, and H. Pak. 1981. The influence of optical water type on the heating rate of a constant depth mixed layer. UGR 86007:6426-6428.

Zentara S.J. and D. Lamykowski. 1977., Latitudinal relationships among temperature and selected plant nutrients along the west coast of North and South America. J. Mar. Res. 35: 321-337.

APPENDIX G. GLOSSARY OF ACRONYMS AND DEFINITIONS

APT	Automatic Picture Transmission
AVHRR	Advanced Very High Resolution Radiometer
CCT	Computer Compatible Tapes
CZCS	Coastal Zone Color Scanner
DOC	Department of Commerce
DOD	Department of Defense
DOMSAT	Domestic Communication Satellite System
EDIS	Environmental Data and Information Service
EROS	Earth Resources Observational System
ESIC	Environmental Science Information Center
ESSA	Environmental Science Services Administration (Predecessor to NOAA)
GEM-10b	A geoid model
GEOS	Geodynamics Experimental Oceanographic Satellite (NASA)
GMT	Greenwich Mean Time
GOES	Geostationary Operational Environmental Satellite (NASA)
GOSSTCOMP	Global Operational Sea Surface Temperature Computation
HRPT	High Resolution Picture Transmission
IFOV	Instantaneous Field of View
IR	Infrared
JPL	Jet Propulsion Laboratory
LAMMR	Large Antenna Multichannel Microwave Radiometer
LANDSAT	Land Observing Satellite (NASA)
NASA	National Aeronautics and Space Administration
NEFC	Northeast Fisheries Center

NESS	National Environmental Satellite Service
NIMBUS	Atmospheric and Oceanic Observing Satellite (NASA)
NMFS	National Marine Fisheries Service
NOAA	National Oceanic and Atmospheric Administration
NODS	NOAA Oceanic Data System
NOS	National Ocean Survey
NOSS	National Oceanic Satellite System
NSTL	National Space Technology Laboratories
NWFC	Northwest Fisheries Center
NWS	National Weather Service
PMEL	Pacific Marine Environmental Laboratory
R&D	Research and Development
SAR	Synthetic Aperture Radar
SASS	Seasat Scatterometer System
SEASAT	Oceanic Observing Satellite (NASA)
SDSD	Satellite Data Services Division
SEFC	Southeast Fisheries Center
SIO	Scripps Institute of Oceanography
SMMR	Scanning Multichannel Microwave Radiometer
SMS	Synchronous Meteorological Satellites
SOSU	Seattle's Ocean Services Unit
SST	Sea Surface Temperature
SWFC	Southwest Fisheries Center
TDRSS	Tracking and Data Relay Satellite System
TIROS	Television and Infrared Observation Satellite (NASA/NOAA)
USGS	United States Geological Survey
VHRR	Very High Resolution Radiometer

VIRR Visible and Infrared Radiometer
VISSR Visible Infrared Spin Scan Radiometer
WHOI Woods Hole Oceanographic Institute
WSFO Weather Service Forecast Office
WWB World Weather Building

$\mu\text{g}/\ell$ (or $\mu\text{g}\ell^{-1}$) - micrograms per liter

primary production - the initial conversion of inorganic to organic material; the conversion of chlorophyll to phytoplankton in the ocean